SHIP PRODUCTION COMMITTEE
FACILITIES AND ENVIRONMENTAL EFFECTS
SURFACE PREPARATION AND COATINGS
DESIGN/PRODUCTION INTEGRATION
HUMAN RESOURCE INNOVATION
MARINE INDUSTRY STANDARDS
WELDING
INDUSTRIAL ENGINEERING
EDUCATION AND TRAINING

May 1, 1998
NSRP 0524
N7-94-1

THE NATIONAL SHIPBUILDING RESEARCH PROGRAM

Welding Over Paint Primer

U.S. DEPARTMENT OF THE NAVY
CARDEROCK DIVISION,
NAVAL SURFACE WARFARE CENTER

in cooperation with
Peterson Builders, Inc.

Report Documentation Page

Form Approved
OMB No. 0704-0188

1. REPORT DATE	2. REPORT TYPE	3. DATES COVERED
01 MAY 1998	**N/A**	**-**

4. TITLE AND SUBTITLE	5a. CONTRACT NUMBER
The National Shipbuilding Research Program, Welding Over Paint Primer	5b. GRANT NUMBER
	5c. PROGRAM ELEMENT NUMBER
6. AUTHOR(S)	5d. PROJECT NUMBER
	5e. TASK NUMBER
	5f. WORK UNIT NUMBER
7. PERFORMING ORGANIZATION NAME(S) AND ADDRESS(ES) **Naval Surface Warfare Center CD Code 2230-Design Integration Tower Bldg 192, Room 128 9500 MacArthur Blvd Bethesda, MD 20817-5000**	8. PERFORMING ORGANIZATION REPORT NUMBER
9. SPONSORING/MONITORING AGENCY NAME(S) AND ADDRESS(ES)	10. SPONSOR/MONITOR'S ACRONYM(S)
	11. SPONSOR/MONITOR'S REPORT NUMBER(S)

12. DISTRIBUTION/AVAILABILITY STATEMENT
Approved for public release, distribution unlimited

13. SUPPLEMENTARY NOTES

14. ABSTRACT

15. SUBJECT TERMS

16. SECURITY CLASSIFICATION OF:			17. LIMITATION OF ABSTRACT	18. NUMBER OF PAGES	19a. NAME OF RESPONSIBLE PERSON
a. REPORT	b. ABSTRACT	c. THIS PAGE			
unclassified	**unclassified**	**unclassified**	**SAR**	**240**	

Standard Form 298 (Rev. 8-98)
Prescribed by ANSI Std Z39-18

DISCLAIMER

These reports were prepared as an account of government-sponsored work. Neither the United States, nor the United States Navy, nor any person acting on behalf of the United States Navy (A) makes any warranty or representation, expressed or implied, with respect to the accuracy, completeness or usefulness of the information contained in this report/ manual, or that the use of any information, apparatus, method, or process disclosed in this report may not infringe privately owned rights; or (B) assumes any liabilities with respect to the use of or for damages resulting from the use of any information, apparatus, method, or process disclosed in the report. As used in the above, “Persons acting on behalf of the United States Navy” includes any employee, contractor, or subcontractor to the contractor of the United States Navy to the extent that such employee, contractor, or subcontractor to the contractor prepares, handles, or distributes, or provides access to any information pursuant to his employment or contract or subcontract to the contractor with the United States Navy. ANY POSSIBLE IMPLIED WARRANTIES OF MERCHANTABILITY AND/OR FITNESS FOR PURPOSE ARE SPECIFICALLY DISCLAIMED.

WELDING OVER PAINT PRIMER

NSRP-SP-7 Project No. 7-94-1

Submitted by:

Kevin S. Johnson, Stephen Liu and David L. Olson
Center for Welding, Joining and Coatings Research
Colorado School of Mines
Golden, CO 80401

Submitted to:

Mr. Lee Kvidahl
Ingalls Shipbuilding
Pascagoula, Mississippi

Mr. John Meacham
SP-7 Welding Panel
Program Manager
Peterson Shipbuilding

May 1998

ABSTRACT

When welding is performed over primer-coated steels such as in the shipbuilding and offshore structures fabrication industry, significant amounts of hydrogen and other gases, e.g., CO and $Zn_{(v)}$ are generated as the welding arc causes the primer to decompose. If entrapped in the weld pool, the hydrogen and other gases will produce porosity. Since hydrogen has been shown to compose most of the gas generated in a flux-cored arc weld over a primer-coated steel, it is also the most detrimental. According to the *hydrogen-oxygen* and *hydrogen-fluorine* equilibrium considerations, an increase in the partial pressure of oxygen or fluorine could decrease the partial pressure of hydrogen within the welding arc. Consequently, a welding consumable that contains chemical ingredients of high oxygen and fluorine potential would be capable of minimizing hydrogen pick-up in the weld pool.

Welds made using a commercially available rutile-based E71T-1 flux-cored consumable produced about 74.3 ml/100g of diffusible hydrogen on a steel sample coated with 5.0 mils of an inorganic, zinc ethyl-silicate primer. The oxygen content for this weld was about 600 ppm. Welds made on a samples coated with 4.0 mils of the same primer, but using an experimental electrode with the addition of $CaCO_3$, SiO_2, Fe_3O_4, and MnF_3 produced only 15.8 ml/100g of diffusible hydrogen with an oxygen content of about 660 ppm. The decrease in diffusible hydrogen content from the experimental electrodes is due

to the effectiveness of the oxide and fluoride flux additions. The welds made with electrodes that contained MnF_3 showed substantial ferrite grain size refinement. This refinement would aid in controlling the increase in grain size and amount of grain boundary ferrite expected with an increase in weld metal oxygen content, while maintaining a sufficient amount of acicular ferrite to produce adequate weld metal toughness. It can be stated that along with helping to lower diffusible hydrogen, the fluorides also help to refine the microstructure.

TABLE OF CONTENTS

ACKNOWLEDGMENTS

The authors would like to thank the National Shipbuilding Research Program, SP-7 Welding Panel for their financial support of this research project. They would also like to thank Mr. Ed Bohnart and Mr. Don Brooks from Miller Electric Manufacturing for their donation and help in setting up the welding equipment used in the research, Mr. Stan Ferree and Mr. Roger Bushey for their help in supplying and manufacturing the FCAW electrodes used, and Mr. Lee Kvidahl, Mr. Tim Warren and Mr. Russ McClellan (formerly of Ingalls) from Ingalls Shipbuilding for their help in supplying the necessary materials for the welding experiments, along with Mr. John Meacham of Peterson Shipbuilding.

Chapter 1

INTRODUCTION

The purpose of this section is to give some background information with regards to the scope of this project, welding over primers, underwater wet welding, and the goals of this research project.

1.1 General Background

Pre-construction primers are used regularly by the shipbuilding industry to protect steel plates from corrosion during storage and construction. Just prior to the plates being welded, the primers are locally removed by blasting or grinding operations because weld quality is often unsatisfactory when welding directly over a primer painted surface. The presence of primer can lead to excessive porosity, arc instability, carbon pick-up, alloying element loss, and hydrogen damage. Elimination of these weld discontinuities will allow for arc welding directly over primer and will eliminate costs associated with blasting and grinding operations, and the rework required by defective weld joints. The success of welding over primer would clearly result in significant increases in shipbuilding productivity.

1.2 Welding Over Primers

It is known that most weld metal porosity results from gas entrapment, with hydrogen and carbon monoxide as the most prevalent products from the pyrolysis of

primer. Suga, Nagaoka, Nakano, and Suenaga (1) showed that when an inorganic-zinc, primer-coated steel is subjected to flux-cored arc welding, the resultant gas produced in the blowholes is about 95 pct. H_2. Under most normal welding conditions, moisture, cutting fluids, and organic solvents are the major sources of hydrogen in the arc environment. In the case of a primer-painted steel, the acrylic-based or epoxy-based resins in the primer can provide large amounts of carbon, hydrogen, and oxygen to the welding arc and to the weld pool. As the weld pool begins to solidify, gases such as hydrogen and carbon monoxide are rejected continuously into the remaining liquid which quickly reaches supersaturation. As a result, gas pores nucleate and grow. Some of the gas bubbles will be eliminated from the weld pool due to turbulence and convective flow of the molten metal, while others are entrapped in the solidifying weld pool. For the zinc-based primers, both the organic materials and the zinc contribute to the formation of weld discontinuities. In particular, zinc easily vaporizes in the welding arc and may be entrapped in the weld pool as pores. Porosity can be the cause for repair or rejection of the resulting weld. Costly repairs and schedule delays result when the porosity exceeds the permitted levels specified in the fabrication code.

Porosity in the weld metal that originates from hydrogen and carbon monoxide can be minimized if the partial pressures of these gases in the weld environment are decreased. A welding consumable that contains ingredients with high oxidizing potential is desirable for this purpose. If the decomposition reaction for water, or the H-O

reaction, is examined, as seen in Figure 1.1, the oxygen in the weld metal is expected to react with hydrogen and decrease the hydrogen concentration in the weld metal. As a result, the amount of porosity is also expected to decrease. The additions of fluxes that generate high oxygen potential during dissociation (e.g. $CaCO_3$, SiO_2, and Fe_2O_3) to the core of a flux-cored arc welding consumable to control weld metal porosity. If this were not possible, an overcoat which contains high oxidizing potential ingredients could be deposited over the primer. The effect of this overcoat to control hydrogen during welding should be comparable to that of the flux additions to an electrode.

Besides modifying welding consumables, the amount of weld metal porosity can also be affected by the choice of welding parameters. However, the effectiveness of weld discontinuity control through welding parameters varies significantly with the primer used (2). Therefore, the best approach is to first identify some high oxidizing potential fluxes, determine the best combination of the fluxes, followed by several welding experiments designed to fine-tune the electrodes and to select the welding parameters that will result in discontinuity- or defect-free welds. The primer used to protect the steel can also affect the level of discontinuities. However, close control of primer thickness has often been deemed impractical in a shipbuilding environment. Depending on the success of the high oxidizing flux additions to the welding consumable, the experimental flux system may be able to handle the large fluctuations in an industrial coating procedure.

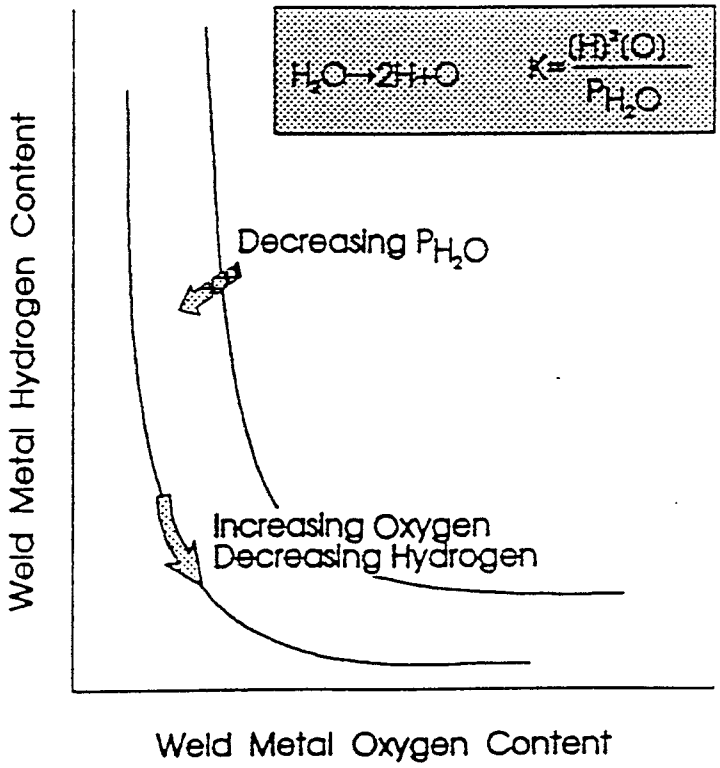

Figure 1.1 Weld metal hydrogen-oxygen equilibrium indicating possible mechanism for weld metal hydrogen control.

The fluxes used in making a flux-cored arc welding consumable very often serve several functions. Ingredients such as SiO_2 and TiO_2 are slag-formers which form long chains of silicates and titanates. Other flux ingredients such as FeO, Fe_2O_3, and CaO (from the decomposition of $CaCO_3$) tend to break down the anion chains and regulate the viscosity of the slag. These ingredients can also release their oxygen into the arc plasma or into the weld pool affecting the oxygen balance of the weld environment. Their addition can be a means of introducing controlled amounts of oxygen into the weld pool and minimizing the amount of hydrogen pick-up in the weld metal. When using $CaCO_3$ as a flux, carbon dioxide is a by-product of the decomposition and will decrease the partial pressure of hydrogen in the arc environment and reduce hydrogen pick-up in the weld pool.

The change of oxygen content in the weld metal is also expected to modify the weld metal microstructure. Any combination of flux and primer will greatly affect what type of microstructure that is obtained when welded over. The microstructure desired can be obtained through fine-tuning of the selected flux systems and through alloy additions. Research work along these lines has been done by Medeiros (3) and Pope (4) at CSM using oxygen to control the production of diffusible hydrogen in underwater wet welds.

Chapter 2

REVIEW OF RELEVANT ISSUES

The purpose of this section is to provide information that must considered during the shipbuilding process. This includes information from flux-cored arc welding to microstructural development.

2.1 Hydrogen-Oxygen Relationship

The effect that oxygen has on diffusible hydrogen has been explained by several experimental programs (5,6,7,8,9) with the objective of establishing a better understanding of the relationship between oxidizing electrodes and diffusible hydrogen. Their results indicated that weld metal oxygen content (or inclusions) alone could not explain satisfactorily the lower hydrogen levels obtained in weld deposits. Some of these studies did indicate that depending on the type and proper balance among the flux constituents, the hydrogen solubility in the slag can be drastically reduced (5,6,7,8,9). If equilibrium is assumed to exist at the slag-metal interface, the lower the hydrogen solubility in the slag, the lower the amount of hydrogen that will be absorbed by the molten weld pool. This

relationship can be seen through some application of thermodynamic principles to the study of oxide stability.

The free energies of formation lines presented in the Richardson diagram (10) for some oxides is shown in Figure 2.1. The oxides which fall above the reaction line for water (shaded portion of the diagram) will be unstable in the presence of water, and will probably decompose into a less stable oxide or metal that will release its oxygen. Metallic elements in this region (e.g. Cu and Ni) will be transferred through the welding arc and consolidate in the weld metal. Oxides that are situated below the water reaction line are stable with respect to water.

Their metallic components (e.g. Fe, Si, and Mn) will react with oxygen to form oxides. These oxides will be incorporated into the slag or entrapped in the weld metal as inclusions. The presence of FeO-rich inclusions was observed by Pope et al. (4). The loss of deoxidant elements and inclusion formation in the weld metal are related to the deleterious action of oxygen.

A conceptual approach was considered when examining possible solutions to the hydrogen and porosity problems. The basic premise is that weld porosity is caused mainly by hydrogen and carbon monoxide. Controlling hydrogen-oxygen and carbon-oxygen equilibrium may result in control of H_2 and CO in the weld pool. This control can be accomplished by modification of the arc atmosphere which changes the partial pressures of H_2 and CO and alters the pick-up of these gases in the weld pool. This effect can be

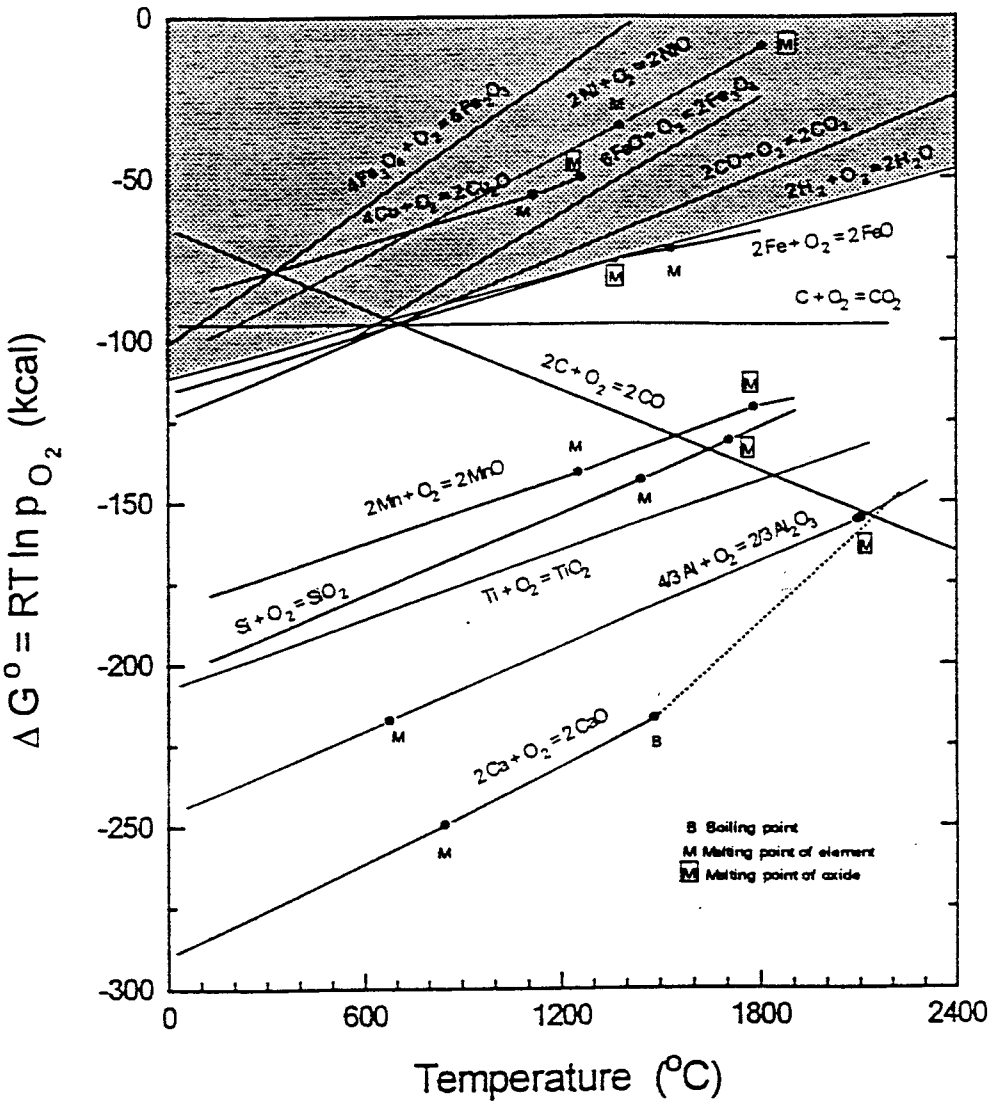

Figure 2.1 Free energy of formation of selected oxides as a function of temperature (10).

observed from the following equilibrium equations:

$$H_2O_{(g)} \Leftrightarrow 2\underline{H} + \underline{O} \quad \text{.....(2.1.1)}$$

$$CO_{(g)} \Leftrightarrow \underline{C} + \underline{O} \quad \text{.....(2.1.2)}$$

From these equilibrium mass reactions, it can seen that if the oxygen level is increased on the right side of the reactions, the reactions will be forced to proceed to the left, removing hydrogen and carbon from the weld pool.

Decreasing hydrogen levels through increased oxygen levels was proposed by Sorokin and Sidlin (11) in their work with alloying elements and marble in electrode coatings and their effects on pore formation. Their results can be seen in Figure 2.2. It clearly shows that as they increased the weld metal oxygen content, the weld metal diffusible hydrogen content decreased. This increase in oxygen was accomplished by introducing fluxes that dissociated in the arc.

The [H]-[O] relationship is something that can be looked at by examining some elementary thermodynamic equations as follows:

$$k = \frac{[H]^2[O]}{P_{H_2O}} \quad \text{.....(2.1.3)}$$

$$\Delta G^0 = 46180 + 1.57(T) \quad \text{.....(2.1.4)}$$

$$\exp\left(\frac{-\Delta G^0}{RT}\right) = k \quad \text{.....(2.1.5)}$$

ΔG^0 is the free energy of decomposition for water, and k is the equilibrium reaction

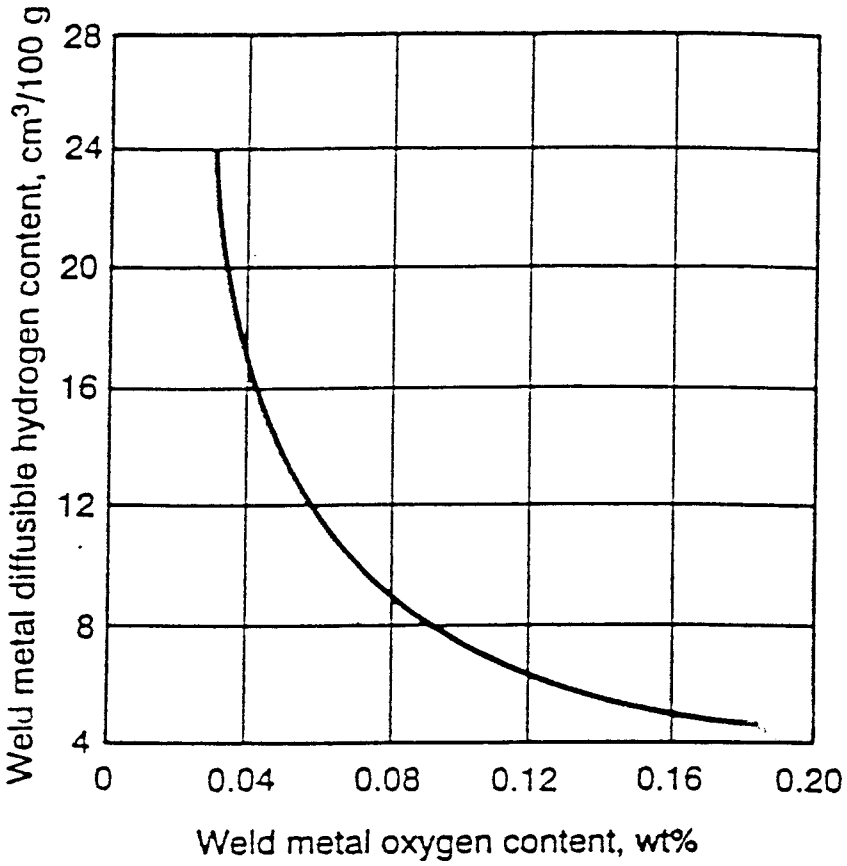

Figure 2.2 Plot of weld metal oxygen content as a function of weld metal hydrogen content when welding with electrodes that contain chromium and niobium in their coatings (11).

constant. Since the ΔG^0 is a function of temperature, the reactions can be calculated and plotted for several different temperatures as shown in Figure 2.3 (12). These curves were calculated for the atmospheric pressure at sea-level which is approximately one atm, and the partial pressure of water in a typical steel-making furnace of about 0.023 atm. According to thermodynamics, a decrease in hydrogen is obtainable with increases in oxygen. This relationship was also proven by Pope (4) examining underwater wet welds.

2.2 Hydrogen-Fluorine Relationship

If the oxygen level in the weld metal is increased too high, the mechanical properties are affected negatively due to the formation of large grain-boundary ferrite in the microstructure. This observation means that the oxygen levels can not be raised indiscriminately without a thought to the consequences. Another mechanism is needed to help lower the hydrogen. The mechanism is the hydrogen-fluorine relationship. This mechanism involves the same type of process as for the hydrogen-oxygen relationship. The reaction involved is the decomposition reaction for $HF_{(g)}$:

$$HF_{(g)} \Leftrightarrow [H] + [F] \quad \text{.....(2.2.1)}$$

From this equilibrium mass reaction, it can seen that if the fluorine level is increased on the right side of the reaction, the reaction will be forced to proceed to the left, removing hydrogen from the weld pool. The premise is the same with increasing the oxygen content

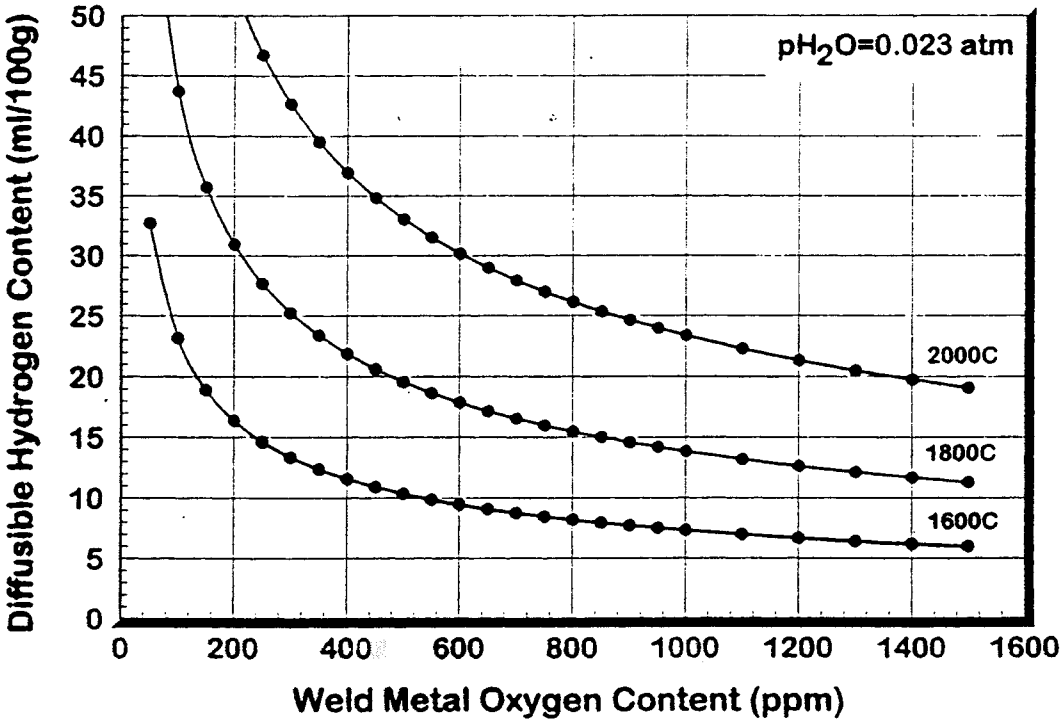

Figure 2.3 Weld metal hydrogen-oxygen equilibrium calculated using thermodynamic equations (12).

of the weld metal. If fluorine-containing fluxes are added to an electrode or placed upon a weld, this would provide fluorine to the weld pool to facilitate removal of hydrogen as does the addition of oxide fluxes. Now, in dealing with fluorine, there are some health concerns that must be dealt with at some point.

2.3 Shipbuilding

The problems involved in the fabrication of ships are different from those problems experienced by designers of buildings, bridges and other land-based structures. The amount of material used in fabrication of a ship is one of the greatest concerns. Any excess material over the minimum required for structural integrity, including a suitable margin for corrosion and wear, leads to an impaired carrying capacity and speed. There are several types of ships used in a number of environments. Some ships, such as a barge, are subjected to smooth water service and the hull stresses are simple and easy to calculate. An ocean-going ship is subjected to much higher stresses due to wind and waves as well as stresses caused by the cargoes being carried. The problem of economical structural design of such vessels is complex and solutions have evolved mainly due to trial and error with regard to scientific analysis and evaluation.

Most all modern ships are fabricated with all-welded construction. There is a trend in shipbuilding toward using higher strength steels with yield points ranging from 47 to 100 ksi (324 to 690 MPa) in the main hull. These steels are produced in many grades

having different strength levels and different chemical compositions. They can be furnished in several conditions (as-rolled, normalized, or quenched & tempered) depending on the grade of the steel, the thickness involved and the properties required. The welding of these higher strength steels is more exacting and complicated than in the case of welding ordinary carbon structural steels. Automation, computers and improved welding processes and consumables have led to improved shipbuilding practices.

2.3.1 Fabrication Materials

The shipbuilding industry has recognized the need for steels possessing both standard mechanical properties with suitable notch toughness and low hardenability in the heat-affected-zone. These requirements can be affected by imposing certain limitations on the composition and steelmaking practice. The notch toughness can also be affected by the thickness of the material. Thicker materials usually require a more notch-tough composition to maintain the toughness. The American Bureau of Shipping specifications for hull steel recognizes variations in notch toughness due to plate thickness by specifying various grades. The rules include specifications for high tensile steels of various strengths as seen in Tables 2.1 and 2.2.

Principal ABS requirements for ordinary strength hull structural steel

Grades	A	B	D	E	DS	CS
Deoxidation	Any method except rimmed steel for plates over 0.5 in. (12.5 mm)	Any method except rimmed steel	Fully killed fine-grain	Fully killed fine-grain	Fully killed fine-grain	Fully killed fine-grain
Chemical composition (ladle analysis)	For all grades exclusive of Grade A shapes and bars the carbon content + ¼ of the manganese content is not to exceed 0.40%. The upper limit of manganese may be exceeded up to a maximum of 1.65% provided this condition is satisfied.					
Carbon %	0.23 max[a]	0.21 max	0.21 max	0.18 max	0.16 max	0.16 max
Manganese %	2.5x carbon min for plates over 0.5 in. (12.5 mm)	0.80-1.10 0.60 min for fully killed or cold flanging	0.70-1.35 0.60 min for thickness 1.0 in. (25 mm) and under	0.70-1.35	1.00-1.35	1.00-1.35
Phosphorus %	0.04 max	0.04 max	0.04 max	0.04 max	0.04 max	0.04 max
Sulphur %	0.04 max	0.04 max	0.04 max	0.04 max	0.04 max	0.04 max
Silicon %	—	0.35 max	0.10-0.35	0.10-0.35	0.10-0.35	0.10-0.35
Heat treatment	—	—	Normalized over 1.375 in. (35 mm)	Normalized	Normalized over 1.375 in. (35 mm)	Normalized
Tensile strength	For all Grades: 58,000-71,000 psi (41-50 kg/mm): for Grade A shapes and bars 58,000-80,000 psi (41-56 kg/mm).					
Yield point, min.	For all Grades: 34,000 psi (24 kg/mm²); for Grade A over 1.0 in. (25.0 mm) in thickness 32,000 psi (23 kg/mm)					
Elongation, min.	For all Grades: 21% in 8 in. (200 mm) or 24% in 2 in. (50 mm) or 22% in 5.65 $\sqrt{A}$ (A equals cross-sectional area of test specimen).					
Impact test Charpy V-notch Temperature	—	32° F (0° C) over 1.0 in. (25 mm)	14° F (− 10° C)	−40° F (−40° C)	—	—
Energy avg. min. longitudinal specimens	—	20 ft-lb (2.8 kg-m)	20 ft-lb (2.8 kg-m)	20 ft-lb (2.8 kg-m)	—	—
or Transverse specimens		14 ft-lb (2.0 kg-m)	14 ft-lb (2.0 kg-m)	14 ft-lb (2.0 kg-m)		
No. of specimens	—	3 from each 50 tons	3 from each 50 tons	3 from each plate	—	—

Note: For complete requirements see ABS Rules for Building and Classing Steel Vessels.

(a) May be 5K up to 1.375 in. (35 mm) provided steel over 1 in. (25.5 mm) is normalized. Si and Al contents do not apply.

Table 2.1 Principal ABS requirements for ordinary hull structural steel (13).

Principal ABS requirements for higher strength hull structural steel for Grades AH32, DH32, EH32, AH36, DH36, and EH36

Grades	AH32	DH32	EH32	AH36	DH36	EH36
Deoxidation	Semikilled or killed	Killed, Fine grain practice	Killed, Fine grain practice	Semikilled or killed	Killed, Fine grain practice	Killed, Fine grain practice
Chemical composition for all grades (Ladle analysis)	Carbon, %	0.18 max	Nickel, %	0.40 max	These elements need not be reported on the mill sheet unless intentionally added.	
	Manganese, %	0.90-1.60	Chromium, %	0.25 max		
	Phosphorus, %	0.04 max	Molybdenum, %	0.08 max		
	Sulphur, %	0.04 max	Copper, %	0.35 max		
	Silicon, %	0.10-0.50	Columbium, % (Niobium)	0.05 max		
			Vanadium, %	0.10 max		
Heat treatment — normalized						
Aluminum treated	Over 2 in. (51 mm) thick	Over 1 in. (25.5 mm) thick	All thicknesses	Over 2 in. (51 mm) thick	Over 1 in. (25.5 mm) thick	All thicknesses
Columbium or Vanadium	same	Over 0.5 in. (12.5 mm) thick	same	same	Over 0.5 in. (12.5 mm) thick	same
Tensile strength		68,000-85,000 psi (48-60 kg/mm)			71,000-90,000 psi (50-68 kg/mm)	
Yield point or yield strength, min.		45,500 psi (32 kg/mm)			51,00 psi (36 kg/mm)	
Elongation, min. For all grades: 19% in 8 in. (200 mm), or 22% in 2 in. (50 mm), or 20% in 5.65 $\sqrt{A}$ (A equals area of test specimen)						
Impact test Charpy V-notch Temperature	32° F (0° C)	−4° F (−20° C)	−40° F (40° C)	32° F (0° C)	−4° F (−20° C)	−40° F (−40° C)
Energy, avg. min Longitudinal specimens	25 ft-lb (3.5 kg-m)	25 ft-lb (3.5 kg-m)	25 ft-lb (3.5 kg-m)	25 ft-lb (3.5 kg-m)	25 ft-lb (3.5 kg-m)	25 ft-lb (3.5 kg-m)
or Transverse specimens	17 ft-lb (2.4 kg-m)	17 ft-lb (2.4 kg-m)	17 ft-lb (2.4 kg-m)	17 ft-lb (2.4 kg-m)	17 ft-lb (2.4 kg-m)	17 ft-lb (2.4 kg-m)
No. of specimens	3 from each 50 tons	3 from each 50 tons	3 from each plate	3 from each 50 tons	3 from each 50 tons	3 from each plate

Note: For complete requ. ements, see ABS Rules for Building and Classing Steel Vessels.

Table 2.2 Principal ABS requirements for higher strength hull structural steel for Grades AH32, DH32, EH32, AH36, DH36, and EH36 (13).

Some commercially available high strength steels are being used in some merchant ship applications. They include as-rolled and normalized steels up to about 50 ksi (345 MPa) yield strength, and quenched and tempered steels up to about 100 ksi (690 MPa) yield strength. The shipyards must take care in selecting such steels to ensure both suitable mechanical properties and adequate weldability. The U.S. Navy Specification MIL-S-22698A (Steel Plate, Carbon, Structural, for Ships) is in agreement with the ABS specifications for ordinary strength hull structural steel. Both specifications contain requirements for normalizing heat treatment to refine the grains and enhance the low-temperature notch toughness for heavier thicknesses. The U.S. Navy Specification for a high-tensile strength steel is MIL-S-16113C, grade HT (14). This is a carbon steel with a UTS of 85 to 92 ksi (586 to 634 MPa) depending on thickness, minimum YS of 42 to 50 ksi (290 to 345 MPa), and an elongation of 20 percent in 8 inches.

An improved HT steel is the HT Type II with lower sulfur and phosphorus contents and a range of vanadium. It is also included in the specification above. The Type II does require ultrasonic testing for quality assurance and is designed for critical applications, such as submarine construction. There are several strength levels of quenched and tempered steels from 50 to 100 ksi (345 to 690 MPa) yield strength that are included in the Naval Material Procurement Specification. Experimental work is being done to develop materials which will possess yield strengths approaching 130 to 150 ksi (896 to 1034 MPa) for weldments of high toughness in the near future.

The U.S. Navy Specification MIL-S-24113 (Ships) covers carbon-manganese steel plates heat treated by quenching and tempering (QT-50). This specification controls the residual elements and has the properties listed for differing plate thicknesses. The specification also contains a normalized grade similar to ASTM A-537. A couple of popular materials used in critical applications such as submarine hulls and in certain areas of naval surface ships are HY-80 and HY-100 steels. These are quenched and tempered, high yield strength, low-alloy materials covered by MIL-S-16216F. The chemical and mechanical properties for these steels are shown in Table 2.3.

2.3.2 Welding Materials

Because shipbuilding involves many materials and processes, great care must be taken to ensure that the proper process is chosen for each material. The normal high-tensile carbon steels (45 to 60 ksi, or 310 to 414 MPa yield strength) are welded using procedures similar to those used for mild steel. Low hydrogen electrodes should be used for welding the higher strength carbon steels, and may be used without preheat except when welding thick plates, restrained structures, or during cold weather. When welding low-alloy quenched and tempered steels having yield strengths of 80 to 100 ksi (552 to 690 MPa), special precautions must be taken such as the use of low hydrogen electrodes to avoid hydrogen cracking problems. Since preheating is required (100 to 300^0F, or 38 to 149^0C maximum) and since high heat inputs are harmful, welding must be done

Chemical composition (ladle analysis)

Element	Percent, maximum, unless a range is shown	
	HY-80	HY-100
Carbon	0.18	0.20
Manganese	0.10–0.40	0.10–0.40
Phosphorus	0.025	0.025
Sulfur	0.025	0.025
Silicon	0.15–0.35	0.15–0.35
Nickel	2.00–3.25	2.25–3.50
Chromium	1.00–1.80	1.00–1.80
Molybdenum	0.20–0.60	0.20–0.60

Residual elements	Maximum percent permitted	
	HY-80	HY-100
Titanium	0.02	0.02
Vanadium	0.03	0.03
Copper	0.25	0.25

[1] Add 0.02% to the maximum for plate 6 in. thick and over.
[2] The percent of phosphorus and sulfur together should not be more than 0.045.

Mechanical properties

	HY-80	HY-100
Ultimate tensile strength, psi	[1]	[1]
Yield strength, 0.2% offset, psi	80,000 to 95,000	100,000 to 115,000
Elongation in 2 in., min %, Type F2 specimen	...	...
Elongation in 2 in., min %, Type R1 specimen	20	18
Reduction in area, min %, Type R1 specimen		
Longitudinal	55	50
Transverse	50	45

[1] To be recorded for information only.

Impact requirements, Charpy V-Notch

Plate thickness (in.) nominal	Specimen size, millimeters	Ft-lb Average of three tests, min	Test (coolant) temperature, degrees F
Up to 1/2 excl.	10 x 5 (1/2 size)	..	−120 + 3
1/2 to 2, incl.	10 x 10	50	−120 + 3
over 2	10 x 10	30	−120 + 3

Table 2.3 Chemical and mechanical properties of HY-80 and HY-100 steels (15).

with small electrodes with control of the minimum and maximum interpass temperatures. The U.S. Navy specifies 55 kJ/in maximum heat input with a minimum preheat of 200^{0}F (93^{0}C) and a maximum interpass temperature of 300^{0}F (149^{0}C) for welding HY-80 or HY-100 steels in thicknesses above 1-1/8 inches (15). These requirements make a high heat input process, like SAW, undesirable unless the heat input is carefully controlled.

In areas of concern, it is suggested that tempering beads should be used and that fillet welds be slightly concave (13). The tempering beads are quite effective in lowering the HAZ hardness, which reduces the possibility of cracking at the toe of the intermediate passes as well as the finish passes. Stress relieving is generally not performed on low-alloy steels. When welding is done with certain classes of electrodes, stress relieving is strictly prohibited. This situation requires that structural design minimize the level of hot forming followed by reheat-treatment that would be required. This situation affects what type of an electrode may be used for a particular base plate. Table 2.4 shows applicable filler metals for base plate combinations.

An electrode is selected so that the deposited weld metal will match the base plate in strength. However, this practice may not always be necessary since lower strength welds are used in some areas while still providing adequate strength. Lower strength welds may have less tendency to crack. When welding low-alloy steels to mild steel, low hydrogen electrodes suitable for the alloy steels should be used. It may only be necessary to match the mechanical properties of the lower strength mild steel. Generally, it is

Applicable filler metal (ABS grade and AWS classification)—base plate combinations

Filler metal properties	Ordinary strength			Higher strength		
Tensile strength (psi) (a) Yield point, min (psi) Elongation in (2 in.), min %	58,300-81,100 (406-567 MPa) 44,100 (308 MPa) 22			71,000-95,000 (497 MPa) 54,000 (378 MPa) 20		
ABS filler metal grade	1 (b)	2 (b)	3 (b)	1Y (b)	2Y (b)	3Y (b)
Charpy V- impacts ft-lb @ °C Manual and semiautomatic Automatic	35 @ 20 25 @ 20	35 @ 0 25 @ 0	35 @ −20 25 @ −20	20 @ 0 20 @ 10	20 @ −20 20 @ −10	20 @ −40 20 @ −30
Equivalent AWS classification Covered electrodes (SMAW)	E6010, E6011, E6027, E7015, E7016, E7018, E7027, E7048 E7028			E7015, E7016, E7028, E7018 E7048, E8016, C3, E8018-C3		E8016-C3 E8018-C3
Wire-flux (SAW)	F6X2, F6X4, F6X6, F7X2, F7X4, F7X6 F6X0 F7X0			F7X4, F7X6, F8X4 F7X0, F7X2, F8X0, F8X2		
Wire-gas (GMAW)	ER70S-2, ER70S-6, ER70S-7, ER70S-3			ER80S-Ni1, E80C-Ni1 ER70S-2, ER70S-3, ER70S-6, ER70S-7, ER80S-D2		
Flux-cored (FCAW)	E6XT-5, E6XT-6, E6XT-8, E7XT-6, E7XT-8 E6XT-1, E7XT-1			E7XT-1, E7XT-5, E7XT-6, E7XT-8		
Applicable ABS Base plate Material grades	A to ½ in. (12.5 mm) inclusive A over ½ in. (2.5 mm) B, D, DS		DN, C5, E	AH to ½ in. (12.5 mm) inclusive AH over ½ in. (12.5 mm)		EH

Suitable for grades 1, 2, or 1Y, 2Y as indicated.
Suitable for grades 1, 2, 3, or 1Y, 2Y, 3Y as indicated.
(a) (psi x 7) ÷ 1000 = MPa
(MPa x 1000) ÷ 7 = psi
(b) Ref: ABS publication: "Rules for Welding Electrodes, Wire Flux and Wire Gas Combinations."

Table 2.4 Applicable filler metal (ABS grade and AWS classification) - base plate combinations (13).

strongly advised that the recommendations of both the steel and electrode manufacturers be followed when welding any higher strength steels or by following established procedures.

The filler metals are qualified for use by the Navy in a Navy-approved laboratory (15). The U.S. Navy also issues lists of qualified filler metals which is done by the Naval Ships Engineering Center. Filler metals for welding on ships classed by the American Bureau of Shipping are qualified by demonstration from the electrode manufacturer, in the presence of an ABS Surveyor. ABS also publishes lists of approved filler metals annually. The U.S. Coast Guard accepts filler metals approved by the ABS without further testing.

There are different grades of filler metals used for various applications in hull construction of low and high strength steels. As mentioned earlier, filler metals are selected to produce welds with strength and toughness comparable to the base plate. Low-hydrogen manual electrodes are usually selected for all higher strength steel, thick section, restrained condition, and crack susceptible welding. There are also electrodes that possess low elongation, as compared to other electrodes of the same strength level. Because of their low ductility, they are not used for joints in shell plating, strength decks, tank tops, bulkheads and longitudinal members of large vessels. They are also not used for welding on galvanized material since their penetration qualities are low.

The U.S. Navy provides an electrode specification, MIL-E-22200/1 with the following classifications and intended uses:

- Type MIL-7018 for welding of medium carbon steels, such as classes A, B and C of Spec. MIL-S-22698, and grade HT (under 5/8 in. thickness) of Spec. MIL-S-16113
- Type MIL-8018 for welding of grade HT (5/8 in. and thicker) plate of Spec. MIL-S-16113 and QT50 of Spec. MIL-S-24113
- Types MIL-9018, -10018 and -11018 for welding of low-alloy high yield strength steel, such as grade HY-80 of Spec. MIL-S-16216
- Types MIL-11018 and -12018 for welding high yield, low-alloy steel, such as grade HY-100 of Spec. MIL-S-16216

All of these electrodes are for SMAW. There are also electrodes for GMAW, FCAW, SAW, ESW and EGW. Due to the diversity of materials joined by these processes, an extensive selection of filler metal chemistries is available. In cases where it is desirable to use a material before it is granted specification coverage, approval can be granted by the U.S. Navy, ABS or U.S. Coast Guard on an individual basis. Presentation of experimental data on tests made by the fabricator is usually required to support such requests.

Filler metals used in shipbuilding are described by a variety of specifications issued by AWS, U.S. Navy and ABS. The following are the specifications most commonly used for ship fabrication (13,15):

American Welding Society

- A5.1 - Covered Carbon Steel Arc Welding Electrodes
- A5.5 - Low Alloy Steel Covered Arc Welding Electrodes
- A5.17 - Carbon Steel Electrodes and Fluxes for Submerged Arc Welding
- A5.18 - Carbon Steel Filler Metals for Gas Shielded Arc Welding
- A5.20 - Carbon Steel Electrodes for Flux Cored Welding
- A5.23 - Low Alloy Steel Electrodes and Fluxes for Submerged Arc Welding
- A5.25 - Consumables Used for Electroslag Welding of Carbon and High Strength Low Alloy Steels
- A5.26 - Consumables Used for Electroslag Welding of Carbon and High Strength Low Alloy Steels
- A5.28 - Low Alloy Steel Filler Metal for Gas Shielded Arc Welding

- A5.29 - Low Alloy Steel Electrodes for Flux Cored Arc Welding

U.S. Navy

- MIL-E-15599 - Electrodes, Welding, Covered, Low-Medium Carbon Steel
- MIL-F-18251 - Fluxes, Welding, Submerged Arc Process, Carbon and Low Alloy Steel
- MIL-F-19922 - Fluxes, Welding, Submerged Arc Process, Carbon and Low Alloy Steel
- MIL-E-19822 - Electrodes, Welding, Bare High Yield Steel
- MIL-E-22200/1 - Electrodes, Welding Mineral Covered, Iron Powder, Low Hydrogen Medium and High Tensile Steel
- MIL-E-22200/6 - Electrodes, Welding Mineral Covered, Low Hydrogen, Medium and High Tensile Steel
- MIL-E-22749 - Electrodes (Bare) and Fluxes (Granular) Submerged Arc Welding, High Yield Low Alloy Steels
- MIL-E23765 - Electrodes and Rods-Welding Bare, Solid, Mild Steel

American Bureau of Shipping

- Rules for Approval of Electrodes for Manual Arc Welding in Hull Construction
- Provisional Rules for the Approval of Filler Metals for Welding Higher Strength Steels
- Rules for Approval of Wire-Flux Combinations for Submerged Arc Welding
- Provisional Rules for the Approval of Wire-Gas Combinations for Gas Metal Arc Welding

As was previously mentioned, electrode coverings are highly hygroscopic and require the need for careful packaging, storage and handling. This situation is the case for filler metal compositions designed to deposit high-strength weld metal when using high strength materials. Since the presence of small amounts of hydrogen in high-strength weldments can lead to cracking in the weld and HAZ, it is mandatory that precautions are taken to prevent moisture pick-up such as detection of damaged packaging and proper baking temperatures. The moisture contents of type E70XX, E80XX and E90XX to

E120XX electrodes can be kept to a minimum by baking the electrodes at temperatures as high as 800^{0}F (427^{0}C) prior to use and holding in ovens at 275 to 300^{0}F (135 to 149^{0}C) until used (15). The 800^{0}F (427^{0}C) temperature can sometimes cause damage to the coating, so baking procedures should be checked with the electrode manufacturer. This potential damage is also the case with granular fluxes used in SA welding and for FCA welding electrodes.

2.4 Primers and Coatings

Coatings are used to protect various structures during fabrication or in service to lengthen the life of the product. The coatings include everything from paints to hot-dip galvanizing. Table 2.5 shows how coatings can protect steel from various corrosive environments. These systems can be expressed in economic terms and calculated in terms of: 1) energy savings, 2) reduced down time, 3) increased life-time, 4) capital savings, and 5) materials substitution (51). Very often, these coatings must be able to protect the steel structures for several months while they are subjected to the environment and until they are used in construction. There are high-performance coatings such as epoxys, polyesters, polyurethanes, vinyl or chlorinated rubbers which help to satisfy the need for corrosion prevention. An uncoated ship in seawater would suffer severe corrosion in five years or less and an adequately coated ship might avoid serious repair for 15 to 25 years (16). Special primers can also be used to provide passivation, galvanic protection, corrosion

Preventive method	Atmosphere	Soil	Freshwater	Seawater	Steam systems	Acids and pickling baths
Metal coatings: electroplating, galvanizing	Galvanizing very effective; plating with other metals used for both decorative appearance and corrosion protection	Galvanized steel widely used in drainage pipe and storm sewers	Galvanizing used in potable water	Not recommended	Not recommended	Not recommended
Painting: chemical treatment, priming, and painting	Economical and effective corrosion prevention	Seldom used	Fairly effective	Special paint systems used	Not recommended	Not recommended
Cathodic protection	Not recommended	Most economical and effective method, especially with organic coatings other than paint	Fairly effective with organic coatings	Very effective	Not recommended	Effective under special conditions
Inhibitors: liquid and vapor	Effective in closed areas	Not recommended	Effective in some applications, especially cooling waters	Fairly effective in some applications	Very effective	Very effective
Alloying additions to steel	Very effective, especially copper-bearing and HSLA steels	Not effective	Not effective	Only effective with much alloying	Chromium-molybdenum steels are very effective	Only effective with much alloying
Removal of oxygen from environment	Not applicable	Not recommended	Seldom used	Very effective, especially in desalination and hot seawater	Very effective	Not recommended
Removal of more noble metals; elimination of galvanic couples	Usually not necessary	Fairly effective	Effective	Necessary	Advisable	Not effective
Organic coatings other than paint	Sometimes used to replace painting	Used to advantage with cathodic protection	Fairly effective with cathodic protection	Used to advantage with cathodic protection	Not recommended	Have been used

Table 2.5 Guide to corrosion prevention for carbon steels in various environments (17).

inhibition, or mechanical or electrical barriers to corrosive action. When welding is performed over some of the so-called "weldable primers", significant amounts of gases are produced which can lead to porosity and weld cracking. As indicated, the correct paint system must be carefully chosen to satisfy all requirements of protection and mechanical properties of the weldment.

Most of these coatings have a binder or film former which is dissolved or dispersed in water or a solvent. Table 2.6 shows some characteristics of solvent classes. This film-forming liquid is the vehicle in which pigments are dispersed to give the film its desired properties. There can be many other ingredients added to the vehicle to achieve special film properties. These ingredients include such things as driers to aid curing, plasticizers to give flexibility, and stabilizers to lessen the harmful effects of heat or sunlight. Table 2.7 provides relative rankings for various coatings. The need for good painting systems has become an ever increasing challenge due to the total national yearly costs of metallic corrosion in the United States, which in 1985 was estimated to be around $167 billion (17). Restrictions dealing with volatile organic compounds have been gradually enacted over the last twenty years to allow formulators to develop comparable paint materials with complying solvents. The Environmental Protection Agency (EPA) has limited the amount of volatile organic compounds that can be emitted from painting facilities. To protect the applicators, the use of active pigments in primers, such as lead compounds and chromates, has been limited by the Occupational Safety and Health Administration (OSHA). It was

Class	Solvent name	Strength/solvency	Polarity	Specific gravity	Boiling range (°F)	Flash point of TCC	Evaporation rate[a]
Aliphatic	VM&P naphtha	Low (32 KB)[b]	Nonpolar	0.74	246-273	52	24.5
	Mineral spirits	Low (28 KB)	Nonpolar	0.76	351-395	128	9.0
Aromatic	Toluene	High (105 KB)[c]	Intermediate polarity	0.87	230-233	45	4.5
	Xylene	High (98 KB)	Intermediate polarity	0.87	280-288	80	9.5
	High solvency	High (90 KB)	Intermediate polarity	0.87	360-400	140	11.6
Ketone	Methyl ethyl ketone (MEK)	Strong	High polarity	0.81	172-176	24	2.7
	Methyl isobutyl ketone (MIBK)	Strong	High polarity	0.80	252-266	67	9.4
	Cyclohexanone	Strong	High polarity	0.95	313-316	112	4.1
Ester	Ethyl acetate	Intermediate	Intermediate polarity	0.90	168-172	26	2.7
Alcohol	Ethanol	Weak	Intermediate polarity	0.79	167-178	50	6.8
Unsaturated aromatic	Styrene	Strong	Intermediate polarity	0.90			
Glycol ethers	Cellosolve	Strong	High polarity	0.93	273-277	110	0.3
	Butyl cellosolve	Strong	High polarity	0.90	336-343	137	0.06

[a]Butyl acetate equals 1.
[b]KB, Kauri-Butanol; a measure of solvent power of petroleum thinners (milliliters of thinner required to produce cloudiness when added to 20 g of a solution of karigum in butyl alcohol).
[c]TCC-TAE closed cup.

Table 2.6 Characteristics of solvent classes (18).

Category key: A, hardness; B, flexibility; C, humidity resistance; D, corrosion resistance to industrial atmospheres; E, salt spray; F, exterior durability, pigmented film; G, exterior durability, clear film; H, paint cure temperature, in °F; I, cost guide. Ratings key: 1, excellent; 2, good; 3, fair; 4, poor; H, high cost; M, moderate cost; L, low cost

Type	A	B	C	D	E	F	G	H	I
Silicone acrylic	1	3	2	2	2	2	1	450	H
Thermoset acrylic	2	2	1	2	1	2	2	430	M
Amine-alkyd	2	3	2	2	3	2	3	340	L
Silicone alkyd	2	3	2	2	2	1	2	420	H
Vinyl-alkyd	2	2	1	2	2	3	3	340	M
Straight epoxy	1	2	1	1	1	4	4	400	H
Epoxy-ester	2	2	1	2	1	4	4	400	M
Organosol	2	1	1	1	1	2	3	350	L
Plastisol	3	1	1	1	1	2	3	350	L
Polyester (oil-free)	1	2	1	2	1	2	3	400	M
Silicone polyester	2	2	1	2	1	1	2	450	H
Poly-vinyl fluoride	2	1	1	1	1	1	1	450	H
Poly-vinyl idene fluoride	2	1	1	1	1	1	1	450	H
Solution vinyl	2	1	1	2	1	2	3	300	M

Table 2.7 Relative rankings of various coating in different performance categories (17).

found that nearly all volatilizing solvents photochemically degrade and were therefore environmentally harmful. This realization, together with the potential for further legislative restriction, has motivated coating formulators to develop water-base paints or high-solids (low-solvent) coating materials.

Paints or organic coatings usually contain three components (18). These components consist of the "volatile vehicle" (solvent or dispersant), the "non-volatile vehicle" (resin), and the pigment. The volatile vehicle is the component that allows application of the coating or spreading. These volatile vehicles may consist of ketone, ester alcohol, petroleum solvent, water, or a combination of these materials. Table 2.6 gives some the characteristics of these solvent classes. The pigment component provides color, opacity, and viscosity control as well as reduced water permeability. Pigments can also provide some corrosion resistance. The following materials are considered pigments: driers, plasticizers, ultraviolet light absorbers, emulsifiers, and dispersing agents. Different combinations are added to modify coating properties.

Several different kinds of resins are used to prepare the coatings. These resins include auto-oxidative cross-linked resins (alkyds, alkyd modification, and epoxy esters); thermoplastic resins (vinyls, chlorinated rubber, acrylics, coal tar, and asphalts); cross-linked thermosetting coatings (epoxies, phenolics, and urethanes); and zinc-rich coatings (17). The advantages and disadvantages for many of the resins can be seen in Table 2.8. The resin or organic binder of the coating material is probably the most consequential in

Resin type	Advantages	Limitations	Comments
Asphalt pitch	Good water resistance and ultraviolet stability. Will not crack or degrade in sunlight. Nontoxic and suitable for exposure to food products. Resistant to mineral salts and alkalies to 30% concentration	Black color only. Poor resistance to hydrocarbon solvents, oils, fats, and some organic solvents. Do not have the moisture resistance of coal tars. Can embrittle after prolonged exposure to dry environments or temperatures above 150 °C (300 °F), and can soften and flow at temperatures as low as 40 °C (100 °F)	Often used as relatively inexpensive coating in atmospheric service, where coal tars cannot be used. Relatively inexpensive. Most common use is as a pavement sealer or roof coating.
Water emulsion latex	Resistant to water, mild chemical fumes, and weathering. Good alkali resistance. Latexes are compatible with most generic coating types, either as an undercoat or topcoat.	Must be stored above freezing. Does not penetrate chalky surfaces. Exterior weather and chemical resistance not as good as solvent or oil-base coatings. Not suitable for immersion service	Ease of application and cleanup. No toxic solvents. Good concrete and masonry sealers because breathing film allows passage of water vapor. Used as interior and exterior coatings
Acrylics	Excellent light and ultraviolet stability, gloss, and color retention. Good chemical resistance and excellent atmospheric weathering resistance. Resistant to chemical fumes and occasional mild chemical splash and spillage. Minimal chalking, little if any darkening upon prolonged exposure to ultraviolet light	Thermoplastic and water emulsion acrylics not suitable for any immersion service or any substantial acid or alkaline chemical exposure. Most acrylic coatings are used as topcoats in atmospheric service. Acrylic emulsions have limitations described under "Water emulsion latex."	Used predominantly where light stability, gloss, and color retention are of primary importance. With cross linking, greater chemical resistance can be achieved. Crosslinked acrylics are the most common automotive finish. Emulsion acrylics are often used as primers on concrete block and masonry surfaces
Amine-cured epoxies	Excellent resistance to alkalies, most organic and inorganic acids, water, and aqueous salt solutions. Solvent resistance and resistance to oxidizing agents are good as long as not continually wetted. Amine adducts have slightly less chemical and moisture resistance.	Harder and less flexible than other epoxies and intolerant of moisture during application. Coating will chalk on exposure to ultraviolet light. Strong solvents may lift coatings. Temperature resistance: 105 °C (225 °F) wet; 90 °C (190 °F) dry. Will not cure below 5 °C (40 °F); should be topcoated within 72 h to avoid intercoat delamination. Maximum properties require curing time of about 7 days.	Good chemical and weather resistance. Best chemical resistance of epoxy family. Excellent adhesion to steel and concrete. Widely used in maintenance coatings and tank linings
Phenolics	Greatest solvent resistance of all organic coatings described. Excellent resistance to aliphatic and aromatic hydrocarbons, alcohols, esters, ethers, ketones, and chlorinated solvents. Wet temperature resistance to 95 °C (200 °F). Odorless, tasteless, and nontoxic; suitable for food use	Must be baked at a metal temperature ranging from 175 to 250 °C (350 to 450 °F). Coating must be applied in a thin film (approximately 0.025 mm, or 1 mil) and partially baked between coats. Multiple thin coats are necessary to allow water from the condensation reaction to be removed. Cured coating is difficult to patch due to extreme solvent resistance. Poor resistance to alkalies and strong oxidants	A brown color results upon baking, which can be used to indicate the degree of cross linking. Widely used as tank lining for alcohol storage and fermentation and other food products. Used for hot water immersion service. Can be modified with epoxies and other resins to enhance water, chemical, and heat resistance
Organic zinc-rich	Galvanic protection afforded by the zinc content, with chemical and moisture resistance similar to that of the organic binder. Should be topcoated in chemical environments with a pH outside the range 5–10. More tolerant of surface preparation and topcoating than inorganic zinc-rich coatings	Generally have lower service performance than inorganic zinc-rich coatings, but ease of application and surface preparation tolerance make them increasingly popular	Widely used in Europe and the Far East, while inorganic zinc-rich coatings are most common in North America. Organic binder can be closely tailored to topcoats (for example, epoxy topcoats over epoxy-zinc-rich coatings) for a more compatible system. Organic zinc-rich coatings are often used to repair galvanized or inorganic zinc-rich coatings.
Inorganic zinc-rich	Provides excellent long-term protection against pitting in neutral and near-neutral atmospheric, and some immersion, services. Abrasion resistance is excellent, and dry heat resistance exceeds 370 °C (700 °F). Water-base inorganic silicates are available for confined spaces and VOC compliance.	Inorganic nature necessitates thorough blast-cleaning surface preparation and results in difficulty when topcoating with organic topcoats. Zinc dust is reactive outside the pH range of 5–10, and topcoating is necessary in chemical fume environments. Somewhat difficult to apply; may mudcrack at thicknesses in excess of 0.13 mm (5 mils)	Ethyl silicate zinc-rich coatings require atmospheric moisture to cure and are the most common type. Widely used as a primer on bridges, offshore structures, and steel in the building and chemical-processing industries. Used as a weldable preconstruction primer in the automotive and shipbuilding industries. Use eliminates pitting corrosion.
Alkyds	Good resistance to atmospheric weathering and moderate chemical fumes; not resistant to chemical splash and spillage. Long oil alkyds have good penetration but are slow drying; short oil alkyds are fast drying. Temperature resistant to 105 °C (225 °F)	Not chemically resistant; not suitable for application over alkaline surfaces, such as fresh concrete or for water immersion	Long oil alkyds make excellent primers for rusted and pitted steel and wooden surfaces. Corrosion resistance is adequate for mild chemical fumes that predominate in many industrial areas. Used as interior and exterior industrial and marine finishes
Epoxy esters	Good weather resistance; chemical resistance better than alkyds and usually sufficient to resist normal atmospheric corrosive attack	Generally the least resistant epoxy resin. Not resistant to strong chemical fumes, splash, or spillage. Temperature resistance: 105 °C (225 °F) in dry atmospheres. Not suitable for immersion service	A high-quality oil-base coating with good compatibility with most other coating types. Easy to apply. Used widely for atmospheric resistance in chemical environments on structural steel, tank exteriors, etc.
Vinyls	Insoluble in oils, greases, aliphatic hydrocarbons, and alcohols. Resistant to water and salt solutions. Not attacked at room temperature by inorganic acids and alkalis. Fire resistant; good abrasion resistance	Strong polar solvents redissolve the vinyl. Initial adhesion poor. Relatively low thickness (0.04 to 0.05 mm, or 1.5 to 2 mils) per coat. Some types will not adhere to bare steel without primer. Pinholes in dried film are more prevalent than in other coating types.	Tough and flexible, low toxicity, tasteless, colorless, fire resistant. Used in potable water tanks and sanitary equipment; widely used industrial coating. May not comply with VOC regulations

Table 2.8 Advantages and limitations of principal coating resins (17).

determining the overall resistance and properties of the coating. As stated earlier, the type and amount of pigments, solvents, and additives such as rheological aids will dramatically influence the application properties and protective capability of the applied film (16).

2.4.1 Auto-oxidative, Cross-linked Resins

Auto-oxidative cross-linked resins dry and cross link through a reaction of oxygen with the atmosphere (17). Coatings that consist of these types of resins contain drying oils, which consist mainly of polyunsaturated fatty acids. They undergo film formation by oxidative drying. The auto-oxidative reaction happens quite rapidly after application of the wet paint, and it continues throughout the life of the coating, although at a much slower rate with time. This auto-oxidative reaction is one of decomposition that results in the formation of hydroperoxides. The cross linking allows the film to attain the ultimate resistant properties. Within weeks after application, the hydroperoxides decompose into organic acid components and the film begins to deteriorate. The reaction also causes hardening and embrittlement of the film which leads to a loss of flexibility and distensibility with the passage of time. The rate at which the coating loses its protectiveness is determined by temperature, thickness, solar exposure, and pigmentation type. Zinc oxide and lead-containing pigments are useful in absorbing the hydroperoxides and slowing the rate of film deterioration.

As previously mentioned, these cross-linked films always contain some sort of drying oil. This drying oil could be a vegetable oil, castor, linseed, safflower, soybean, and tall oil or fish oil. The drying oil is mixed with a resin (alkyd, epoxy ester, or polyurethane) by heating or cooking. Figure 2.4 shows the molecular structure of a linseed oil alkyd. The resin adds toughness and chemical resistance to the oil, increasing its chemical and moisture resistance. The protective capability of the resulting film is influenced by the amount of oil combined with the resin. Most commonly, alkyds, epoxy esters, and urethane resins are used in conjunction with the drying oils to form the auto-oxidatively cross-linked coatings.

Alkyd resins are derived as the reaction product of polyhydric alcohols and polybasic acids, which also includes polyester resins (17). The main difference between an alkyd and a polyester is that the alkyd uses a polybasic acid derived from semidrying or drying oils. The resin formed can then undergo auto-oxidation at ambient temperatures through reaction with atmospheric oxygen at the unsaturated groups present in the fatty acid molecules. The curing reaction of a polyester resin is a free radical initiated cross-linking. This condition is why polyesters are referred to as chemically cross-linked coating systems. The properties of alkyd coatings are mainly derived from the properties of the drying oil used during manufacture. Drying time, hardness, color, and moisture sensitivity all depend to a great extent on the drying oil used and its type and degree of unsaturation (available cross-linking sites).

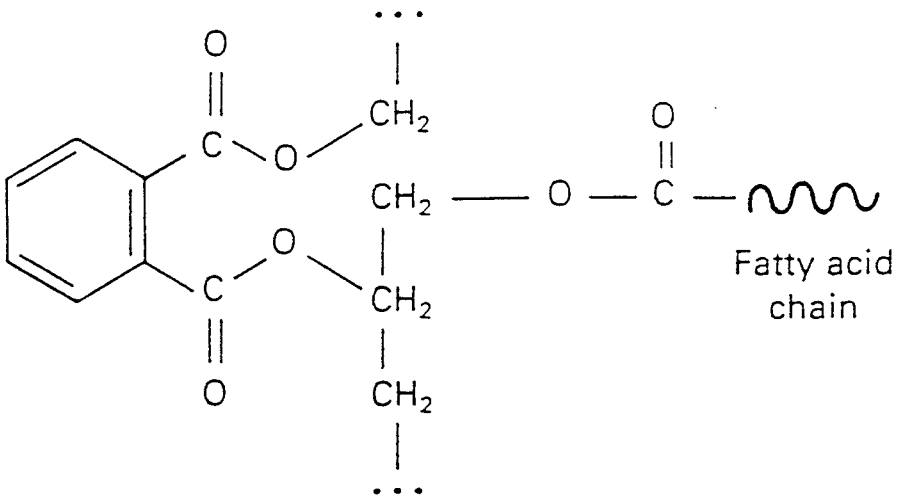

Figure 2.4 Molecular structure of a linseed oil alkyd obtained from the reaction of a linseed oil monoglyceride and phthalic anhydride (17).

Alkyds can also be modified with a variety of other different resins to improve specific properties, such as drying time, color retention, and moisture and chemical resistance. If you modify an alkyd with a chlorinated rubber resin, the result is a resin with improved toughness and adhesion as well as an increase in acid, alkali, and water resistance. These types of coatings are used on concrete floors and as highway-marking paints. A phenolic resin will improve gloss retention and water and alkali resistance. Phenolic-alkyd resins have performed quite well in water immersion. However, non-phenolic modified alkyd resins are not suitable for this type of service. Alkyd-vinyl resins are commonly formulated as universal primers upon which topcoats may be placed. The alkyd part of the alkyd-vinyl resin improves adhesion, film build, solvent resistance, and thermal resistance. The vinyl modification improves recoatability, and chemical and moisture resistance. Alkyd-silicone resins are perhaps the most widely promoted modification for corrosion-protective coatings. Adding up to thirty percent silicone to the alkyd resin provides polymers with greatly improved durability, gloss retention, and heat resistance (17). Moisture resistance is also greatly improved with the silicone modification which makes it suitable for marine and maintenance paints. Alkyds can also be modified with polyisocyanates to improve drying rates and chemical and abrasion resistance. These chemicals are referred to as uralkyds and are available in a variety of colors and usually exhibit excellent gloss and color retention. Similarly, epoxy-alkyd resins have improved

adhesion to metal, better gloss and color retention, and much improved water and chemical resistance.

Epoxy esters differ from epoxy-modified alkyds in that the epoxy is a direct reaction product of an epoxy resin and a fatty acid. Epoxy esters resins are like alkyds in that they are usually prepared by reacting the drying oil with the epoxy resin at a temperature of about 220 to 290^{0}C (425 to 550^{0}F) in the presence of esterification catalysts (17). The same drying oils used to prepare the alkyd resins are also used to prepare the epoxy esters. Generally, the epoxy resins, when compared to the alkyds, have better adhesion and moisture and chemical resistance, although they are slightly more expensive.

2.4.2 Thermoplastic Resins

Thermoplastic resins are characterized by a softening at elevated temperatures. The molecular structure of the thermoplastic paint system is not cross linked into a rigid molecule, as are the chemically cross-linked or the auto-oxidized coating systems (17). The resinous binder is dissolved in a suitable solvent, mixed with pigment and other constituents making up the paint, and packaged. The solvent will volatilize when applied, and the resinous binder and pigment are deposited onto the substrate as a solid film. These resins have a large, linear, molecular structure which provides a layering effect when coiled or tangled (16). This layering effect, along with the pigmentation and

sufficient thickness, provides the characteristic moisture and chemical resistance of the resin system used.

For corrosion protection, the most useful thermoplasic resins are the vinyls, chlorinated rubbers, thermoplastic acrylics, and bituminous resins (coal tar and asphalt). Like all other resins, each one has its own special properties. However, since no chemical change takes place to the resin upon application and drying, it is reasonable to assume that the applied coating will redissolve if it is exposed to the same solvents it was originally dissolved in. This situation causes the coatings in which these resins reside to have no resistance to the solvents in which they were originally dissolved, or in solvents of equal or greater solvency for that particular resin. Although the resistance to solvents may be poor, such coatings are rarely exposed to a solvent-laden atmosphere. They are usually asked to resist weathering, acid, or alkali exposures, and moisture. On the other hand, the solvent susceptibility of these thermoplastic coatings can be an advantage. When maintenance repainting is required, the same system can be reapplied, and the solvents in the new topcoat can partially redissolve the existing old coat. This practice results in intermolecular entanglement of the new coating with the old and giving excellent adhesion (17). This entanglement behavior is one advantage of using a thermoplastic resin as compared to either the auto-oxidative cross-linking coatings or the chemically cured coatings. Also, the characteristics of the thermoplastic resins are derived mainly from their molecular structure.

Coatings with vinyls are applied as a solvent-deposited solution. It may consist of either a polyvinyl chloride-polyvinyl acetate (PVC-PVA) copolymer. Figure 2.5 shows the reaction of PVC and PVA to form the copolymer. The ratio of each is about 86 pct. PVC and 13 to 14 pct. PVA, or is a high molecular weight emulsion of the same copolymer (e.g. latex or water-based paint) (17). Most thermoplastic vinyl solution coatings contain oxygenated solvents such as ketones and glycol ethers. Solvents range from 75 to 90 pct. of the total volume of the paint mixture. This concentration prevents the use of these solution vinyl coatings in areas where coating legislation is enforced.

Polyvinyl chloride is a very inert material with high symmetry, an extremely stable carbon-to-carbon backbone, and stable carbon-to-hydrogen and carbon-to-chlorine pendant sidegroups. This structure gives PVC its inert property, and the ability not to be dissolved by some stronger solvents used in coatings manufacturing. However, without the PVA modification, the PVC can not be used in paint manufacturing. The PVA retains its stable carbon-to-carbon backbone, but does have an ester sidechain that lends itself to solvent attack. This situation means that PVA can be readily dissolved by stronger solvents. PVA coatings have only a limited moisture and chemical resistance and are suitable for only interior decoration.

When the PVC and PVA are mixed in the above mentioned levels with about 1 pct. or less maleic acid to form a copolymer, this formulation is the basis for most solvent-deposited vinyl coatings used for corrosion protection (17). Due to the sensitivity of the

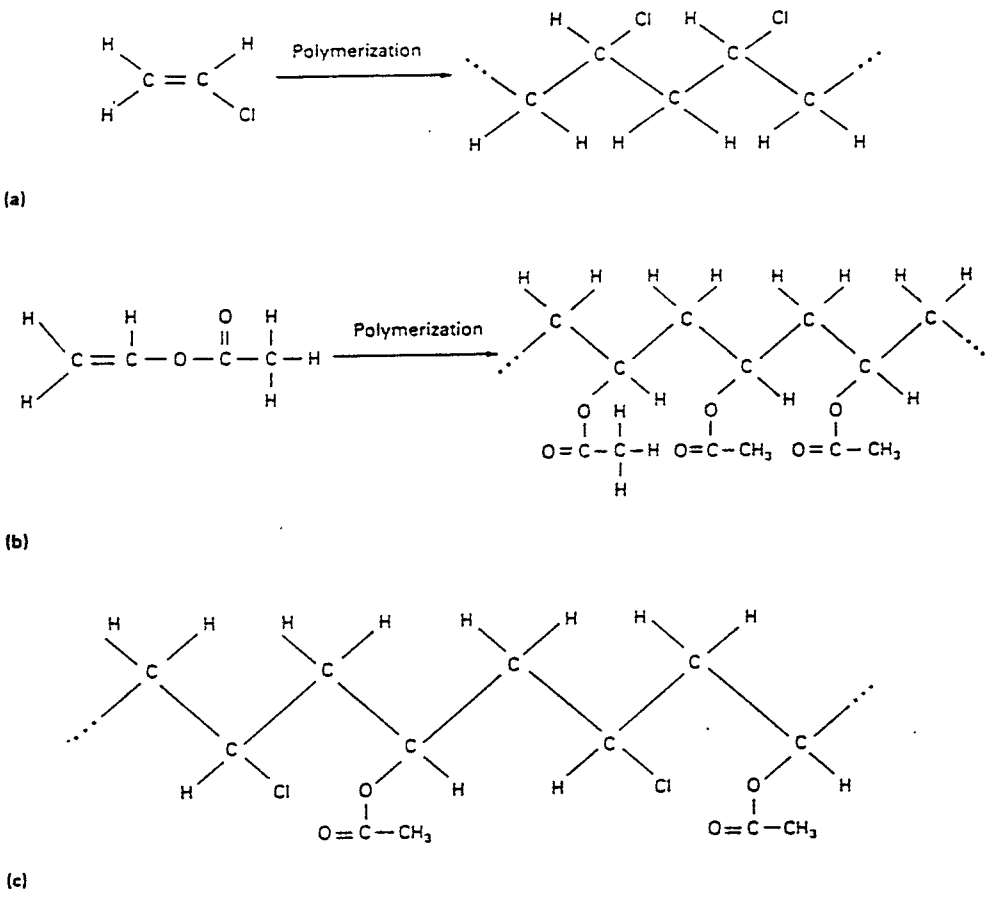

Figure 2.5 Reaction of a PVC (a) and PVA (b) polymers to form a PVC-PVA copolymer (17).

vinyl resin to ultraviolet light, an ultraviolet scattering pigment such as rutile (TiO_2) must be used to minimize chalking or degradation of the coating. Other pigments can be used along with the rutile, but they act more as filler and reinforcing pigments. Zinc oxide and zinc dust can be used as pigments. However, due to the acidic nature of the vinyl, care must be taken since they have a tendency to curdle the paint while in solution. Vinyl solution coatings are known for their excellent toughness and water resistance, and they can be used as complete systems (vinyl primer, intermediate, and topcoat).

Chlorinated rubber coatings are also considered to be solvent-deposited coatings because there is no chemical change that happens upon application, and the coating film forms on the surface after the solvent evaporates. Coating systems based on chlorinated rubber have excellent resistance to acids, alkalies, oxidizing agents and have very low water vapor transmission rates (about 10 pct. that of an alkyd resin coating). These coating systems are generally non-flammable because of their chlorine content, and are also, non-toxic. Paints made with chlorinated rubber are used primarily as chemical- and corrosion-resistant coatings, marine coatings, building masonry and swimming pool paints, highway marking paints, fire-retardant and mold-resistant paints, and primers for hot applied coal tar or asphaltic enamels.

Chlorinated rubber resins are made by adding chlorine (65 to 68%) to natural rubber. The molecular structure of a chlorinated rubber resin can be seen in Figure 2.6. Next, the resin must be plasticized and stabilized against light, heat, and gelation to allow

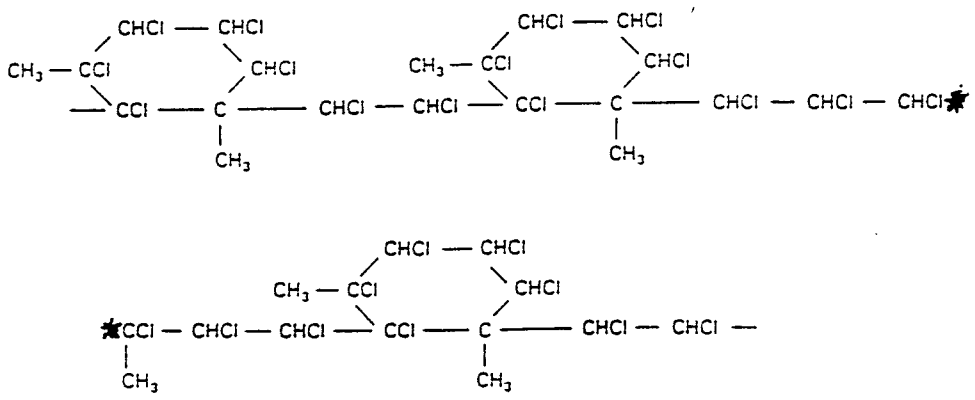

Figure 2.6 Molecular structure of a chlorinated rubber resin (17).

the resin to be used as a binder in protective coatings. Heat stability is brought about by incorporating low molecular weight epoxy compounds or epoxidized oils into the resin. The amount of plasticizer added to the coating directly affects the film properties. Too little plasticizer results in a film which is harder, more brittle, and will exhibit poor adhesion. Too much plasticizer will result in a film that is soft and exhibits tackiness resulting in higher dirt retention. This condition also leads to increased water transmission rates or water permeability through the film, diminishing the corrosion protection. The presence of ferrous (Fe^{+2}) or ferric (Fe^{+3}) ions may cause gelation of the chlorinated rubber coating (16). This result means that care must be taken to avoid excessive contact with iron or steel during manufacturing. Any storage containers should be coated to minimize corrosion and to prevent possible contamination by the ferrous or ferric ions.

Acrylic coatings can be made much in the same manner as the thermoplastic, solvent-deposited coatings. These acrylic resins consist of polymers and copolymers of the esters of methacrylic and acrylic acid (17). The repeating units for methacrylate and acrylate can be seen in Figure 2.7. When mixed with the proper pigmentation, the resulting resins provide excellent film-forming coatings with superb light fastness, gloss, and ultraviolet stability. Nearly all acrylic coatings are not well suited for immersion service or strong chemical environments due to the fact that the ester group is present on both the polymethyl methacrylate and ethyl acrylate resins. However, this ester group is present only as a pendant sidechain. The carbon-to-carbon backbone chain of the acrylic

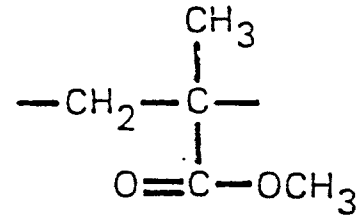

Polymethylmethacrylate

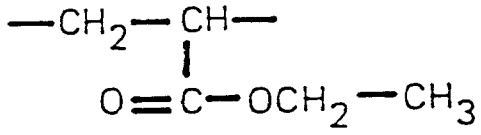

Polyethylacrylate

Figure 2.7 The repeating units for the methacrylate and acrylate molecules (18).

resins does provide very good chemical and moisture resistance.

Acrylate, methacrylate, or higher homopolymers can be used to formulate some coatings. Formulations of both types of resins are also commonly used for corrosion protection. Most often, coatings made from the acrylates or from copolymers with a dominance of the acrylate ester are softer and more flexible than the corresponding methacrylates. The acrylate has a somewhat lower resistance to ultraviolet radiation than that of the methacrylate due to the presence of a tertiary hydrogen attached directly to a carbon comprising the molecular backbone. This active hydrogen is vulnerable to photo-oxidative and thermo-oxidative attack. As a result, the acrylate esters have a greater susceptibility to ultraviolet light and oxygen. The methacrylates have a harder and more brittle film, but with less adhesion, and they also possess better chemical and moisture resistance and heat tolerance. Greater flexibility, toughness, and resistance to abrasion can be obtained in both resins by increasing the molecular weight. However, hardness decreases as the flexibility and elongation increase in both resin types. If the molecular weight is increased too much, the viscosity becomes excessive, and solvent release is excessively slow. Acrylic resins are characteristically soluble in moderately hydrogen-bonded solvents, such as ketones, esters, aromatic hydrocarbons, and some chlorinated hydrocarbons.

Thermoplastic acrylics are solvent-deposited coatings that do not undergo any chemical change during or after application. Upon application, the solvent vehicle

volatilizes, and the coating sets, hardens, and attains its final properties as the solvent evaporates. To accelerate the evaporation, heating or baking may be used. Solvent-deposited acrylics are also used for maintenance finishes, but more commonly, the acrylic monomer or copolymer is added to an alkyd. The resulting acrylic-modified alkyd has excellent penetration properties, adhesion, and ease of application of the alkyd, combined with the improved ultraviolet resistance, gloss, and color retention of the acrylic.

Cross-linking (thermosetting) acrylics are obtained by combining the methacrylate or acrylate esters with a reactive non-acrylic polymers (17). These cross-linking agents are usually epoxy resins, the urea or melamine-formaldehyde resins, and the vinyl resins. The non-acrylic polymer usually is the major component present in the coating film. The arcylic modification is only done to enhance color, gloss, and ultraviolet stability of the non-acrylic component. The resulting thermoset acrylic films are harder, tougher, and more resistant to heat and solvents than thermoplastic acrylics. However, thermoset acrylics are generally less resistant to ultraviolet light and usually require heating or baking after application to achieve the desired properties. The coatings have good adhesion and detergent resistance. Also, they have short curing times at relatively low temperatures. The major advantages of these types of coatings are the high gloss, range of colors, and lack of yellowing or darkening upon exposure to sunlight.

The water-based acrylic coatings market is quite large. Water-based acrylics have a number of advantages over the oil-based coatings. They have a much faster drying time,

and can be recoated within one hour. They also have better alkali resistance, excellent adhesion, large color choices, good sunlight and ultraviolet light resistance, and excellent long-term flexibility and toughness. The biggest advantage is that they can be cleaned up with water. The disadvantages are that oil-based paints have better penetration and better initial adhesion. Water-based paints will sometimes peel or lose adhesion on smooth surfaces, while an oil-based paint will wet sufficiently to maintain good adhesion. However, water-based acrylics have better resistance to blistering due to their breathing ability and have better resistance to chalking and yellowing. Water-based acrylics may adhere better to damp wood and masonry substrates than oil-based paints.

Water emulsion coatings have a complex chemistry. The molecular weight of the acrylic polymers is quite high and polymerization takes place in a water emulsion. Pigments are dispersed throughout the emulsion, and the required additives are added, followed by tinting and color pigments. Rutile (TiO_2) is the most widely used white-hiding pigment, although most other water-insoluble alkali resistant organic and inorganic pigments can also be used. Wetting agents must be added to ensure complete pigment wetting in the water vehicle. Anti-foaming agents are added to prevent foaming during the manufacturing process. Thickening agents are also used to maintain the proper viscosity of the coating to keep the pigments from settling and running after application. Surfactants are added to strengthen the pigment dispersion. It is these surfactants that provide water sensitivity to most water-based coatings after application. The surfactants

possess a hydrophobic (water-hating) and a hydrophilic (water-loving) end, which orients itself around the emulsified resin and the pigment particles (17). The hydrophobic end is next to the resin particle surface, while the hydrophilic end is attracted to the water carrier. After application of the coating, many of the surfactants remain entrapped within the film cross-section. The hydrophilic end of the surfactant attracts water from the environment, which tends to soften and swell the coating. In atmospheric service, there is not enough water to cause a problem. However, in prolonged water immersion, water may be attracted by the surfactant, penetrate the film, and cause softening and swelling of the coating and a loss of adhesion. As a result, nearly all water-based coatings are not suitable for prolonged water immersion as they are currently formulated.

A coalescing solvent is added to most air dry applications. This organic solvent evaporates slowly, is miscible with water and is added to the water carrier. As the water evaporates, the resulting solvent concentration in the solvent/water mixture grows larger. When the concentration has reached a level at which the solvent can partially solvate the resin particles, they soften and meld together as the drying proceeds. The coalescing solvent helps to convert the emulsified particles into a relatively smooth, homogenous film. However, the residual solvent may be entrapped within the drying film, and it too can lead to water sensitivity.

A new technology in the area of acrylics is the photopolymerization of the homo- and copolymers located within the coatings. Cross linking can be initiated in a susceptible

binder system through the use of ultraviolet light (about 200 to 400 nm) or visible light (about 400 to 800 nm) (17). Acrylic esters show a very rapid response to photoinitiation as compared to other commonly used coating resins. Within the arcylic family, the acrylate is at least ten times more reactive to the ultraviolet of visible light radiation than the methacrylate. All types of resins can be modified with acrylate esters, and the combination can be mixed with a suitable photoinitiator to aid in the radical polymerization mechanism. After setting up and exposure to an intense source of ultraviolet or visible light, they cross link through a photoinitiated free radical polymerization, which leads to thorough cross linking, hardening, and almost immediate attainment of chemical and moisture resistance. The great potential of this technology is quite evident in that the sun might be able to act as a cross-linking agent.

Bituminous coatings are those that involve the use of coal tar or asphalt (17). These bitumens are distinctly different physically and chemically. As coatings, they can be applied as hot melts, solvent cutbacks, or emulsions. Hot melt applications involve heating the coal tar or asphalt to around 175 to 245^{0}C (350 to 475^{0}F) so its viscosity is close to that of water. Asphaltic or coal tar bitumens dissolved in a suitable solvent (normally aliphatic and aromatic hydrocarbons) are termed solvent cutbacks. The viscosity of the bitumen is lowered as it is dissolved in the solvent sufficiently enough to allow for application by the appropriate method. After application, the solvent volatilizes and the bitumen resolidifies into a film. The coating thicknesses of solvent cutbacks are

usually much less than hot melts, but the ease of not having to heat the bitumen at the job site immediately before application is a major advantage.

Water emulsions of the bitumens are prepared by suspending minute particles in water using emulsifying agents, and by combining with inert fillers. These inert fillers include pulverized talcs (hydrated magnesium and aluminum silicates), coal dust, powder silica, mica, and limestone dust. After application, the water evaporates and coalescence takes place in the typical fashion of any emulsion coating, and a protective film is formed. The hot melt application provides the best moisture and chemical resistance, followed by the solvent cutback and water emulsion. Asphaltic materials have much better atmospheric weathering resistance and are less deteriorated by ultraviolet light than are the coal tar coatings. However, coal tar coatings have much better resistance to moisture, acids, and alkalies than the asphaltics. The asphalts and coal tars are usually incompatible due to their chemical make-up and should not be used as mixtures or applied one type over another.

The coal tar enamels (or pitches) are made from the coking of coal (17). When the coal is heated in the absence of air to a temperature of about $1095^{0}C$ ($2000^{0}F$), it decomposes partially into a gas and coke. The gas is condensed and coal tar is formed. Lighter fractions are removed from this tar by reheating and gas extraction until the desired coal tar fraction is obtained. The coal tar compounds range from low-boiling, low molecular weight benzene to complex, high molecular weight, aromatic hydrocarbons.

There are basically three types of coal tar enamels. The first one is a straight pitch that is relatively hard and brittle, but has great chemical and moisture resistance. The second one is a plasticized enamel that is more flexible and has greater cold weather application tolerance, but poor chemical and moisture resistance. The third one is an intermediate grade of the other two (50 pct. of each) with intermediate properties. The natural asphalts are being replaced by those obtained as residues from the distillation of crude petroleum. Asphaltic compounds are made up of complex polymeric aliphatic hydrocarbons. They have good water and chemical resistance, and like coal tars, they are sensitive to oils and solvents.

2.4.3 Cross-Linked Thermosetting Coatings

Coatings that harden or cure and attain their final resistant properties by virtue of a chemical reaction either with a copolymer or with moisture are referred to as chemically cured coatings (16). These types of coatings, which chemically cross link by copolymerization, include epoxies, unsaturated polyesters, urethanes in which the isocyanate is reacted with a polyol, high temperature curing silicones, and phenolic linings. Chemically cured coatings that react with water include moisture-cured polyurethanes and most of the inorganic zinc-rich coatings. Even though drying-oil-base coatings are also chemically linked upon their reaction with oxygen from the air, they are excluded from this

category because the auto-oxidative, cross-linking mechanism is a sufficiently distinct class of chemical cross linking.

The main goal of chemical cross-linking is to formulate a coating using a resin, or binder of low molecular weight. After being mixed and applied, a reaction takes place with moisture from the atmosphere, or with a co-reactant. This reaction results in cross linking and a substantially larger three-dimensional molecular structure (16). This coating may be placed on the inside of a large tank or vessel, and upon completion of the application (many hours later), the film may cure into one large macro-molecule. This macro-molecule may cover many thousands of square feet of surface area. A suitably formulated coating of this type may provide a tough, flexible, and highly chemical-resistant corrosion protection barrier over the underlying surface. A macro-molecule of this type would be impossible to obtain in a pre-reacted binder system.

There are coatings which are based on chemically converted binders, and they can generally be made to have excellent resistance to acids, alkalies, and moisture. They can also be made to resist abrasion, ultraviolet degradation, and thermal degradation. Generally, the toughness and flexibility of the coating increase as the molecular length increases. The chemical and moisture resistance can also increase as the cross-linking density increases within the macro-molecule. However, the constituent chemical groups within any type of molecular structure may result in characteristic strengths and weaknesses within the molecular chain.

The properties of any given molecular structure can be further altered by the arrangement and composition of the pendant sidegroups. Sites within the molecule that remain reactive can lead to a decreased chemical, moisture, or thermal resistance. These reactive sites are referred to as "unreacted moieties" (17). The rate of cross linking depends not only on the reacting moieties, but also on the mechanism of cross-linking. Other factors such as temperature and humidity can play a major role in affecting the rate of cross linking. This rate of cross linking means that chemically converted coatings must set after application through solvent or water volatilization, and then harden and attain their final cured properties through the cross-linking reaction, which is temperature and/or moisture dependent. If the rate is too fast, the coating may become overcured, hard, and impervious which would not allow for proper adhesion of a subsequent topcoat.

For some chemically cross-linked systems, the curing and hardening is so fast (polyesters and vinyl-esters) that multi-component spray application systems are necessary. These types of systems actually mix the co-reactants at the time of spray application within the spray gun or outside the spray, gun nozzle. The chemical cross-linking reaction begins almost immediately so that by the time the coating has been deposited on the surface, it is beginning to set up. Even though these coatings are hard within minutes, solvent volatilization and additional cross linking should be allowed to continue for days before exposure to a severe chemical environment. Generally, the curing of most cross-linked systems should take place for about 7 days at 25^0C (75^0F)

before the coating is exposed to severely corrosive conditions, immersion, or acid or alkali splash or spillage. The resins used for these types of coatings include epoxies, phenolics, and urethanes.

Epoxies that are chemically cross-linked generally come in two packages. The first package consists of the epoxy resin, pigments, and some solvent. The second package has the copolymer curing agent. Both packages are mixed together immediately before application, and upon curing, it develops the large macro-molecule structure. The properties of the epoxy coating come from the type and molecular weight of the epoxy resin and from the copolymer curing agent used for cross linking (19). For industrial maintenance coatings, the most common type of epoxy resin is the glycidyl ether type that is derived from bisphenol-A and epichlorohydrin as seen in Figure 2.8. Cycloaliphatic epoxies were developed to offer improved light stability and ultraviolet degradation. However, they do not possess the adhesion, chemical resistance, and flexibility of the resins derived from bisphenol-A and epichlorohydrin. Epoxy cresol novolacs were developed to provide greater high-temperature resistance and chemical resistance at the expense of brittleness and a lack of flexibility.

The cross-linking reaction for the epoxies is actually a copolymerization, and not a catalyzed reaction. The curing reaction takes place primarily through the epoxy ring endgroups or the mid-chain hydroxyls of the epoxy resin. The curing agent is usually an amine or polyamide, with the cross linking derived through the active hydrogens attached

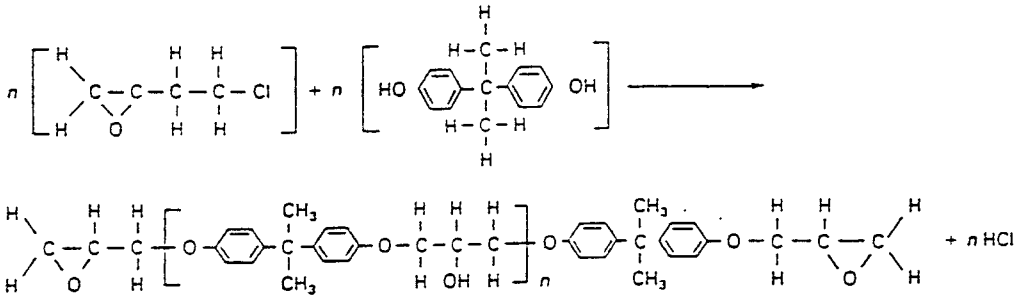

Figure 2.8 Reaction of epichlorohydrin and bisphenol-A to form a glycidyl ether type epoxy resin (17).

to the amine nitrogen (19). There are numerous cross-linking agents that can be used such as mercaptans, polybasic acids and anhydrides, and phenol-formaldehyde and phenol resins. However, the polyamines, the amine adducts, and the polyamides are the most common types used.

The polyamines are small molecules with a low molecular weight (e.g. diethylene-triamine, hydroxyethyl diethylene triamine, bishydroxydiethylene triamine) compared to the epoxy resin. This physical characteristic means that when reacted, they lead to tight cross linking and high chemical and moisture resistance. During the cross-linking reaction, there may be some unreacted amine that is squeezed out of the film to the surface. This behavior is called "amine blush", which is a hazy white coloration on the coating surface (17). Amine blush can be minimized by allowing a 15 to 30 minute induction period after mixing prior to application. This practice allows initial cross linking to occur before the paint is applied. Several small amine molecules will partially cross link with epoxy resin molecules which reduces the tendency for amine blush to occur. Coating manufacturers often supply the amine as a pre-reacted amine adduct. In this case, the epoxy pigment and solvents are packaged as before in one container, but an excess of the amine is pre-reacted with some of the epoxy resin to increase its molecular size. The amine adduct is then packaged in a separate container, sometimes with additional pigment and solvent.

The polyamide curing agents come from the condensation products of a dimerized fatty acid with a polyamine (17). Cross linking occurs as with a straight amine, although

the polyamide molecule is much larger. The resulting film has improved flexibility, improved gloss and flow, excellent water resistance, and good chemical resistance. Polyamide-cured coatings do have less solvent and alkali resistance than amine and amine adduct-cured epoxies do. There are specially formulated polyamide-cured epoxies that have the ability to displace water from the substrate surface. These materials can be applied and cured underwater to form corrosion resistant coatings.

Ketimine is another curing agent that allows the application of a high molecular weight, high solids, or solventless epoxy resin with standard spray equipment. Figure 2.9 shows the curing reaction of a ketimine cured epoxy. Epoxies that are more viscous can be mixed with the low molecular weight ketimine curing agent and applied to a surface by spraying. Until the ketimine decomposes in the presence of atmospheric moisture, no reaction will occur to form a polyamine or ketone. The ketone volatilizes from the film and the amine reacts as described above to cross link with the epoxy resin after application. These systems result in tightly cross-linked epoxy films. They do require relative humidity in excess of fifty pct. and good ventilation to expose the ketimine to moisture and to remove the residual ketone and other solvents from the paint film.

The coal tar epoxies are a combination of a coal tar mixed with an epoxy resin packaged separately in one container. The curing agent is an amine, amine adduct, or polyamide as previously described and is packaged in a separate container. Also, the cross-linking reaction is the same as discussed earlier. The coal tar material acts as a filler

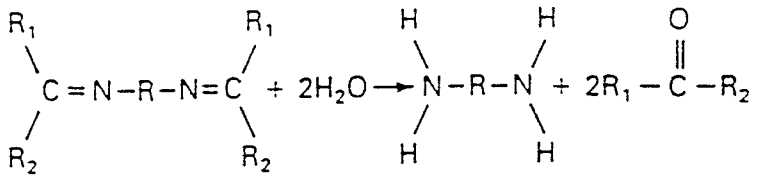

Figure 2.9 Curing reaction of ketimine-cured epoxies where the ketimine decomposes in the presence of atmospheric moisture to form a polyamine plus a ketone (17).

within the cross-linked epoxy matrix. The resulting film has good toughness, adhesion, ultraviolet resistance, and thermal stability much like the epoxies. It also has the high moisture resistance of the coal tar. The amine-cured coal tar epoxies usually have better chemical and moisture resistance, but are more brittle and harder to apply and topcoat than the amine adduct- and polyamide-cured coal tar epoxies. However, the polyamide coal tar epoxies are more flexible, easier to topcoat, and more tolerant of application variables.

Phenolic cross-linked epoxy coatings are extremely resistant to acids, alkalies, and solvents. The high molecular weight epoxies that have a high proportion of hydroxyl functional groups available for reaction are used. The epoxy is packaged with a phenolic resin (e.g. phenolformaldehyde resin) which can be seen in Figure 2.10, pigment, and an acid catalyst. The coating is applied after mixing by spraying, and then it is baked at temperatures ranging from 150 to 205^{0}C (300 to 400^{0}F) in order for cross linking to proceed. The cross linking that results is between the hydroxyl groups along the epoxy chain and the methylol groups present in the phenolic resin. A secondary reaction is possible between the terminal epoxide groups of the epoxy resin and the hydroxyl groups of the phenolic resin (17). Phenolic linings are formed by the reaction of a phenol with a formaldehyde to form the phenolformaldehyde compound. The methylol group can react on the two ortho positions and the paraposition on the benzene ring to form phenolformaldehydes with possible reaction sites. When these compounds are heated, a

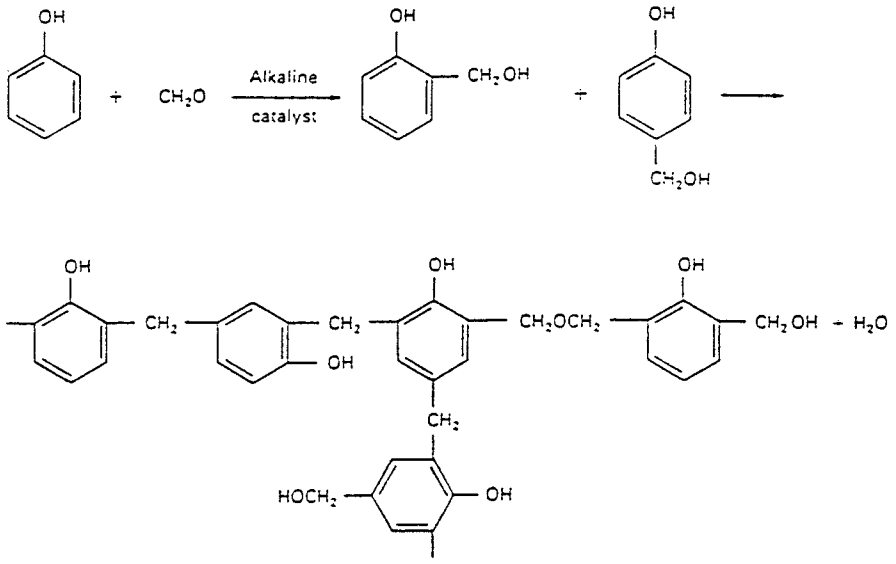

(a)

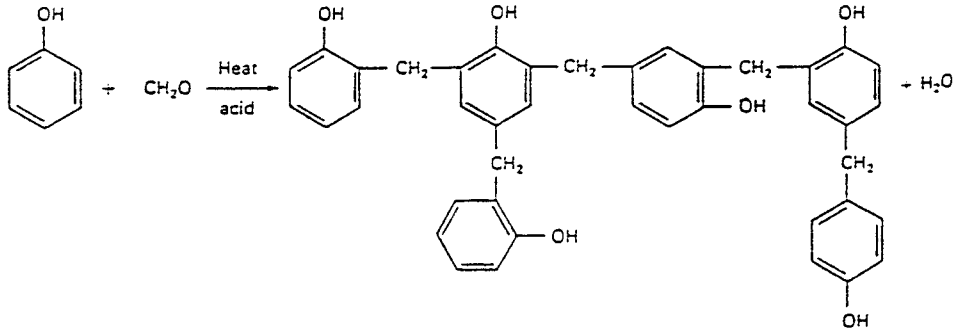

(b)

Figure 2.10 Reaction of phenol and formaldehyde to form a phenolic resin by (a) reaction using an alkaline catalyst, and (b) reaction using an acid catalyst (17).

condensation reaction occurs between methylol groups on the adjacent molecules that cross link the film and release water.

The coatings must be applied in multiple-coat systems. Each coating is about 0.025 mm (1 mil) thick and must be baked for a few minutes at 120 to 205^{0}C (250 to 400^{0}F) between coats. This baking partially cross links the coating, but more importantly, it volatilizes the water formed during the cross-linking reaction. After the final application, a post-bake at higher temperatures and longer times is performed. It is relatively easy to determine when the coating has baked long enough to ensure proper curing and cross linking. The phenolic resin darkens when exposed to heat, and a properly cured coating is a uniform, light chocolate brown color. The phenolic coatings are odorless, tasteless, and non-toxic after curing. This condition makes them ideal as linings for vessels and tanks which support food production. They also have excellent resistance to boiling water and hot aqueous solutions of mild acid. However, the phenolic coatings have a major weakness in that they have a lack of alkali resistance. Unless they are modified with epoxies, they should not be used for alkaline service.

Urethane coatings have moisture and chemical resistance similar to that of epoxies. They can also be mixed in a variety of light-stable colors that maintain their gloss and "wet look" upon extended exposure. The chemistry involved in the urethane coating curing is not complex and usually consists of the reaction of an isocyanate-containing (-N=C=O) material with a polyhydroxylated (-OH containing) co-reactant as seen in Figure 2.11.

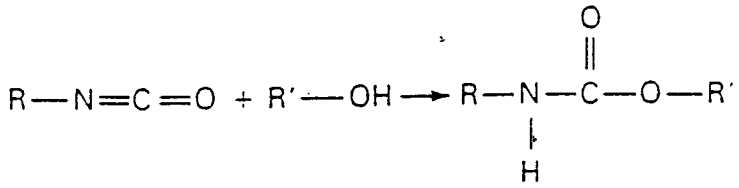

Figure 2.11 Reaction of an isocyanate and a polyol to form a urethane where R and R' are different aromatic or aliphatic groups (17).

The cross linking occurs because of the highly reactive nature and affinity of the isocyanate group for the active hydrogen of the polyol hydroxyl or any active hydrogen atom attached to a nitrogen or oxygen atom. The rate of this cross-linking reaction depends on the type and configuration of both the isocyanate and polyol materials and the temperature. The cross-linking reaction occurs with most formulations at temperatures a low as -18^{0}C (0^{0}F) or less.

There are several types of isocyanates used in making urethane coatings. The final properties of the urethane coatings are based upon the number of isocyanate groups available for reaction (functionality) as well as the molecular weight and structure (16). The different polyol structures, such as acrylics, epoxies, polyesters, polyethers, and vinyls, when reacted with a particular isocyanate will result in various combinations of physical and chemical properties. The isocyanates are generally referred to as either aromatic (having a benzene ring) or aliphatic (straight-chained or cyclical) hydrocarbons. Toluene di-isocyanate (TDI) was the first aromatic isocyanate used in urethane coatings. The resulting urethane coating had suitable chemical-resistance, but it was generally undesirable because of its low viscosity and toxic irritating vapors that were produced. To make a safer co-reactant, TDI was reacted further to make a higher molecular weight polyisocyanate that contains less than 1 pct. of the original TDI monomer (Figure 2.12). The higher molecular weight aromatic isocyanates can form useful chemical-resistant coatings that can be cured at low temperatures when reacted with a polyol. However, the

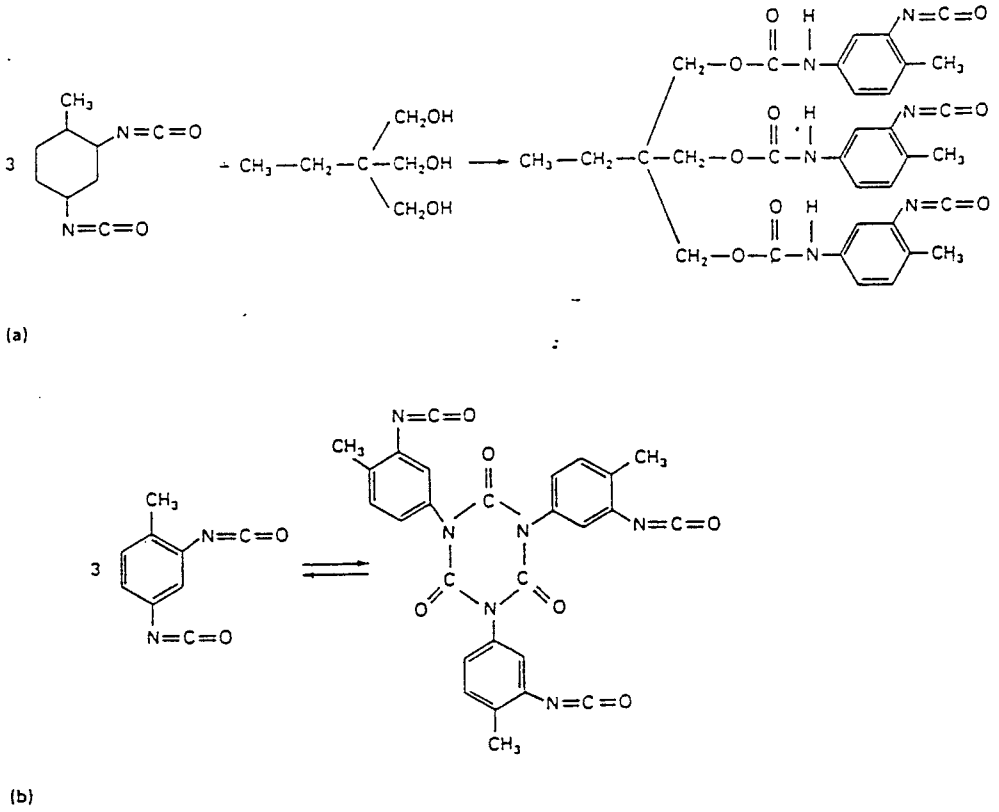

Figure 2.12 Modifications of TDI to form higher molecular weight polyisocyanates by (a) polymerization of TDI with an alcohol to produce a TDI alcohol adduct, and (b) condensation of TDI monomer to produce an isocyanate ring (17).

urethanes that are formed have a tendency to chalk, yellow and darken when exposed to sunlight.

Aliphatic isocyanates were developed in the early 1970's and were more expensive than the aromatic isocyanates, but the allowed the formulation of non-yellowing, light-stable, high-gloss finish coats (17). The appearance of the urethane coatings that were made with aliphatic isocyanates was unmatched by the epoxies, acrylics, or any other coating material available in the industrial marketplace. An important aliphatic isocyanate is hexamethylene diisocyanate (HDI) and its molecular structure can be seen in Figure 2.13. When the HDI is in its monomer form, it is an irritant. The HDI can also be reacted with water to form a larger molecule much like the TDI. Several different combinations of aromatic and aliphatic isocyanates can be made, including specialty isocyanates, to make high-solids or solvent-free coatings, elastomeric coatings, or coatings designed for baking or curing at elevated temperatures. However, as previously mentioned, the aromatic isocyanates have a tendency to discolor. Both the straight-chained and cyclical aliphatic isocyanates, although non-yellowing, are much slower to react and cross link than aromatic isocyanates.

The polyols co-react with isocyanates to form the polyurethane film (16). The polyol is packaged with the pigment, most of the solvent, and any additives used for flow, thixotropy, antisetting properties, and so on. The long, repeating carbon-to-carbon backbone chains with very little branching (e.g. vinyl) result in tough, flexible resins.

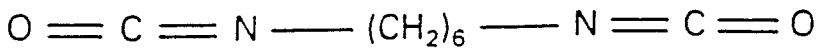

Figure 2.13 Molecular structure of HDI, an aliphatic isocyanate used in urethane coatings (17).

Aromatic groups add rigidity to the chain as does the cross linking. The presence of several ester, ether, and urethane groups reduces the chemical and moisture resistance. For corrosion-resistant coatings, the polyol is usually an acrylic, polyester, polyether, epoxy, vinyl, or alkyd. One may add asphalt and coal tars to any of the polyols. However, it is felt that the bitumen behaves as a filler in the urethane matrix because they are essentially non-reactive. They may also provide the cured coating with good chemical resistance, high moisture resistance, and high film build at a relatively low cost.

Acrylic urethanes are the most widely used urethanes for corrosion protection in atmospheric service. These coatings can have excellent weatherability, gloss and color retention and have good chemical and moisture resistance. The acrylate polymer family is softer and more flexible than the corresponding methacrylates. An increase in the molecular weight of the monomers, such as methyl acrylate to butyl acrylate, leads to softer, more flexible polymers for both families. The acrylate and methacrylate blends are also used as reactive polyols. Acrylic urethanes are not used for immersion service, and they don't have the chemical resistance of the polyester urethanes. They do have excellent weathering properties when an aliphatic isocyanate is used.

Polyesters come about from the condensation reaction of a dibasic acid and a polyhydric alcohol (17). A hydroxylated polyester is formed when an excess of the hydroxyl functionality from the alcohol is allowed over that of the acid. The result is a polyester molecule with a mid-chain and end-chain hydroxyl functionality. Due to the high

isocyanate demand when co-reacted, polyesters result in relatively hard chemical-resistant polymer films. However, alkaline attack and water sensitivity can occur at locations where the ester group is exposed because the ester linkages occur in the molecular backbone. In other words, this behavior happens at areas of low cross-link density or where less branching of adjacent molecules occurs. Because of this fact, polyester urethanes are not normally used for immersion service.

The polyol of choice for use in making elastomeric coatings, coal tar urethanes, and other urethanes that are protected from light are the polyethers. The polyether prepolymer is much less expensive than acrylic or polyester polyols. Polyethers are quite sensitive to ultraviolet-induced oxidative degradation. Also, the ether linkages (-C-O-C-) are water sensitive. In polyethers, they are repeated throughout the polymer chain without separation by long, water-insensitive, hydrocarbon chains or aromatic groups that can minimize water sensitivity.

Vinyl urethanes use a linear, long chain, hydroxyl-bearing PVC/PVA resin that is reacted with a polyfunctional isocyanate prepolymer. Urethane coatings that use vinyl polyols combine the abrasion resistance of the urethane with the toughness, flexibility, and chemical resistance of the vinyl. These types of coatings are promoted for use where flexibility and abrasion resistance are important factors. However, vinyl urethane coatings are susceptible to chalking or fading upon exterior exposure and do not have the color, gloss, weatherability, or solvent resistance of the acrylics and polyesters. Because the

vinyl is thermoplastic and is attacked and softened by solvents, recoatability after extended times is not a problem and is a big advantage of vinyl urethane systems.

Isocyanates are reacted with alkyds to form what is called a uralkyd or urethane oil coatings (17). This reaction decreases the drying time of the coating and provides enhanced resistance to chemicals, moisture, weathering, and abrasion. Uralkyds harden by auto-oxidation of their unsaturated oleoresinous sidechains. The resultant coating system is an upgrade over the non-urethane system. However, because of the isocyanate reaction, the cost of this particular system is higher than those systems that are not urethane modified. If some of the dibasic acid is replaced with an isocyanate to form a cross-linked polymer, this is called a uralkyd. The resulting urethane alkyd resin still has the oleoresinous sidechains, and although it is cross linked and upgraded by the isocyanate, it is still sensitive to water and chemicals through the ester and urethane links.

Moisture-cured urethanes are formed when an isocyanate reacts with the hydroxyl group in water. Single-package moisture-cured urethanes use an isocyanate prepolymer that, when applied, reacts with the humidity in the air to form a hard, tough, resinous film. The curing reaction can be seen in Figure 2.14. Aromatic isocyanates are used primarily in moisture-cured urethanes because of their rapid rate of reaction. The pigments must be essentially non-reactive with the isocyanate (e.g. aluminum leaf). It should be pointed out that the isocyanate/water reaction produces CO_2 gas. Some of the CO_2 is evolved in the curing of all urethane coatings, because of the humidity present in the atmosphere. In

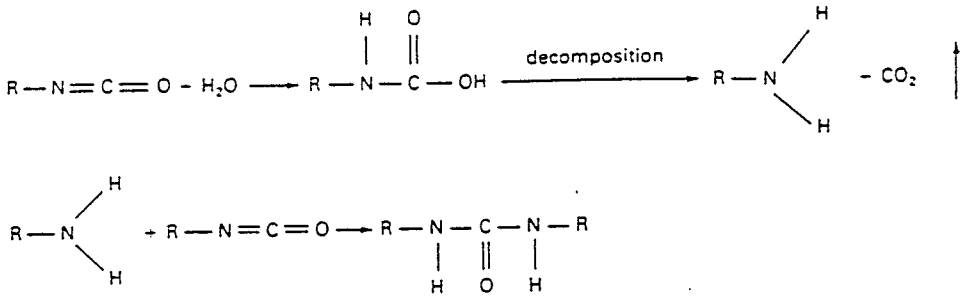

Figure 2.14 Curing reaction of a single-package moisture-cured urethane (17).

areas where the relative humidity is low or where assurance of a more complete cure is necessary, a small amount of a tertiary amine catalyst (e.g. dimethylethanolamine) can be added. This catalyst is added to the isocyanate just before use.

2.4.4 Zinc-Rich Coatings

In recent years, a number of coatings have been developed that will deposit a film of metallic zinc and have many of the same properties in common with zinc coatings applied by other methods (hot-dip galvanizing, electro-plating, etc.). The zinc-rich coatings are a unique class of cross-linked coatings that provide galvanic protection to a ferrous substrate. These coatings are referred to as "zinc-rich primers". The binder is highly loaded with a metallic zinc dust pigment. The binder, once the coating is applied, holds the metallic zinc particles in contact with the steel and other zinc particles. Once the metal-to-metal contact of the two dissimilar metals is made, a galvanic cell results. Paint films that contain 92 to 95 pct. metallic zinc in the dry film along with the film being in electrical contact with the steel surface at a sufficient number of points, results in the film protecting sacrificially (20). The zinc becomes the anode which sacrifices itself to protect the underlying cathodic steel. The biggest advantage in using zinc-rich coatings for corrosion protection is that pitting corrosion and subfilm corrosion is eliminated. This advantage is also true at voids, pinholes, scratches, and abrasions in the coating system.

This can not be said of other types of protective coatings which makes zinc-rich coatings special and widely used.

There are certain disadvantages that accompany this protective advantage. The underlying steel substrate must be cleaned of all rust, old paint and other contaminants that may interfere with the metal-to-metal contact. Surface preparation must be quite thorough. Blast cleaning should produce a Commercial Blast Cleaning minimum and for immersion service, a White or Near-White surface (21). There are several organizations, such as the Steel Structures Painting Council (SSPC) and the National Association of Corrosion Engineers (NACE), that issue standards for the surface preparation of metals for several coatings. If the steel is cleaned by power tools, the surface must be cleaned to bright metal. Zinc-rich coatings can be applied to pickled steel, but the surface must be clean. Due to the high reactivity of the zinc-dust pigments, zinc-rich coatings are not suitable in condensing of hydrolyzing environments outside the pH range of about 5 to 10. The acids and alkalies will attack the zinc-dust pigments, even when topcoats are used. The chemicals may penetrate the top coat through pinholes, scratches, voids, or discontinuities within the topcoat and cause aggressive attack of the zinc-rich primer.

Because of the high zinc loading, the zinc-dust pigment should be suspended in the spray pot during spray application. An "agitator" or stirrer must be used in the spray pot as a result of this high zinc loading. Also, because of this high pigment loading, long hoses from the spray pot to the spray gun should not be used to minimize settling in the

lines. Care must be taken so that the primer does not begin to set up in the spray lines on warm days. This situation is a problem with most inorganic zincs, especially when application is interrupted for more than just a few minutes without first draining the paint from the hose. If there is no movement in a warm paint hose, plugs of paint may begin drying and hardening such that when spraying resumes, the paint doesn't readily move through the fluid line to the gun. When blockage of the line occurs and the gun only works intermittently, hardening of the paint may occur to such an extent that the entire line must be thrown away.

The rapid drying characteristic that many of the inorganic zincs possess may result in a greater amount of dry spray than would occur with conventional non-zinc-rich coatings. This means that care must be taken during application to make sure the zinc-rich primer is deposited in a smooth, wet application. These types of coatings generally have more porosity because of the high zinc loading over the pigment volume concentration of the binder. Because of this porosity, they are harder to top-coat. When topcoats are placed over both organic and inorganic zinc-rich primers, they will often exhibit bubbles or voids in their cross-sectional thickness and bubbles or pinholes extending down through their surface to the underlying zinc-rich coating. This situation is due to entrapped air, solvents, and moisture within the zinc-rich primer before or during topcoating. These liquids or gases must be able to pass through the coating to the atmosphere. As the topcoat dries, some of the escaping gases form bubbles or blisters, or the path of the

escaping gas hardens into a pinhole. If the zinc-rich binder does not cure properly before application of the topcoat, poor adhesion or cohesion within the zinc can eventually lead to peeling of the topcoat.

Inspite of these disadvantages, the elimination of subfilm and pitting corrosion makes zinc-rich coatings quite advantageous. They are one of the most widely used corrosion prevention coatings for painting steel in industrial, marine, and other severe service environments. Zinc-rich coatings used as primers with topcoats are widely used for the corrosion protection of steel substrates. They can also be used extensively in the marine industry (inorganic zinc-rich systems) for the protection of exterior hulls, cargo and ballast tanks, offshore platforms, and other areas of high marine corrosion. Inorganic zinc-rich coatings are also used in applications requiring abrasion and high heat resistance (to 370^0C, or 700^0F) when not topcoated.

The inorganic zinc-rich coatings use a completely different binder system and so, they are different from the organics. According to the Federal Specification TT-P-641 which covers primer paints and zinc dust/zinc oxides for galvanized surfaces, there are three types of zinc dust/zinc oxide paints:

- *Type I*: zinc dust/zinc oxide linseed oil for outdoor exposure, recommended as a primer or finish coat for broad, general use, especially when there is widespread rusting of the steel surfaces; air dried only

- *Type II*: zinc dust/zinc oxide alkyd resin paint, a heat-resistant paint sometimes sold as a stack paint, may also be used for outdoor exposures where rust is not severe; quick drying; can be air dried or baked at temperatures to 150^0C (300^0F)

- *Type III*: zinc dust/zinc oxide phenolic resin paint; used for water immersion and other severe moisture conditions; may be air dried or baked at temperatures to 150^{0}C (300^{0}F)

The zinc dust/zinc oxide paints possess high covering power. Because the protection provided by the paint is directly related to its thickness, the necessary protection can not be guaranteed unless the dry film thickness is enough for the environment. Therefore, care must be taken to avoid spreading the paints too thin. The type of zinc dust used is a heavy powder, light blue-grey in color, with spherically shaped particles with an average diameter of about 4 μm (17). This powder usually contains 95 to 97 pct. free metallic zinc with a total zinc content exceeding 99 pct. Zinc-rich coatings can be placed into categories depending on the type of binder material used. The coatings with organic binders are similar to coating systems that have been previously discussed, except that zinc-dust pigment is added for galvanic protection. The inorganic solvent-base types are derived from organic alkyl silicates, which become totally inorganic upon curing.

Urethane, vinyl, chlorinated rubber and epoxy polyamide binders are most commonly used to make the organic zinc-rich coatings. Coatings have been made with alkyds for air-dry or baking compositions in the automotive industry. The zinc-dust pigment can not be substituted for the normal inhibitive and filler pigments when making an organic zinc-rich coating. There needs to be careful formulation to maintain a balance between galvanic protection and storage, application, and physical properties of the coating. Such a coating has the physical attributes as determined by the organic binder,

along with the galvanic properties and chemical liabilities of the zinc-dust pigment.

Vinyl and chlorinated rubber zinc-rich primers are easier to topcoat than epoxy and urethane zinc-rich primers for the same reasons that vinyl and chlorinated rubber primers are easier to topcoat than overcatalyzed or excessively hardened epoxies urethanes. Also, the heat resistance of the thermoset epoxies and urethanes is greater than that of the thermoplastic vinyls and chlorinated rubbers. For any of the coatings, the zinc-dust pigment is attacked by acids and alkalies when not topcoated. The binder is resistant to such chemicals, but organic zinc-rich primers should not be used in aggressive environments. The binder determines the drying, hardening, and curing of the coating. The curing and hardening mechanisms of the various binders that have been discussed in the previous sections do not change for the zinc-rich coatings.

The organic zinc-rich coatings are more merciful of poorly prepared surfaces because they wet more readily and seal the rust or old paint that remains on the surface. There is no reaction with the underlying surface other than for the organic vehicle to wet the steel surface thoroughly and to obtain mechanical adhesion. Organic zinc-rich coatings do not require a white blast preparation (21). If the coating is to be used in a mild-service environment, it can be applied to a well-hand-cleaned surface. Topcoating with the same generic type of topcoat (e.g. a vinyl zinc-rich coating covered with a vinyl topcoat) is more readily accomplished, because organic zinc-rich coatings of all types have a less porous surface and are more like conventional organic coatings. This totally organic

system allows for better resistance to continuous exposure to salt water and to acid or alkali chemical fumes.

The advantages of the organic zinc-rich coatings include less critical surface preparation, greater variation in application techniques, less sensitivity to varying climatic conditions (level of humidity) during application and curing, and more flexibility and more resistance to chemical environments. The disadvantages include flammability, blistering, harmful solvent effects, sensitivity to atmospheric influences, and relatively low heat resistance.

Inorganic zinc-rich coatings have been placed into three major groups by the Steel Structures Painting Council (SSPC) (21). These groups are as follows: 1) postcured water-base alkali metal silicates, 2) self-cured water-base alkali metal silicates, and 3) self-cured solvent-base alkyl silicates. In each case, the binder is an inorganic silicate (e.g. glass or sand), but the curing of the binder is different in all three cases.

The postcured water-base inorganic silicates come as three-package systems (17). These components include the zinc dust, silicate binder, and curing solution which are packaged separately. The first postcured zinc-rich coatings were based on a sodium silicate vehicle, and many commercial products still have the same chemistry. There are other formulations based on lithium or potassium silicates that self-cure, but will cure faster by use of a curing solution. Dehydration is the first step in the curing process. The water (or solvent) evaporates from the surface of a clean piece of steel which leaves the

zinc and alkali silicate on the surface as a coating. The coating is very hard and metallic. After the initial drying process, an acid phosphate curing solution is sprayed or brushed over the zinc-rich coating to wet out the entire surface. The initial reaction for the acid is to neutralize the sodium in the sodium silicate solution and create a mildly acidic surface condition. Next, during the initial curing, the pigment components may react with the silica matrix. This reaction, along with further neutralization of the silicate alkalinity, insolubilizes the film.

When an acidic curing solution is added to the surface of the zinc coating, the zinc is ionized in the coating as well as the lead oxide pigment mixed with it (17). While this situation is going on, the active silicate groups and the lead and zinc react quite rapidly to insolubilize the silica matrix. The acid phosphate also reacts with the zinc and lead to form very insoluble zinc and lead phosphates within the silicate matrix. This situation causes the coating to become insoluble to water and resistant to exposure to weather. Further hydrolysis and improvement of film properties, continue after the initial curing over time. After the application and reaction of the curing agent, the remaining soluble salts on the surface are removed with clean water or by weathering. The coating is now dense, relatively nonporous, insoluble in water, and resistant to marine and mild chemical atmospheres. Post-cured coatings are usually the best overall performing of the inorganic zinc-rich coatings because of the properties of the coatings after curing. Maximum protective properties of the coatings are obtained shortly after application of the curing

solution. On the other hand, self-cure coatings rely on ambient atmospheric conditions to cure completely. They do not usually obtain their ultimate resistance and protective capabilities until long after their original application.

The self-curing water-base alkali silicates commonly use potassium and lithium silicates or a combination of these as the silicate binders (18). They can also use lithium hydroxide-colloidal silica and quaternary ammonium silicate as binders. The reactions that the self-cure water-base inorganic zinc-rich silicates undergo is similar to that of the post-cured sodium silicates, but the curing solution isn't applied. The metal silicate vehicle has a higher ratio of silica to metal oxides and a lower alkalinity than the post-cured vehicles before the addition of the zinc-dust pigment. After the water evaporates and the insolubilization resulting from the silica reaction with the pigment, enough neutralization and cure are attained by further reaction with acid formed by the atmospheric hydrolysis of carbon dioxide which forms a weak carbonic acid. These coatings become hard within minutes and are considered generally resistant to precipitation within thirty minutes of application. For a more rapid cure or insolubilization, heat or an acidic curing solution can be applied. The reaction chemistry would then be identical to that of the post-cured sodium silicate matrix.

The self-cured solvent-base alkyl silicates use binders that are basically modified alkyl silicates consisting of partially hydrolyzed members of the series methyl through hexyl or glycol ether silicates (17). The ethyl silicate is the one most commonly used. The

reaction chemistry of the ethyl silicates can best be described by the hydrolysis of tetraethyl orthosilicate in the presence of an acid or alkali catalyst. This reaction goes to partial completion with the degree of hydrolysis ranging from 70 to 95 pct. Because of the volatilization of the alcohol that results from the ester exchange, the reaction is considered irreversible. If the silicate should gel, alcohol can be added to redissolve the gel. While condensation is taking place, the partially polymerized silicate combines with atmospheric moisture to eliminate alcohol, which vaporizes.

When the hydrolysis is complete, the cross-linked network forms a structure to hold the pigment particles. It is a distinct possibility that the zinc and other metallic pigment additives, including the ferrous substrate, may react with the silicate in a manner similar to that of postcured sodium silicate where the silica matrix is insolubilized. The single-package inorganic zinc-rich primers based on the ethyl silicate chemistry previously described have been developed. The coating manufacturer adds the zinc dust in the manufacturing plant along with additives to keep the zinc dust in suspension. Extreme care is taken to keep the zinc-dust pigment and additives moisture free. Also, the ethyl silicate vehicle is somewhat less prehydrolyzed and is usually catalyzed with an acid catalyst such that upon application and curing the reaction with moisture occurs at a faster rate than with two-package ethyl silicate zinc-rich primers. The properties of these single-package primers are similar to those of dual-package primers where the zinc dust is packaged separately from the liquid silicate binder. However, the single-package

inorganic zinc-rich primers do not cure as fast or as hard as dual-package primers. Also, they do not provide as long a corrosion protection, but do maintain excellent protection.

The inorganic zinc-rich coatings do provide somewhat longer galvanic protection than do the organics, but they are less tolerant of poor surface preparation. Generally, they are slightly harder to mix and apply along with being difficult to topcoat. They also have a tendency to mudcrack at increasing thicknesses. The organic zinc-rich coatings have limited temperature resistance which is brought about by which binder is used. Inorganic zinc-rich coatings can withstand dry heat to over 370^{0}C (700^{0}F) (17). If the primer is topcoated with a silicone or ceramic coating, it can be used at temperatures of 650^{0}C (1200^{0}F) or higher. The inorganic zinc-rich coatings also possess superior abrasion and impact resistance. All of the water-base zinc-rich coatings, including post- and self-cured, must have greater surface cleanliness to be able to provide good adhesion and environmental protection. These coatings have a greater possibility to mudcrack at high thicknesses than do the solvent-base inorganics. The water-base coatings also have a greater tendency to form zinc surface reaction products with sodium and lithium silicate vehicles. The biggest advantage of the water-base zinc-rich coatings is that they do not have a flash point and can be used in confined spaces such as tanks, ship holds or poorly ventilated areas. These coatings do require good ventilation or dehumidification to properly cure. Solvent-base inorganic zinc-rich coatings can be modified to increase their flash point, but they often form a softer, less resistant film.

2.5 Welding of Primers

The use of primer-coated steel plate in the fabrication of ships and other structures is increasing more and more. The object is to protect the steel against atmospheric corrosion while it sits in the shipyard waiting to be used for a period of several months. The thickness of these primers is usually not more than 25 ☞m or 1 mil. When primer-coated steel plate is welded, there are various conditions which affect the quality of the welds. The primer can add hydrogen to the weld metal, affect slag and weld metal fluidity, affect weld metal ductility, and produce hygienic dangers. One particular condition of interest is the level of porosity generated within a weld. Research has been conducted to gain insight into the large number of factors which influence the levels of porosity obtained in welds.

Porosity can be affected by the following factors in primer-coated plates: primer pigments, primer binders, coating thickness, electrode type, plate thickness, welding position, heat input, joint geometry, and welding current (22). There are other conditions which affect the quality of a weld, such as the different types of cracking which can be affected by certain types of primers and the hydrogen they provide. These primers can also affect the levels of fumes generated during welding with FCAW consumables and other flux-related welding processes. These fumes may necessitate the need for special equipment to remove the fumes from the welding environment and protect the welder at

the same time. This observation shows that great care must be used when welding over primer-coated steel plates.

2.5.1 Primer-related Weld Discontinuities

For welding steels with higher strengths, hydrogen is extremely detrimental. This is because they are more susceptible to hydrogen assisted cracking, which was discussed previously. The manufacturer of welding materials is usually required to make consumables that produce very low amounts of hydrogen in the arc. It is undesirable for the primer to contribute to the development of hydrogen. The primer supplier should therefore be aware that the dry residue of the primer must not give rise to an increased hydrogen content in the weld metal. An increased level of weld metal hydrogen will lead to cracking in the HAZ and other areas where stresses are high.

Certain components of primers can change the fluidity of the slag and weld metal when mixed together. In such cases, the covering of slag differs from the normal pattern, and may be difficult to remove. Slag rims at the top of the joint are also a result of this fact. Increased fluidity of the weld metal results in a change of the bead profile. This causes a sunken profile to be obtained in a standing fillet weld which is undesirable. A weld cross-section or throat thickness which is too small leads to reduced fatigue strength. These drawbacks appear to occur when zinc is present in the primer (23). The welding

processes behave differently in regards to zinc level and slag/weld fluidity when making comparative tests.

There has been extensive research carried out at several facilities regarding primer-coated steel welding and levels of porosity. Because there are so many factors which can affect the level of porosity in a weld, it is very difficult to look at all of them at once without letting the scale of the experiments become too large. Welding tests conducted at the Philips Welding Development Laboratory, Utrecht in the Netherlands in the early 1970's came to some conclusions about welding primers (22). They examined welding position, current type, plate thickness, electrode type, and five different kinds of primers. They showed that the primer pigment has no influence on the development of porosity, and zinc-epoxy and zinc-ethyl-silicate primers yielded the poorest results regarding the levels of porosity obtained. The conclusions had to be drawn with some reservation because the primer manufacturers do not give detailed compositions of their primers, and only the main constituents were examined. Unfortunately, these tests revealed no applicable guidelines.

In 1987, work was done at BOC, Ltd. in Morden, UK to identify an optimum gas/consumable package for welding primered plate by British shipbuilders (24). Prefabrication primers were developed on the basis of their corrosion resistance, but their ability to be welded over was gaining in importance. A British Standard (BS 6084: 1981) test was developed to assess the porosity level produced in submerged arc welds made

over these primers. They examined two typical primers used by British shipbuilders: NEA407/NEA409 (iron oxide, epoxy) and NQA021/NQA026 (zinc silicate). Porosity became severe and was visible on the surface of the weld bead at low paint thicknesses. The arc stability was also poor, especially with zinc-silicate type primers. The influence of zinc on vapor jet formation in the arc is believed to be responsible for the erratic transfer and spatter encountered with the zinc silicate system.

There was some indication that increasing the CO_2 content delays the onset of porosity, but argon improves arc stability. Gas mixtures with higher levels of oxidizing components improved arc stability and porosity. Asnis et. al. (25) stated that sound welds could be made adding up to 30 pct. oxygen to CO_2. The oxygen improved degasification of the molten weld pool. The use of FCAW electrodes improved the arc stability due to arc stabilizers, slag/metal reactions and a modified transfer mode. The study did suggest that control of paint thickness was poor and needed to be controlled to minimize porosity. It also showed that zinc silicate primers appeared more weldable than iron oxide types when using SAW, but give greater problems when used with GMAW or FCAW (24).

Any paint or primer left in a weld joint will generate gases during subsequent arc welding which may be trapped in the molten weld pool forming porosity. It is normal to remove the primer prior to welding by grinding or grit blasting. Japanese companies have reported that they improved weldability of primers by lower the zinc content of the primer. A new generation of primers, termed "third generation" primers, now claim to be weldable

primers (26). Results have been variable because of primer type, primer thickness, quality control of application, and the welding process. High zinc primers give off excessive amounts of zinc fume which lead to arc instability. Zinc silicate primers also use incombustible ethylsilicate as a polymer/binder. Most developments over the last decade have been to reduce the zinc content to improve their weldability and to decrease the tendency to form porosity. The first zinc silicate primers had up to 90 pct. by weight. The second generation primers contained 40 to 50 pct. zinc and the current third generation primers contain zinc as low as 20 to 30 pct.

Most primers have little or no heat resistance, typically up to 300^0C in the metal surrounding the weld pool, and then only for short periods. Incombustible zinc ethylsilicates can withstand temperatures up to 1000^0C for short periods of time (26). During arc welding, the temperature of the base plate approaches 1600^0C, but the boiling temperature of zinc is about 906^0C. Zinc easily vaporizes and is the major cause of arc instability and porosity in a weld as mentioned before. This can also be the case when welding galvanized steel sheet if the zinc is not removed ahead of the weld according to the Japanese Welding Society (27).

High zinc contents in primers can contribute to occupational sickness called "zinc fever" which requires special precautions. Reducing the zinc level improves welding behavior and reduces the level of spatter. High spatter levels restrict the use of high and medium zinc silicate primers in positional welding. Apart from the primer composition

and thickness, the joint type, welding process and consumable type are process factors which can affect the level of porosity that will be formed in the weld. It is important to note that even though porosity-free welds can be made with the third generation primers, there will always be a risk of porosity under specific process conditions.

According to several investigations, acid-type, rutile and rutile/iron powder electrodes are insensitive both to zinc and iron oxide primers (22,25,26). Low hydrogen electrodes are slightly sensitive to iron-oxide primers and are highly sensitive to zinc primers. Iron oxide primers tend to decrease welding speeds because at higher speeds, porosity is likely to occur. This is also the case with aluminum primers. In general, the zinc primers are more likely to produce more porosity than the others. However, one does get the impression that there are a wide variety of possible primer formulations that might solve the porosity problems.

Porosity is more likely to occur in fillet welds as compared to butt welds. The reason can be attributed to the amount of primer consumed and the ease with which gas can escape. In fillet joints, more primer is trapped within the joint and consumed during welding. This leads to more gas being produced and entering the weld pool. The gases produced from the trailing arc will be sealed in the joint with the only escape route being through the weld pool. Primers have been developed which eliminate the need for removing the primer prior to making a mechanized double fillet weld in the 2F position at high welding speeds (28). The extent of porosity formed is influenced by joint fit-up

which affects gas pressure build up between the plates. The position of the welding gun and the distance between the leading and trailing guns can also have a significant influence on the level of porosity.

A literature review conducted by the Canadian Coast Guard in 1989 on the effect of porosity on mechanical properties stated that between 5 and 10 pct. porosity could be tolerated in fillet welds made with primer coatings (29). However, they did say that further investigations should be made to substantiate this claim. They also stated that for butt welds, the quantity of porosity introduced is not large and current acceptance levels were adequate. Tensile and toughness data taken from several of the butt welds that were welded, which also contained primer, showed no deterioration in properties. They felt that the contribution to the hydrogen content of weld metals from the primer was not critical. This has been shown to be a false assumption. Their results did show that none of the so-called "weldable" primers could be considered as such across the procedure spectrum used, and that their inherent weldability can vary greatly with the welding process position and electrode type.

Flux-cored arc welding electrodes are more prone to produce the various types weld porosity than SMA welding when welding in the flat position. This result is due to the higher welding speeds and faster cooling rates. This is usually the same case for MIG or GMA welding, minus the slag covering. Rutile-based FCA welding electrodes produce a rapidly freezing slag and does not allow sufficient time for gas to escape from the weld

pool. Basic-cored FCA welding electrodes have a more fluid slag which makes them more tolerant to primers in the same manner as the SMA welding electrodes. The more fluid slag allows more time for the gas to escape from the weld pool. This aspect would result in less porosity being produced.

2.5.2 Primer Weldability Tests

Most standards relating to the quality of welds done on primed plates do not provide a clear assessment of the weldability of primers or their tendency to form porosity in production. These standards include the following (30):

- BS6084:1981 - Comparison of Prefabrication Primers by Porosity Rating in Arc Welding
- Lloyds Register of Shipping:1985 - Approval Prefabrication Primers and Corrosion
- DVS 0501:1976 - Testing the Tendency for Porosity when Welding Over Shop Primers
- MIL-STD-248C:1989 - Welding and Brazing Procedure and Performance Qualification
- Bureau Veritas - Rules and Regulations for the Classification of Steel Ships
- Det Norske Veritas - Rules for Classification, Steel Ships
- DAST 006:1980 - Overweldability of workshop primers in steel construction
- NF J 177-115:198 - Shipbuilding, Shop primers influence on the welding ....

The Welding Institute (TWI) developed a test procedure that was aimed at evaluating the third generation primers for arc welding. The test considers the following factors to be important for reproducibility of results:

- The joint type is the T-joint which is the more sensitive joint type.

- The joint fit up is ensured by hydraulic clamping the plates together so that the gap is less than 0.005 inches and provides a barrier to escaping gas.
- The joint is welded in the horizontal-vertical position to reproduce the most severe welding position.
- Welding is carried out by fillet welding to seal one side of the joint before carrying out the second fillet weld on the other side of the standing plate.

The test piece length is about 1 meter long and the clamping force is about 2,000 psi. The welding process used for the test should be the one used in production.

Upon completion of the welding, the test piece is examined visually for porosity. It is then subjected to air-arc gouging to remove the surface metal and submitted for radiography. The level of porosity generated in the weld metal is assessed by visual examination and is quantified by a percentage area of surface breaking indications in any 500 mm of the joint length. The air-arc gouging exposes sub-surface porosity and is measured in the same manner used in the visual examination. This test method also includes a method for accurately measuring the coating thickness over a small area. It was successfully used to evaluate several commercially available primers at the time of development when welded using SMAW, SAW, GMAW and FCAW. A list of these primers can be seen in Table 2.9. The equipment and test procedures were considered by the British Standards Committee WEE 42 for inclusion in the new standard that would replace BS 6084:1981.

Certain professionals might say that a satisfactory weldable primer is impractical, while other sources claim varying degrees of experimental success. Nevertheless, work continues to be done to further develop procedures to evaluate the weldability of primers.

Generic type	International Courtaulds Coatings	SIGMA Coatings
Iron Oxide Epoxy	*Interplate NEA 407/9*	*Weldarite EV 65*
Zinc, Epoxy	*Interplate NLA 230/1*	*Proferral EV*
Zinc Silicate, High Zinc	*Interplate NQA 021/6*	*Proferral MC*
Zinc Silicate, Low Zinc	*Interplate NQA 400/1* *Interplate NQA 805/6*	*Sigmaweld MC*

Table 2.9 A selection of commercially available weldable primers (26).

The National Shipbuilding Research Program (NSRP) SP-3 Panel started a project in 1992 committed to the development of a comprehensive weldable primer system. This involved a literature review, evaluation of conflicting data, experimental analysis, analyzing variable effects, and determining standardized methods and criteria for qualification of primers. They did come up with a list of information that would be needed for a comprehensive certification process that included steel/surface preparation, coating, curing, weld process, and test process that is used. These are all referenced by MIL-STD-248D, ABS Rules and Canadian Coast Guard Standards.

The certification procedure is supposed to qualify the production coating and welding processes applicable to any primer used in shipbuilding. The preparation and testing required in this certification are directed to both the initial qualification of a process and production-quality assurance of the same. The level to which any weld discontinuities affect the performance of a weld during ship construction are set forth as "passable" limitations in the MIL-STD-248D. This is one aspect that makes determining how weldable a primer is very difficult. Many professionals have different ideas about how much porosity determines a weldable primer, as was stated above. They must also include surface preparation of the steel, coating type and manufacture, coating application and dry-film thickness, welding process and consumables, and the fit-up of steel parts.

In the early 1970's, the National Shipbuilding Research Program conducted an extensive evaluation of some commercially available primers (31). They tested 14

different zinc silicate-based, 7 epoxy based, 2 epoxy ester based, 1 phenoxy based and 1 polyurethane based primers. They were evaluated on the basis of application, corrosion resistance, drying time, impact resistance, flexibility, topcoat compatibility and weldability. These were broken down even further to subcategories such as the several different welding processes for the weldability category were included. Around 1,450 steel plates were prepared for the various testing that was performed. The results of this survey were made available to the various shipyards to determine which of the tested primers had the properties best suited to fill their particular requirements. The results were extensive and no particular primer won more than one category. The best overall performance was obtained by the zinc silicate primers. This study reinforces further the fact that primer chemistry greatly affects how a primer will perform, and that work must continue to be done to come up with a universally accepted test for determining a weldable primer.

2.6 Weld Specifications and Testing

Welds can be described by numerous criteria, including welding process used, size, shape, mechanical properties, chemical composition, and a number of others. These criteria will help determine the metallurgical and mechanical responses of the weld metal. It is necessary to characterize weld metal composition and microstructure for welds which the goal is to avoid failures due to inadequate strength, ductility, toughness, or corrosion

resistance (32). In general, the most important goal of weld characterization is to assess the ability of a weld to successfully perform its function.

It is not practical to fabricate an entire structure to evaluate its ability in service due to the high cost that would be encountered. The next best thing is to use some weldability testing and to follow standards and specifications to minimize any problems that might be encountered during fabrication. The standards and specifications provide a guideline for making satisfactory welds with pre-approved welding procedures. The weldability testing helps to determine if two materials (base material and filler metal) can be welded without encountering any cracking problems. In other works, the weldability testing is basically cracking sensitivity testing.

2.6.1 Welding Standards

The purpose of having any kind of standard is to provide a guide to help minimize any kind of problems that might be encountered, for example, during the fabrication of a ship. These standards are the result of numerous hours of experimental study and conversation between governing bodies, such as the AWS (American Welding Society) and the IIW (International Institute of Welding), and industry leaders. These standards cover many areas associated with fabrication from welding consumables to actual fabrication procedures. Many of these specifications dealing with shipbuilding were

covered in the section concerning "Shipbuilding". There are several other standards that are used or considered in some manner.

Most merchant vessels are fabricated conforming with the requirements established by the U.S. Coast Guard an by the American Bureau of Shipping. Most combat and many merchant-type Naval vessels are fabricated according to U.S. Navy specifications. The American Bureau of Shipping (ABS) requirements can be found in its *Rules for Building and Classing Steel Vessels*. The ABS also has separate specifications for river service ships, steel barges, offshore mobile drilling units and manned submersibles.

The Coast Guard regulations are a part of the Code of Federal Regulation and come under Title 46, Shipping; Chapter 1, Coast Guard: Inspection and Navigation. Table 2.10 indicates some of the U.S. Coast Guard Regulations that deal with welded ships. The U.S. Navy specifications concerning welding are presented in five basic documents which were talked about in the section on "Shipbuilding". The detail specifications for each class of ship refer to the basic documents where appropriate. The shipyards that are involved in Naval shipbuilding and repair realize that requirements vary for different ships.

There are specifications that pertain to the base metals used in welding. The ABS has published specifications for hull steel since 1948 which recognizes variations in notch toughness due to thickness of plates by specifying various grades. The U.S. Navy Specification MIL-S-22698A, *Steel Plate, Carbon, Structural for Ships* agrees quite

Sub-Chapter	Subject	Section
D	Tank Vessel	31.10-1, 33.01-5, 35.01-1, 38.05-10
E	Load Lines	43.15-17
F	Marine Engineering	50.25-20, 50.30, 52.05, 52.15-5, 53.13, 54.01-5, 54.05, 54.22, 56.70, Part 57, 59.10
H	Passenger Vessels	72.01-15, 72.01-20, 72.05-10,
I	Cargo and Miscellaneous Vessels	92.01-10, 92.01-15, 98.15-40, 98.20-30, 98.20-70, 98.25-20, 98.25-40, 98.25-90
T	Small Passenger Vessels	177.01-1, 177.10-1
Q	Specifications	160.032-3(f), 160.035-3(e), 160.035-6(e)
Other Sources		
Navigation and Vessel Inspection Circular No.		
7-68	Notes on Inspection and Repair of Steel Hulls	
2-63	Guide for Inspection and Repair of Lifesaving Equipment, p. 4-3 Par. 7, p. 4-7 Par. 5	
11-63	LSTs as unmanned barges; structural reinforcement and drydocking; hull inspection requirements	
1-66	Requirements for Hull Structural Steel—Structural Continuity	
12-69	Special Examination in lieu of drydocking for large mobile drilling rigs	
Equipment Lists	Items Approved or Accepted under Marine Inspection and Navigation Laws CG-190 (Includes list of approved electrodes)	

*From "Code of Federal Regulations," Title 46, Shipping; Chapter 1, Coast Guard; Inspection and Navigation.

Table 2.10 U.S. Coast Guard regulations* pertaining to welded ships (15).

closely with the ABS specifications. The U.S. Navy has other specifications concerning steel plate. MIL-S-16113C, grade HT deals with high-tensile strength steels (85 to 92 ksi) depending on grade or chemistry. MIL-S-24113 covers C-Mn steel plates heat treated by quenching and tempering (QT50). The popular HY-80 and HY-100 steels used for submarine hulls and in certain areas of naval surface ships are covered in MIL-S-16216F.

The filler metals used for Navy ships are qualified for use by tests in a Navy-approved laboratory (15). Lists of qualified filler metals are issued at intervals by the Naval Ships Engineering Center. Filler metals for welding on ships classified by the ABS are qualified by demonstration by the electrode manufacturer, in the presence of a Surveyor of ABS. Lists of the approved filler metals are issued annually by ABS, and they are also accepted for use by the U.S. Coast Guard. The U.S. Navy provides an electrode specification, MIL-E-22200/1 with several classifications and intended uses. These classifications can be seen in the section on "Shipbuilding" and include:

American Welding Society

- A5.1 - Covered Carbon Steel Arc Welding Electrodes
- A5.5 - Low Alloy Steel Covered Arc Welding Electrodes
- A5.17 - Carbon Steel Electrodes and Fluxes for Submerged Arc Welding
- A5.18 - Carbon Steel Filler Metals for Gas Shielded Arc Welding
- A5.20 - Carbon Steel Electrodes for Flux Cored Welding
- A5.23 - Low Alloy Steel Electrodes and Fluxes for Submerged Arc Welding
- A5.25 - Consumables Used for Electroslag Welding of Carbon and High Strength Low Alloy Steels
- A5.26 - Consumables Used for Electroslag Welding of Carbon and High Strength Low Alloy Steels
- A5.28 - Low Alloy Steel Filler Metal for Gas Shielded Arc Welding

- A5.29 - Low Alloy Steel Electrodes for Flux Cored Arc Welding

U.S. Navy

- MIL-E-15599 - Electrodes, Welding, Covered, Low-Medium Carbon Steel
- MIL-F-18251 - Fluxes, Welding, Submerged Arc Process, Carbon and Low Alloy Steel
- MIL-F-19922 - Fluxes, Welding, Submerged Arc Process, Carbon and Low Alloy Steel
- MIL-E-19822 - Electrodes, Welding, Bare High Yield Steel
- MIL-E-22200/1 - Electrodes, Welding Mineral Covered, Iron Powder, Low Hydrogen Medium and High Tensile Steel
- MIL-E-22200/6 - Electrodes, Welding Mineral Covered, Low Hydrogen, Medium and High Tensile Steel
- MIL-E-22749 - Electrodes (Bare) and Fluxes (Granular) Submerged Arc Welding, High Yield Low Alloy Steels
- MIL-E-23765 - Electrodes and Rods-Welding Bare, Solid, Mild Steel
- MIL-E-24403A - Electrodes - Welding, Flux Cored, General Specification
- MIL-E-24403/1D - Electrodes - Welding, Flux Cored, Ordinary Strength and Low Alloy Steel
- MIL-E-24403/2C - Electrodes, Welding, Flux Cored, Low Alloy Steel

American Bureau of Shipping

- Rules for Approval of Electrodes for Manual Arc Welding in Hull Construction
- Provisional Rules for the Approval of Filler Metals for Welding Higher Strength Steels
- Rules for Approval of Wire-Flux Combinations for Submerged Arc Welding
- Provisional Rules for the Approval of Wire-Gas Combinations for Gas Metal Arc Welding

The filler metals used in shipbuilding are described by a variety of specifications issued by AWS, U.S. Navy and ABS, and are updated on a regular basis. They cover all types of

electrodes used in the different welding processes. They deal with how to package, store and handle the electrodes to sample preparation for testing.

The standards named above deal with several aspects of a particular welding process. As an example, AWS A5.29, *Low Alloy Steel Electrodes for Flux Cored Arc Welding* covers everything from method of manufacture to details of tests performed on the weld metal (33). It begins by explaining how electrodes are classified according to shielding gas, weld current, weld position, chemical composition, and mechanical properties of the weld metal. Then, it lists some of the acceptance requirements for procurement, chemical composition, and mechanical testing performed. The mechanical tests include radiographic soundness, all-weld-metal tension, vertical and overhead fillet weld, and Charpy V-notch impact tests. There are tables that list mechanical property requirements for strength and elongation, and impact requirements as well as guidelines for the mechanical tests. The method of manufacturing is also covered with reference to standard sizes and lengths of electrodes to standard forms. They give dimensions for winding requirements around spools, packaging and marking.

2.6.2 Welding Specifications

There are several welding specifications that govern how a weld metal is examined or tested. As mentioned earlier, the weld metal can be subjected to several mechanical tests. These tests are governed by the AWS specification B4.0, *Standard Methods for*

Mechanical Testing of Welds (34). It covers the following tests: bend, fillet weld break, tension, fracture toughness, and fillet weld shear. Each one of the tests listed in the specification has the same general procedure. It begins with the scope of the test and what it hopes to accomplish.

Next, it relates any applicable documents and standards that should be consulted for the test. These include any ANSI, ASTM, and AWS standards. It also gives a brief summary of the test method and the significance of the test. The apparatus that are used for the test are then discussed and shown in several figures. There are usually several types of specimens that can be used for the tests and these are discussed. This section is where the effects of primers could be examined. The last things looked at are the procedures and reports to be made upon completion of the tests.

The weld can be looked at visually to see if it is acceptable in terms of appearance and porosity. This visual inspection is governed by AWS B1.11, *Guide for the Visual Inspection of Welds* (35). It starts off by stating some general provisions, prerequisites and fundamentals for visual inspection. These might include equipment, experience, safety, welding procedures, joint fit-up, and discontinuities. It then talks about general weld surface conditions from the point of the weld discontinuities and what to look for. It also talks about arc strikes, spatter, slag inclusions, and weld profiles. The equipment used in examination is also covered. It talks about ammeters, temperature sensitive crayons, weld gages, ferrite gages, and several others. This standard also lists several

other applicable standards from groups such as ASME, ANSI, API, AISC, ABS, and AWS.

The military specifications are quite similar. As an example, MIL-E-24403/2C begins with its scope stating that the specification covers low alloy steel FCA welding electrodes for the fabrication of HY-80 and HY-100 steel weldments (36). It briefly states several applicable documents whether they are Federal, Military, or non-Governmental publications such as ASTM and AWS. This specification also gives many of the same requirements that the AWS specification does as far as conformance, chemical composition and mechanical properties. These requirements are listed in tables as in the AWS specification. It also mentions some of the guidelines used for the mechanical testing done on the weld metal deposits.

There is one difference in that the military specification makes reference to diffusible hydrogen requirements. These requirements are determined using diffusible hydrogen tests over mercury or using gas chromatography. Hydrogen is considered the most harmful to welds because of its ability to increase cracking problems. Therefore, it is important to determine hydrogen values generated by the weld metal and consumables.

The specification for this hydrogen test is given in the AWS specification A4.3, *Standard Methods for Determination of the Diffusible Hydrogen Content of Martensitic, Bainitic, and Ferritic Weld Metal Produced by Arc Welding* (37). This specification begins by stating its scope, units of measure, followed by preparation of the weld test

assembly. The test assembly consists of three pieces (starting weld tab, run-off tab and test piece) of A36 or SAE1020 nonrimming quality steel. The cross-section of the three pieces should be 25 x 12 mm ± 2 mm (1 x 1/2 in. ± 1/16 in.). The length of the test piece should be 80 mm ± 5 mm (3-1/8 in. ± 1/4 in.). The length of the weld tabs are arbitrary as long as they comply with certain requirements as seen in Figure 2.15.

The test assembly is degassed for one hour minimum in air, vacuum, or inert gas at 400^0 to 650^0C (750^0 to 1200^0F) to remove any hydrogen present in the material. If the assembly was machined to size prior to heat treatment and no scale appears on the test pieces, then no descaling is required. If scale is present, then the test assembly must be descaled by some "dry" method to avoid contamination. The test pieces should be stamped to allow for easy identification, but not to interfere with proper welding. The test pieces are weighed to the nearest 0.1 g or less and recorded for future use. Just before the samples are welded, the test assembly is degreased in alcohol or acetone. After this point, the samples are handled with rubber gloves or clean tongs.

The test assembly is placed in a copper holding fixture to keep the three pieces in alignment and in firm contact, and also to serve as a heat sink. A schematic of the copper holding fixture can be seen in Figure 2.16. The copper foil seen in the schematic is used to protect the copper clamping fixture from errant arc strikes. It can also be used to contain fluxes used during submerged arc welding. Quick release devices or clamps should be used to facilitate easy removal of the test assembly. It is also recommended that the weld

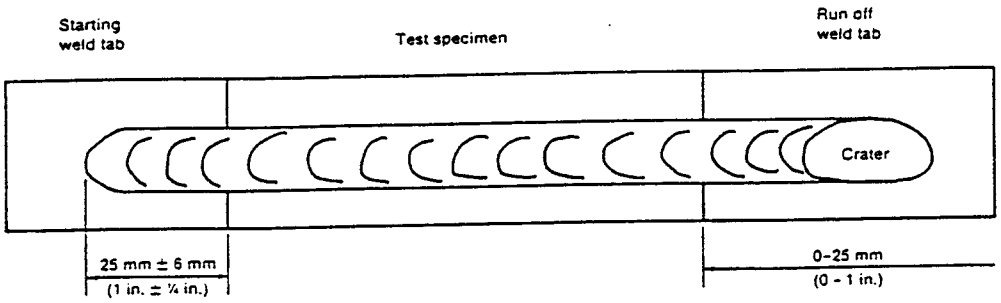

Figure 2.15 Weld test assembly after welding, with correct dimensions for weld bead length on the weld tabs (37).

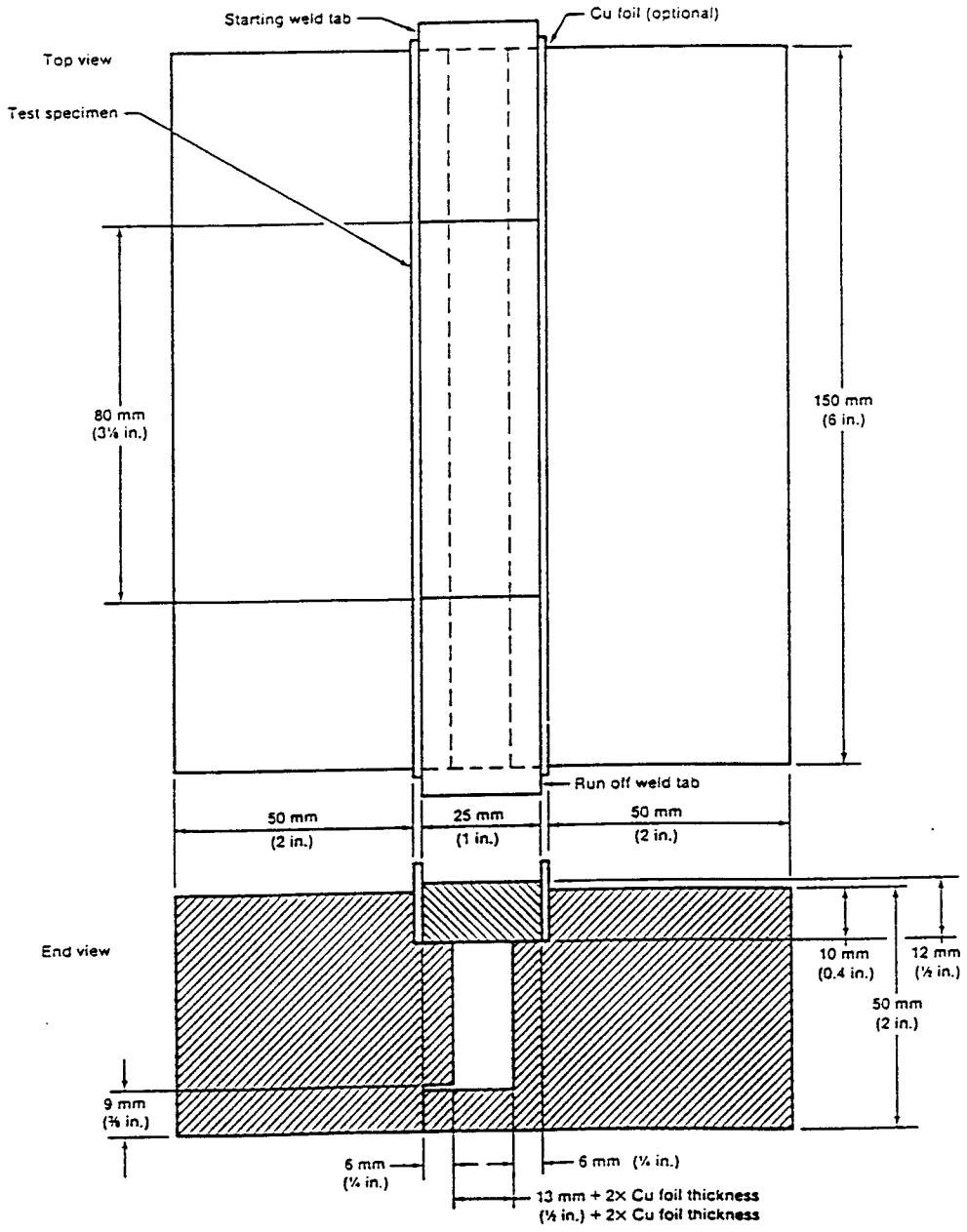

Figure 2.16 Weld test assembly in suggested copper clamping fixture (37).

tabs extend a short distance beyond the ends of the copper fixture to aid in the easy removal of the test assembly. The copper clamping fixture should be cool to the touch before each test assembly is welded. Water cooling may be used, but the fixture needs to be free of condensation or moisture when welding.

Before welding can begin, welding parameters should be adjusted to the desired settings and not changed during the tests. The parameters are recorded for future use. A bead-on-plate technique is used on the test assemblies to deposit the weld metal. The arc is initiated on the start tab and continued uninterrupted until the specified position of the crater is reached on the run-off tab. Decreasing the travel speed for crater filling is not permitted. Within five seconds of extinguishing the arc, the test assembly is removed from the copper fixture and plunged into ice water. The test assembly is stirred vigorously for about thirty seconds, rinsed off with acetone to remove the water, and then placed into a low temperature liquid bath of dry ice and ethanol or liquid nitrogen. All the weld test assemblies shall be completed within sixty minutes after beginning the first weld.

After the temperature of the liquid nitrogen has stabilized with the test assemblies in it, the test assemblies can be removed one at a time for cleaning. The maximum time out of the bath is no more than one minute. A power brush is used to remove any adhered slag and oxide on the test piece. After cleaning, the weld tabs are broken off and the test piece is placed back in the bath. Any samples not corresponding to the specification are discarded. After the temperature of the liquid nitrogen has again stabilized, the samples

can then be removed and placed in the testing apparatus or stored for up to three weeks in the liquid nitrogen.

There are two types of analytical apparatus that can be used for collecting diffusible hydrogen. One is a mercury-filled eudiometer tube (seen in Figure 2.17), and the other one is a gas chromatograph. The specification contains procedures for both. Both apparatus involve loading the test piece into an isolation chamber where the hydrogen diffuses out of the test piece and is recorded. All moisture should be removed from the samples before they are placed in the isolation chambers. A sample is removed from the liquid nitrogen bath and stirred in cold water to remove any ice present on the sample. The sample is then rinsed with acetone or ethanol to remove the water, or blown dry before loading. The sample is then immediately loaded into the eudiometer tube, and the mercury is drawn up around the sample with a vacuum pump. The time from the test piece reaching 0^0C to sealing the isolation chamber or eudiometer shall not exceed 150 seconds. Any delays in placing the sample in the eudiometer or isolation chamber can cause the results to be thrown off.

The bottles of mercury are placed in a heated water bath. The temperature of the mercury bath is about 45^0C. At this temperature, the samples will require 72 hours or 3 days to allow at least 90 pct. of the diffusible hydrogen out of the test piece. If the temperature of the bath can be raised to 150^0C, the diffusion time is reduced to six hours. The amount of diffusible hydrogen collected is converted to Standard Temperature and

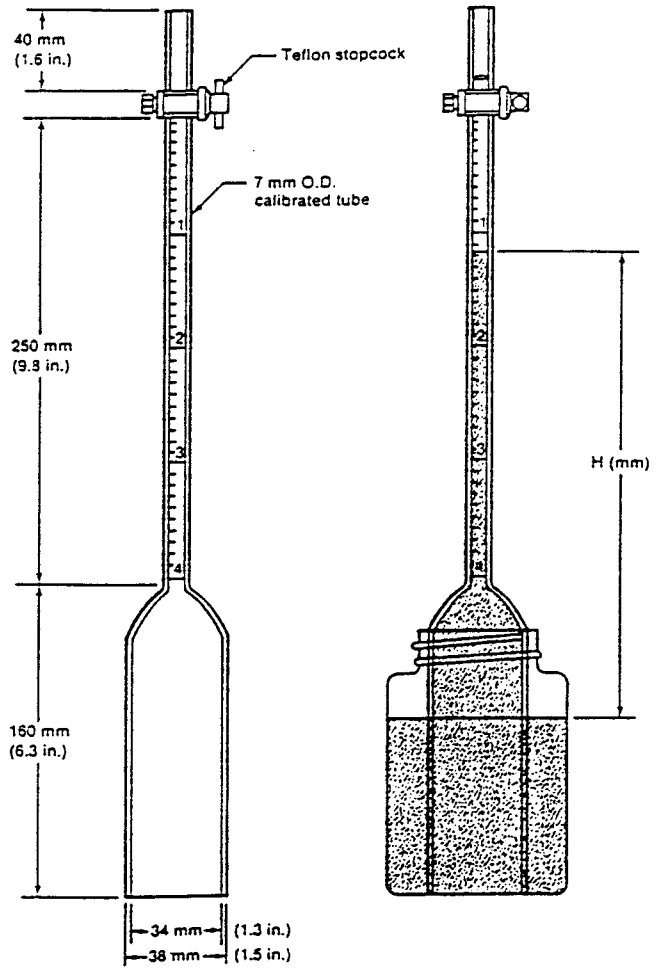

Figure 2.17 Eudiometer tube and assembly for standard mercury displacement procedure (37).

Pressure [0^0C (32^0F) and 760 mm Hg (14.7 psia)] by the following equation for mercury displacement:

$$VH = \frac{273}{(273 + T)} * \frac{(P - H)V}{(760)} \quad \text{.....(2.6.1)}$$

where T is the gas column temperature (^{0}C) at time of measurement, P is the barometric pressure (mm Hg) at time of measurement, V is the measured volume of gas in the eudiometer tube (ml), H is the head of mercury (mm) at time of measurement, and VH is the volume of hydrogen gas converted to STP (ml). The equation used for gas chromatography doesn't account for the H. After the hydrogen analysis, the test piece is removed from the mercury and cleaned. The sample is then weighed to the nearest 0.1 g and recorded. The increase in weight is taken as the weight of deposited weld metal. Then the hydrogen volume, converted to STP, is multiplied by 100 and divided by the deposit weight to obtain the diffusible hydrogen value in ml/100 g of deposited metal. It is preferable to run four nominally identical tests to allow an average to be calculated, and to throw out any samples which are unsatisfactory. This average is then reported as the diffusible hydrogen value for the particular welding process and set-up used.

From the previous sections, it is easy to see that there are numerous standards and specifications that must be followed in the fabrication of a welded ship. The purpose of these standards is to help minimize any complications that may be encountered when

trying to make satisfactory welds. This minimization of complication can also be helped by actual weldability testing.

Chapter 3

EXPERIMENTAL APPROACH

This section will give a brief description of the problems encountered with hydrogen production during welding over primer-coated steels followed by a description of the experimental phases used to verify some of the discussion developed concerning the solutions to the hydrogen problems encountered to ensure that as many aspects concerning the project were covered as possible. Many of the experimental phases were changed slightly as new concerns or problems arose.

3.1 Definition of Problem

It is commonly known that one of the most potent problems in welding steels is the production of hydrogen gas, which can be absorbed into the weld pool. This hydrogen in turn will lead to cracking problems as the hydrogen diffuses to areas of higher stress concentration in C-Mn and low alloy steel welds (38). The welding process generates high stress concentrations as the weld pool cools. In higher carbon and higher strength steels, this cracking problem can be quite detrimental to the integrity of the weld, requiring special precautions before welding or special consumables be developed to minimize any potential problems (39).

This hydrogen can come from several sources such as moisture in the air, moisture absorbed by the fluxes, moisture in the shielding gas, or contamination of the weld joint. In the case of shipbuilding, hydrogen can be absorbed by the weld pool when a primer is welded over. Because many primers contain compounds that contain hydrogen such as alcohols, benzenes, epoxies, and ethyl silicates, when the primer decomposes it produces gases. These gases include, but are not limited to carbon monoxide, carbon dioxide, hydrogen, water vapor, and if the primers contain zinc, zinc vapor and zinc oxide gases. Most of these gases lead to porosity problems which can affect the mechanical properties of the weld. However, the most detrimental gas is hydrogen, and it can negatively affect mechanical properties by increasing cracking sensitivity and impact strength through porosity levels.

The best way to minimize hydrogen problems is to avoid absorption of hydrogen by the weld pool. This approach has been attempted by electrode manufacturers and electrode users through baking of the electrodes, cleaning the weld surfaces, and purifying the shielding gas. As was previously stated, one possible way to minimize hydrogen pick-up by the weld pool is by affecting the equilibrium hydrogen content in the weld pool through welding consumable design. To test this proposed approach, the research project was divided into four experimental phases.

3.2 Experimental Phases

The main goal of this research project is to decrease hydrogen pick-up in the molten weld pool when welding over paint primer, which during decomposition acts as a contaminant and increases the level of hydrogen produced. To achieve this goal, a clear understanding of the interactions that take place between the paint primer and the welding fluxes needs to be developed. From this information, a methodology for the development of a flux-cored arc welding consumable that controls hydrogen pick-up in the weld pool and the associated weld discontinuities will be developed though these experimental phases.

Phase I of the research began with verification of the [H]-[O] relationship. Several test welds were made using a pre-selected FCA welding base electrode. These experiments involved using no paint primer on the weld samples. The samples were prepared by Ingalls Shipbuilding and sent to CSM for testing. Several high oxidizing potential fluxes which included Fe, Fe_2O_3, FeO, SiO_2, and $CaCO_3$ were chosen for testing. CO_2 shielding gas perturbed with hydrogen was used to increase to increase hydrogen pick-up in the weld pool. By combining the fluxes in varying amounts and combinations, the [H]-[O] relationship could be verified. The tests performed in Phase I involved diffusible hydrogen, oxygen analysis, and macro- and microstructural examination.

Phase II involved welding experiments with the high oxidizing potential fluxes in various combinations and the Phase I electrode. Two different paint primers were used in

the welding experiments: an inorganic, zinc ethyl-silicate based primer and an organic, epoxy-zinc-based primer. The inorganic primer was tested at several thicknesses as compared to only one thickness of for the organic primer. Of the oxidizing fluxes used in Phase I, only the FeO, SiO_2, and $CaCO_3$ were used in Phase II, and Fe_2O_3 was substituted for FeO. Since fluorides were suggested to behave in the same manner as the oxidizing fluxes in their removal of hydrogen from the weld pool, several fluorides were also added. The addition of fluorides would be beneficial because if the oxygen level in the weld gets too high, mechanical properties deteriorate. These experiments would determine, what type of additions would be beneficial to add to the pre-selected FCA welding electrode for further testing. The tests performed here involved oxygen analysis, selected chemical analysis, and macro- and microstructural examination along with some selected diffusible hydrogen.

Phase III of the research involved manufacturing four different electrodes based on the results from Phase II. The manufacturing of the electrodes was done by ESAB with the CSM recommendations for flux additions. The Phase III weld experiments involved both primer types at three different primer thicknesses. The tests performed here included diffusible hydrogen, oxygen analysis, selected chemical analysis, Charpy V-notch tests, tensile tests, hardness measurements, and macro- and microstructural examination.

Phase IV of the research involved incorporating results from Phase III into two more fine-tuned FCA welding electrodes for manufacture by ESAB. They might also

recommend additions that would aid in the fine-tuning of the electrode. The electrodes manufactured were distributed to several shipyards for round-robin testing. The results from these tests would allow for the determination of the performance of the electrodes recommended by this research, in controlling hydrogen pick-up by the weld pool and minimizing discontinuities.

3.3 Goals

The specific goal of this research project was to establish a methodology for the development of a flux-cored arc welding consumable that would allow for direct welding over primer-coated steel while maintaining adequate mechanical properties. Direct welding over primer would eliminate the need for removing the primer prior to welding which would result in a savings of time, grinding or blasting media, and disposal of spent products. This cost savings could result in lower fabrication costs of future ships. Modification of any flux system is complicated because of the numerous competing reactions that take place in the welding arc and weld pool. Adding the primer to this equation can further complicate the analysis. In addition to cost reduction, it is also the objective of the program to minimize weld discontinuities originated by the primer. This objective could be accomplished by minimizing hydrogen pick-up in the weld pool or increasing gas removal from the weld pool. Increasing gas removal from the weld pool would involve changing the viscosities and cooling characteristics of the slag and weld

metal which would result in greater gas permeability. However, it was decided that minimizing hydrogen pick-up by affecting the equilibrium hydrogen content in the weld pool by changing the welding consumable design would prove to be more successful.

There were two main objectives that acted as a guide toward our goal. The first objective was to characterize the influence of the preconstruction primers on arc welding performance and weld discontinuity formation. The second objective was to develop a clear understanding of the interaction between a primer and the welding arc, and the strategies necessary to eliminate weld discontinuities originated from the decomposition of the primer. By focusing on these objectives, it should be possible to develop the guidelines necessary for the manufacture of a FCA welding consumable that would meet the requirements set forth in this program.

Chapter 4

EXPERIMENTAL PROCEDURE

This particular section will describe all materials (e.g. base material, FCA welding electrode, primers, oxide fluxes, fluoride fluxes), equipment and procedures used in the experimental work.

4.1 Base Material

The base material used in these experiments was a DH-36 plate supplied by Ingalls Shipbuilding. The overall composition of DH-36 can be seen in Table 4.1. It has a carbon equivalent of 0.134 wt. pct. using the Ito-Bessyo equation (40). The plate was 3/8 in. (9.5 mm) thick and was flame-cut into sizes according to AWS A4.3 to allow for diffusible hydrogen testing. The sizes of the run-off tabs were 1 x 2 in. (25.4 x 50.8 mm) and the test specimens were 1 x 3-1/8 in. ± 1/4 in. (25.4 x 79.4 mm ± 6.4 mm) long. The samples were ground flat, degassed, ground to remove scale, and degreased with acetone prior to welding. Samples not used for diffusible hydrogen testing were 1 x 8 in. (25.4 x 203.2 mm) long. Samples were also coated with primers to be used for diffusible hydrogen testing. Because of the primers, they could not be machined, degassed, or degreased. The

Chemical Species	Wt. Pct.
Carbon	0.05
Sulfur	0.009
Phosphorus	0.006
Silicon	0.24
Chromium	0.04
Nickel	0.05
Manganese	1.33
Copper	0.04
Molybdenum	0.01
Columbium	0.025
Titanium	<0.01
Aluminum	<0.01
Vanadium	0.067
Cobalt	<0.01
Boron	.—
Tungsten	<0.01
Iron	Base
Lead	<0.01

Table 4.1 Chemical composition of DH-36 base plate (CE=0.134 wt. pct.).

difference in specimen preparation resulted in slightly more hydrogen being introduced into the diffusible hydrogen tests since the guidelines of A4.3 could not be followed exactly.

4.2 Welding Electrode

The electrodes used in these experiments were all flux-cored welding consumables. The base FCAW electrode was the Dual Shield II 71 Ultra (0.052" dia.), and was supplied by ESAB Welding and Cutting Products in 50 lb boxes (5 - 10 lb spools). The AWS classification of the electrode is E71T-1 and corresponds to the AWS A5.20, *Carbon Steel Electrodes for Flux-Cored Welding.* The sheath of the electrode is a low carbon steel whose chemistry can be seen in Table 4.2.

The flux is a rutile-based mixture with about 50 pct. being rutile. There are also additions of sodium and potassium compounds for arc stability along with small additions of a fluoride, possibly CaF_2. The alloy additions include manganese and ferro-silicon. The deoxidizers present include aluminum, magnesium, and silicon. There are also additions of iron powder to increase the deposition rate. There are other components present, but the exact amounts are not known. The spools were baked in an oven at 150^0C overnight before being used in welding. This particular electrode uses CO_2 as the shielding gas. For Phase I of the research, 4 pct. hydrogen was added to increase the chance of hydrogen pick-up in the weld pool. The base electrode was used in both Phase I and II. The

Chemical Species	Wt. Pct.
Carbon	0.025
Manganese	1.11
Silicon	0.3
Phosphorus	0.012
Sulfur	0.012
Titanium	0.021
Boron	0.0044

Table 4.2 Chemical composition of 0.052 in., Dual Shield II71 Ultra FCAW electrode.

experimental electrodes manufactured for Phase III of the project were done so by ESAB Welding and Cutting Products. The experimental consumables were based upon the Dual Shield commercial product.

4.3 Pre-Construction Primers

There were two types of primers used in these experiments. One was an inorganic, zinc-ethyl silicate based primer and the other was an organic, zinc-epoxy based primer. The inorganic primer was Interplate NQA238 supplied by International Marine Division and is used extensively by Ingalls Shipbuilding. Ingalls coated the samples with this primer since they had the facilities for the job. The thicknesses of the Interplate NQA238 includes 1.0, 1.5, 2.0, and 4.0 mils. The color of the primer was a pale green. The higher thicknesses are rarely used in ship fabrication, but they were used here to determine their effects on welding. The exact composition of the primer is also proprietary, much like the electrode. Information about the primer can be seen on its MSDS (Material Safety Data Sheet) as far as physical data, health concerns, and storage procedures.

Even though the focus of the experiments was on the Interplate NQA238, it was decided to examine the effect of an organic primer at the 4.0 mil thickness. The organic, zinc-epoxy based, water reducible primer chosen was the Valspar V13F40 supplied by Jotun Valspar. Because Ingalls did not have experience in applying this particular primer, samples were coated by Valspar and shipped to CSM. The color of this primer was also

green. Before any of the steel coupons were coated with the primers, they were blast cleaned to an acceptable "Near White" SSPC-SP 10 condition to provide and adequate profile for coating.

After the samples were coated by Ingalls, they were shipped to CSM so that the primer thickness could be monitored. A digital thickness gauge (Positector 6000: Model F2) was used to measure the coating thickness with the ability to determine the variance, or standard deviation, of the measurements. The following guidelines were used in measuring the primer thicknesses. Each sample was measured five times. For a sample to fit into a particular thickness range, its average had to be within ±10 pct. of the specified value (e.g. a 2.0 mil sample → 1.8 to 2.0 mils) and have a variance or standard deviation of no more than ±20 pct.. Any samples that did not fit these requirements were sent back for recoating. This was done with both the Interplate and Valspar coated samples.

4.4 Flux Additions

The focus of this research was to decrease hydrogen levels in welds by increasing the oxygen potential of the flux. This goal was accomplished by adding several high oxidizing potential fluxes: $CaCO_3$, SiO_2, Fe_2O_3, and FeO. FeO was obtained from CF&I Steel as mill scale. The FeO was ground and sized to -70 and +200 mesh. The flux was analyzed using X-ray diffraction and found to be a 50/50 wt. pct. mixture of FeO and

Fe_2O_3. The Fe_2O_3 was made by Fisher Scientific Company. The $CaCO_3$ was made by Merck and Company, Incorporated. The SiO_2 manufacturer was not known.

All the particle sizes were relatively fine and their apparent densities were determined by ESAB to be 0.83 g/cc for the SiO_2, 0.33 g/cc for the $CaCO_3$, and 0.60 g/cc for the Fe_2O_3 which is quite different from the actual bulk densities (SiO_2 = 2.635, $CaCO_3$ = 2.71, Fe_2O_3 = 5.24). Iron powder ($\approx$ 225 mesh) was also used to help with deposition rates. There were several different combinations of these fluxes used to perturb the oxygen levels in the weld metals in each of the various phases. These combinations will be presented when discussing the results of the experiments. The fluxes were baked in an oven at 400^{0}C overnight to remove any absorbed moisture before use.

Besides the oxidizing fluxes, fluorides such as AlF_3, MnF_3, and ZrF_4 were also used to see how they might help control hydrogen levels in weld metal. These fluorides were chosen because of their different properties (melting temperature, alloying ability, deoxidation ability, amount of fluorine, etc.). These fluorides were subjected to many of the same types of tests and preparation as the oxidizing fluxes. These fluorides did not have information about their particle size on the labels, nor did the manufacturers have that information. ESAB did some analysis on only the MnF_3 and found it to be quite fine with an apparent density of 1.06 g/cc (bulk density is 3.54).

4.5 Welding Operation

The welding experiments at CSM involved making bead-on-plate welds on the DH-36 base plate using a semi-automatic, flux-cored arc welding system. The power source used was the Miller Maxtron 450. It is a constant current/constant voltage, direct-current welding power source. It has multi-process capabilities such as GMAW, GTAW, SMAW, and air carbon arc cutting and gouging, along with the ability of pulsing. The Maxtron 450 is rated at 450 A, 38 V DC at 100 pct. duty cycle and equipped with 14-pin and 17-pin remote control receptacles which allows for an automatic wire feeder to be used, such as the Miller S-64M Wire Feeder.

This wire feeder is microprocessor-controlled, constant speed wire feeder. It is used with our FCA welding, but also with GMA welding and GMA-pulsed welding. It can handle wire sizes from 0.023 to 0.125 inch (0.6 to 3.2 mm) wires. Wire feed speeds of 50 to 780 IPM can be handled by the wire feeder. The wire feeder can be programmed for any typical weld cycle desired (pre-flow time, run-in time & speed, weld time & speed, crater time & speed, burnback time, and post-flow time) with the weld current being controlled by the wire feed speed (WFS).

To make the set-up mechanized, the welding torch (Miller GW-60A, water-cooled gun) was placed upon a tractor and track system. The tractor used was the AIRCO No. 41 Radiagraph Tractor System and the welding torch was cooled using a Miller Coolmate 3 recirculating coolant system for water-cooled GMA welding guns. The Coolmate 3 was

hooked up to the Maxtron 450 so when its power was turned on, the Coolmate 3 would also be running. The tractor system had to be turned on separately before the welding cycle could be initiated.

The welding cycle was turned on using an ordinary light switch which activated the welding cycle. This switch had been wired into the S-64M Wire Feeder to activate this welding cycle. The CO_2 shielding gas was plugged into the rear of the wire feeder to provide shielding to the weld pool through the welding torch. The following welding parameters were used during the experiments: 25 V, 220 A, and 14 ipm travel speed (Phase I); and 27 V, 260 A, and 14 ipm travel speed (Phase II and III). These parameters produced heat inputs of 0.70 to 0.89 KJ/mm. The contact-tip-to-work distance (CTWD) was fixed at ¾ inch. The bead-on-plate welds were made using the experimental set-up pictured in Figure 4.1. This copper fixture is the one described in the AWS specification A4.3-86.

4.6 Chemical Analysis

Chemical analysis of the base material and weld metal was done by Colorado Metallurgical Services using an ARL 3460 Optical Emission Spectrometer. Analysis results of the welding wires were provided by ESAB Welding and Cutting Products. CSM performed the oxygen and hydrogen analysis. The oxygen was determined using a Leco TC-136 analyzer. Some selected carbon analysis was done using the Leco CS-244 analyzer.

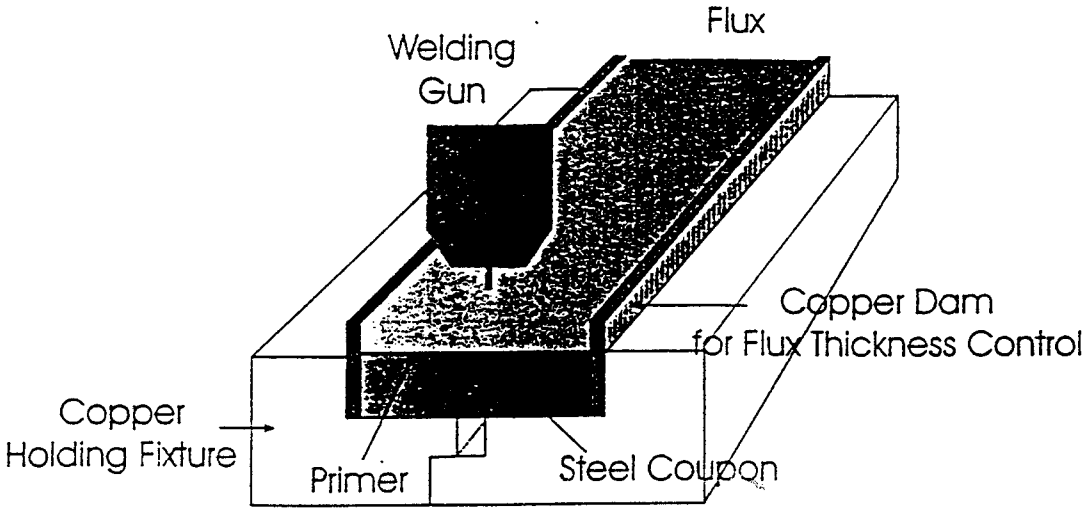

Figure 4.1 Schematic set-up used for welding experiments (corresponds to set-up used in Ref. 37).

Preparation of the weld samples for oxygen analysis involved removing the base metal and the weld bead reinforcement, and any remaining undiluted base material with a belt grinder. The samples were then cut into approximately 0.5 gram pieces to use for analysis. Five specimens were run for each sample to help remove any variation in oxygen levels that were outside normal values, so an average was taken after running 3 to 5 specimens and was reported as the level of interstitial oxygen in the weld metal.

4.7 Mechanical Testing

The mechanical properties were determined using all-weld metal tensile, transverse tensile, Charpy V-notch samples, and fillet weld break tests. All the tests were governed by AWS B4.0 as far as size requirements and test conditions. The tensile and Charpy samples were machined from multi-pass welds which were made by Ingalls Shipbuilding because they were better equipped to make those types of weldments. They also conducted the transverse tensile and fillet weld break tests.

The all-weld-metal tensile specimens were 0.5 ± 0.010 in. (12.7 ± 0.25 mm) in diameter with a gage length of 2.0 ± 0.005 in. (50.8 ± 0.13 mm) and a minimum length reduced section of 2.25 in. (57.2 mm). A description of the all-weld-metal tensile specimens can be seen in Figure 4.2. A description of the transverse tensile samples can be seen in Figure 4.3. The samples were tested on an MTS testing apparatus. The fillet weld break test samples can be seen in Figure 4.4. The plates 3/8 in. (9.5 mm) thick,

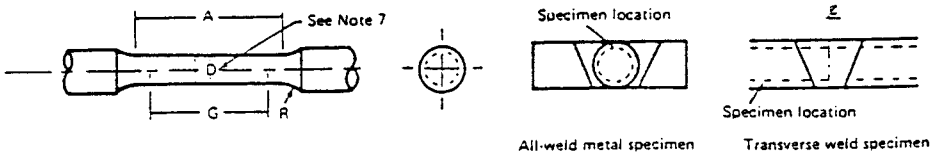

All-weld metal specimen Transverse weld specimen

Dimensions

Nominal Diameter	Standard specimen		Small-size specimens proportional to standard							
	in. 0.500	mm* 12.5	in. 0.350	mm* 8.90	in. 0.250	mm* 6.35	in. 0.160	mm* 4.05	in. 0.113	mm* 2.85
G gage length	2.000 ± 0.005	51.0 ± 0.125	1.400 ± 0.005	35.5 ± 0.125	1.000 ± 0.005	25.5 ± 0.125	0.640 ± 0.005	16.0 ± 0.125	0.450 ± 0.005	11.5 ± 0.125
D - diameter (Note 1)	0.500 ± 0.010	12.5 ± 0.255	0.350 ± 0.007	8.90 ± 0.180	.250 ± .005	6.35 ± .125	.160 ± 0.003	4.05 ± 0.075	.113 ± 0.002	2.85 ± 0.05
R - radius of fillet min	3/8	9.5	1/4	6.5	3/16	5.0	5/32	4.0	3/32	2.5
A - length of reduced section, min (Note 2)	2-1/4	57.0	1-3/4	44.5	1-1/4	32.0	3/4	19.0	5/8	16.0

Standard 0.500 in. round tension test specimens with 2 in. gage length and examples of small-size specimens proportional to the standard specimen. *Not identical to ASTM data. Calculated to the nearest 0.5 mm.

Notes:

1. The reduced section may have a gradual taper from the ends toward the center, with the ends not more than 1 percent larger in diameter than the center (controlling dimension).

2. If desired, the length of the reduced section may be increased to accommodate an extensometer of any convenient gage length. Reference marks for the measurement of elongation should, nevertheless, be spaced at the indicated gage length.

3. The gage length and fillets shall be as shown, but the ends may be of any form to fit the holders of the testing machine in such a way that the load shall be axial. If the ends are to be held in wedge grips, it is desirable to make the length of the grip section great enough to allow the specimen to extend into the grips a distance equal to 2/3 or more of the length of the grips.

4. On the round specimens, the gage lengths are equal to 4 times the nominal diameter. In some product specifications other specimens may be provided for, but unless the 4-to-1 ratio is maintained within dimensional tolerances, the elongation values may not be comparable with those obtained from the standard test specimen.

5. The use of specimens smaller than 0.250 in. diameter shall be restricted to cases when the material to be tested is of insufficient size to obtain larger specimens or when all parties agree to their use for acceptance testing. Smaller specimens require suitable equipment and greater skill in both machining and testing.

6. Five sizes of specimens used have diameters of approximately 0.505, 0.357, 0.252, 0.160, and 0.113 in., the reason being to permit easy calculations of stress from loads, since the corresponding cross-sectional areas are equal or close to 0.200, 0.100, 0.050, 0.0200, and 0.0100 in., respectively. Thus, when the actual diameters agree with these values, the stresses (or strengths) may be computed using the simple multiplying factors 5, 10, 20, 50, and 100, respectively. (The metric equivalents of these fixed diameters do not result in corresponding convenient cross-sectional areas and multiplying factors).

7. For transverse weld specimens, the weld shall be approximately centered between gage marks.

Figure 4.2 Schematic of round (all-weld-metal) tensile specimens (34).

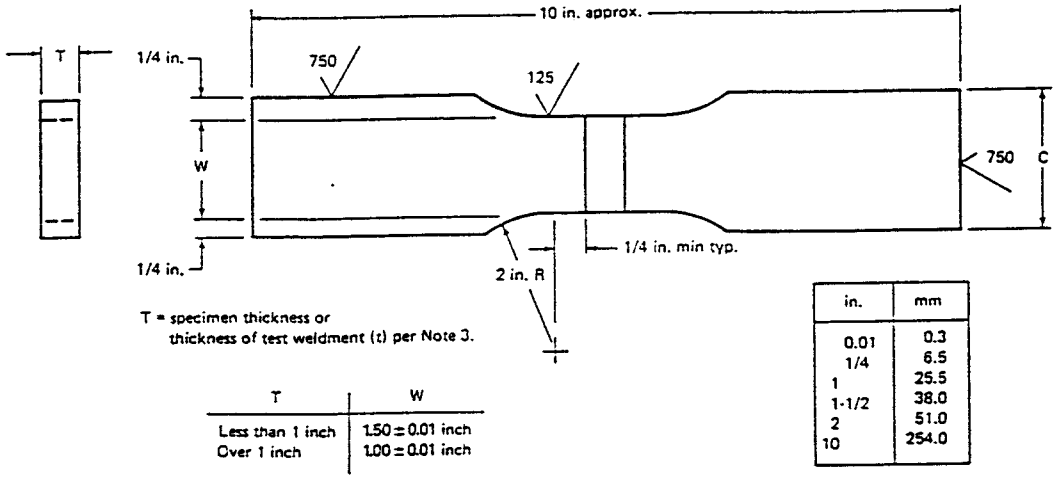

T	W
Less than 1 inch	1.50 ± 0.01 inch
Over 1 inch	1.00 ± 0.01 inch

in.	mm
0.01	0.3
1/4	6.5
1	25.5
1-1/2	38.0
2	51.0
10	254.0

Notes:

1. Thin sheet metal being tested tends to tear and break near the shoulder. In such cases, dimension C shall be no greater than 1-1/3 times times W.
2. Weld reinforcement and backing strip, if any, shall be removed flush with the surface of the specimen.
3. When the thickness, t, of the test weldment is such that it would not provide a specimen within the capacity limitations of the available test equipment, the specimen shall be parted through its thickness into as many specimens as required.
4. The length of reduced sections shall be equal to the width of the widest portion of weld, plus 1/4 in. (6.5mm) on each side.

Figure 4.3 Schematic of transverse rectangular tension test specimens (34).

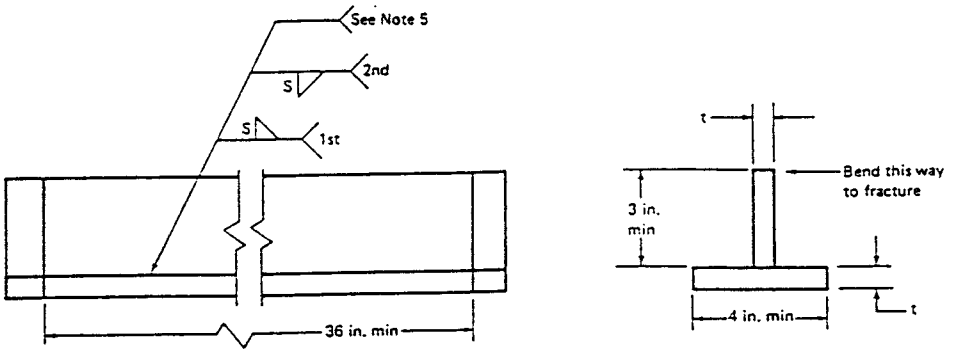

in.	mm
3	76.0
4	101.5
36	914.5

Notes:

1. t = full plate thickness (T).
2. S = specified fillet size.
3. Base plate should be same grade and specification material as that used in production.
4. Base plate shall be primer coated to maximum thickness which will be applied in production.
5. The first side weld shall be removed by gouging or mechanical means and the second side shall be tested.
6. Although entire 36 in. (914.5 mm) length is to be tested, the test assembly may be cut into shorter lengths after welding to facilitate fracturing for examination.

Figure 4.4 Fillet weld break specimens for primer coated materials (34).

4 in. (101.6 mm) wide, and 3 feet (914.4 mm) long. The Charpy samples can be seen in Figure 4.5. These samples were also considered to be standard sizes, and were broken on the Charpy Testing Machine. The test temperature range was only 20^0C to -40^0C due to the limited number of samples.

4.8 Diffusible Hydrogen Measurements

Diffusible hydrogen was determined according to the AWS A4.3-86 specification, *Standard Methods for Determination of the Diffusible hydrogen Content of Martensitic, Bainitic, and Ferritic Weld Metal Produced by Arc Welding.* Because many of the samples for analysis were coated with primers, the specification could not be followed exactly in the area of degreasing and degassing. Several tests were run to determine how the lack of degreasing and degassing would affect the levels of hydrogen, and they appeared to have no significant effects. Figure 4.6 shows a picture of the diffusible hydrogen measurement apparatus.

4.9 Metallography

Due to the large number of weld samples made, only a selected number were chosen for metallographic examination. The weld specimens were sectioned transverse and parallel to the welding direction, mounted, and polished through 0.25 μm.

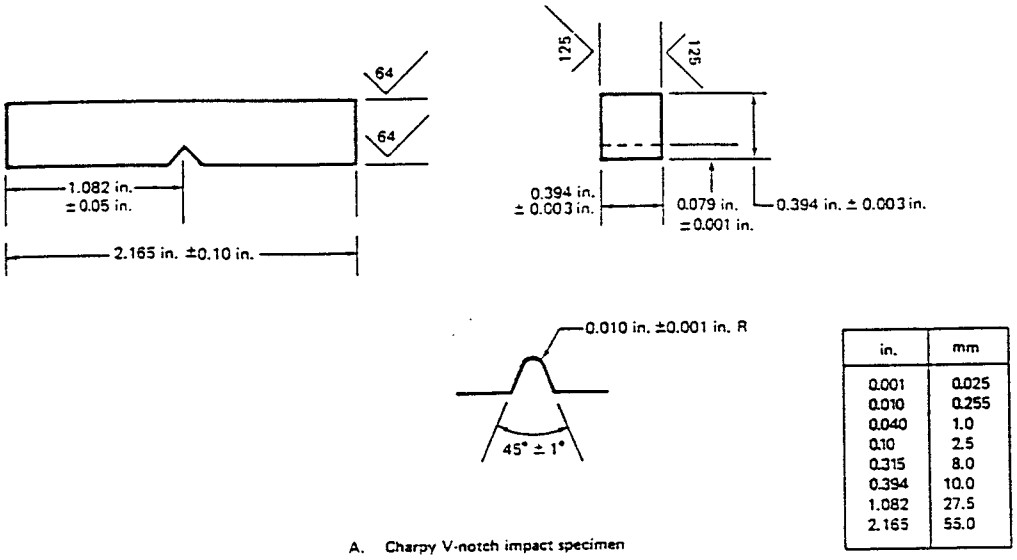

in.	mm
0.001	0.025
0.010	0.255
0.040	1.0
0.10	2.5
0.315	8.0
0.394	10.0
1.082	27.5
2.165	55.0

A. Charpy V-notch impact specimen

Figure 4.5 Charpy V-notch impact toughness specimens (34).

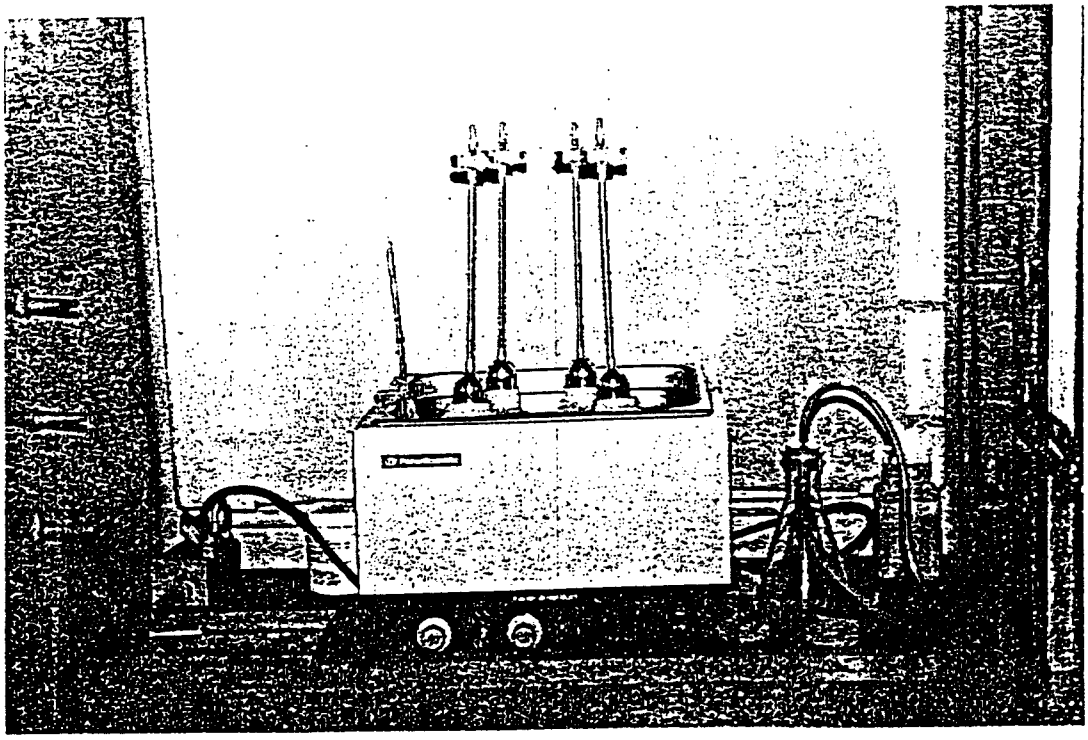

Figure 4.6 Diffusible hydrogen collection over mercury equipment (41).

Photomicrographs and macrophotographs were taken of the welds by a Neophot Metallograph after they had been etched with a 2 vol. pct. nital solution. If this solution was not strong enough to show the necessary features, then a steel weld macroetchant (850 ml water, 150 ml nitric acid, and 50 ml methanol) was used.

The volume fractions of ferrite sideplates (FS phase), acicular ferrite (AF phase), and primary ferrite (PF phase), if necessary, were determined by point counting according to the IIW Document IIW-IX-1533-88. One hundred points were counted in ten fields (for a total of one thousand points) to quantify the microstructure at 200X. Distinction could be made between the different FS or PF phases such as grain-boundary and intragranular polygonal ferrite, or ferrite with aligned and non-aligned second phases when classifying the microstructures if so desired.

The welds that were used for metallography were then subjected to hardness testing. The crown of the weld beads were ground flat to provide an adequate surface for the hardness measurements. Because the base material was low in carbon (0.06 wt. pct.), some of the welds were not very hard. Most welds were measured using the "B-scale". The welds were tested on a Macromet Hardness Tester using a 100 gram load with a 1/16 in. ball. Some welds were tested on a Rockwell Hardness Tester using the "C-scale". This scale makes use of a 150 kg load and a diamond cone indenter.

Chapter 5

RESULTS AND DISCUSSION

The purpose of this section is to present results from the experiments that were performed during this project and the subsequent explanation of these results. As indicated earlier, the basic reason for this particular research project was to help minimize the production of diffusible hydrogen from flux-cored arc welds made over primer-coated steels used in the fabrication of ships. The project was conducted in four phases in which several particular tasks were performed to reach the goal. These tasks would be accomplished through welding experiments, chemical analysis, interstitial analysis for oxygen, diffusible hydrogen collection (over mercury), and quantitative analysis of the results.

5.1 Phase I: Hydrogen-Oxygen Relationship Verification

To minimize the level of diffusible hydrogen produced in a weld, several basic premises were considered. First, weld porosity is caused mainly by hydrogen and carbon monoxide. Second, controlled perturbation of the *hydrogen-oxygen* and *carbon-oxygen* equilibria may result in control of H_2 and CO in the weld pool. The last premise is that

modification of the arc atmosphere changes the partial pressures of H_2 and CO, which alter the pick-up of these gases in the weld pool.

With these premises in mind, the technical approach began by focusing upon the *hydrogen-oxygen* relationship. The equilibrium reactions for water and carbon monoxide showed that if the oxygen level is increased, hydrogen and carbon could be removed from the weld pool. Figures 1.1 and 2.2, which show that increasing oxygen in the weld pool decreases hydrogen produced in the weld pool.

5.1.1 [H]-[O] Welding Experiments

Welding experiments were used to verify the [H]-[O] relationship. These experiments involved no primers on any of the samples. To increase the oxygen level in the weld pool, it was necessary to add flux ingredients with a high oxidizing potential. The flux ingredients chosen were FeO, Fe_2O_3, SiO_2, and $CaCO_3$, along with iron powder. These fluxes were used because each of them would provide unique properties to the weld pool.

The fluxes were placed upon the samples prior to welding as shown in Figure 4.1. The copper mold is the one described in the AWS A4.3 specification for diffusible hydrogen testing. Iron and Fe_2O_3 were used in the following weight percent combinations: 100/0; 75/25; 50/50; 25/75; and 0/100. These welds did not perform very well from an appearance standpoint, with pool wetability of the welds was quite poor.

Thus, SiO_2 was added to increase the fluidity of the weld metal. Several more welds were performed with these fluxes in various mole fractions to determine the optimal combinations to give good weldability. These mole combinations were determined to be:

Weld	Fe_2O_3	Fe	SiO_2
1	0	1	3
2	0.5	1	3
3	1	1	3
4	1.5	1	3
5	2	1	3
6	0	1	4
7	0	0	0
8	0	0	0

It was noticed from these welds that increasing the Fe_2O_3 appeared to help the fluidity of the weld metal and also the arc stability. The welds were made with a 96 pct. CO_2/4 pct. H_2 mixture to ensure hydrogen pick-up in the weld pool and make analysis easier. The welding parameters used were 25V, 230 ipm WFS, and about 14 ipm TS. Sample #7 was done with no flux and the 96/4 CO_2-H_2 gas mix, while #8 was done with no flux and 100 pct. CO_2 shielding gas.

5.1.2 [H]-[O] Analysis

After the samples were welded, they were taken to the diffusible hydrogen testing apparatus for analysis. When the tests were completed, the welds were sectioned for

interstitial analysis of oxygen. The data obtained from these tests allowed were plotted in Figure 5.1. This graph clearly shows that the basic premise holds true that an increase in weld metal oxygen would result in a decrease of diffusible hydrogen. It was not possible to achieve oxygen levels below about 600 ppm because that was the "base weld" composition or the weld done with 100 pct. CO_2 and no flux additions.

There were also a few weld tests done to determine the effect of welding parameters on diffusible hydrogen production in the welds. The following parameters were used for the tests (volts/ipm): 25/230; 26/270; and 27/310. The results of those tests are given in the following table:

Sample	Volts	WFS(ipm)	H_{dif} (ml/100g)
9	25	230	7.44
10	26	270	7.91
11	27	310	8.02

Despite the slight changes in diffusible hydrogen content, these results indicate that diffusible hydrogen is not strongly dependent upon the parameters used at these levels.

5.1.3 Weld Metal Chemical Analysis

The welds used in the hydrogen-oxygen analysis were also analyzed for chemical composition. The results of those tests can be seen in Table 5.1. Only a few elements

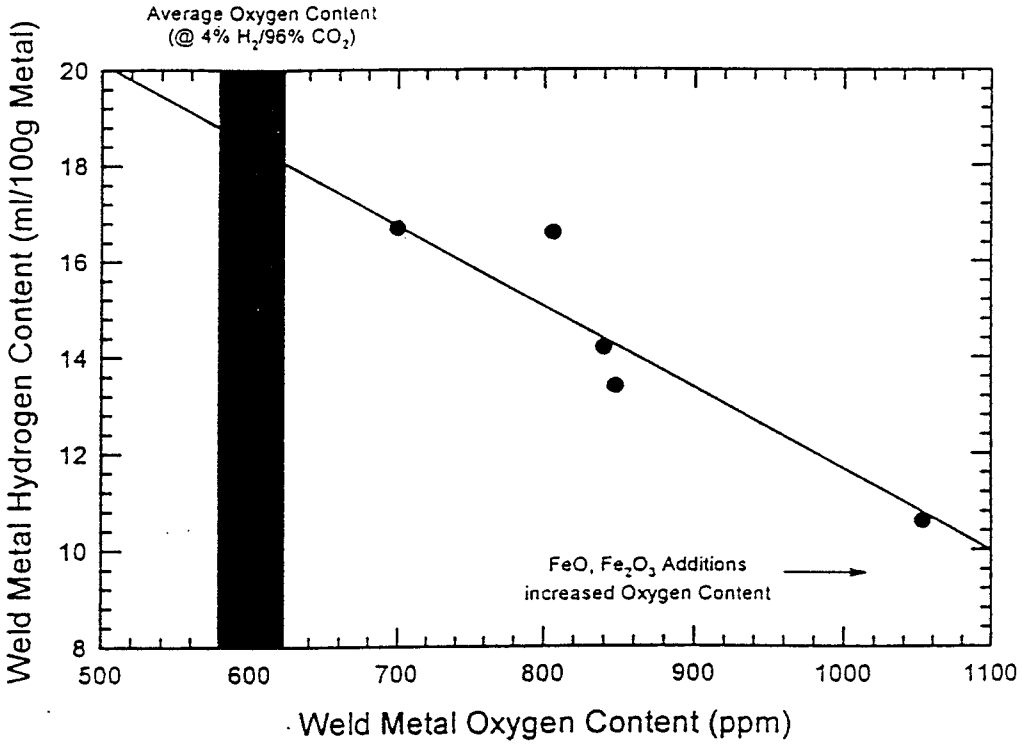

Figure 5.1 Plot of weld metal diffusible hydrogen as a function of weld metal oxygen content from Phase I welds.

Weld	C	S	P	Si	Cr	Ni	Mn	Cu	Mo	Ti	Al	V
1	0.06	0.012	0.01	0.46	0.04	0.03	0.66	0.03	0.01	0.017	<.01	0.027
2	0.07	0.014	0.011	0.26	0.04	0.03	0.76	0.02	0.01	0.019	<.01	0.024
3	0.06	0.01	0.009	0.24	0.04	0.04	0.81	0.02	0.01	0.024	<.01	0.026
4	0.06	0.013	0.011	0.2	0.04	0.04	0.73	0.02	0.01	0.015	<.01	0.024
5	0.06	0.014	0.011	0.19	0.04	0.06	0.7	0.02	0.01	0.015	<.01	0.022
6	0.06	0.012	0.01	0.49	0.04	0.04	0.76	0.02	0.01	0.016	<.01	0.026
7	0.07	0.015	0.008	0.3	0.04	0.04	1.18	0.02	0.01	0.03	<.01	0.034
8	0.06	0.012	0.01	0.29	0.04	0.04	1.25	0.02	0.01	0.026	<.01	0.04

Table 5.1 Chemical analysis of selected Phase I welds.

such as silicon and manganese showed any great changes from the "base weld" (#8) composition, which was done with the 100 pct. CO_2. In the first five samples, the only variable was the amount of Fe_2O_3 in the flux. Increases in the amount of Fe_2O_3 appears to cause less recovery of silicon and a greater recovery of manganese from the slag to the weld metal. This suggests that the increased oxygen levels from the addition of Fe_2O_3 results in the manganese forming an oxide inclusion, such as MnO, in the weld metal causing an increase in the manganese weld metal content. The silicon is kept from reacting to form inclusions in the weld metal, and helps to form an easily detachable slag.

5.1.4 Thermodynamic Verification

As mentioned earlier, simple thermodynamic calculations can be used to verify this [H]-[O] relationship. The equations used here were:

$$\log k = -(10610 / T) - 0.99 \quad \text{.....(5.1.1)}$$

$$[H] = \sqrt{\frac{k}{[O] \div 10{,}000}} \quad \text{where [O] is in ppm; [H] is in \%.....(5.1.2)}$$

$$[H](\%) * 11{,}200 = [H](ml / 100g) \quad \text{.....(5.1.3)}$$

With these equations, an [H]-[O] curve could be calculated. It is not shown, but it is assumed that the partial pressure of water for the decomposition reaction of water is one atm which simplifies the calculations. These calculations are similar to those used in

calculating Figure 2.3, but they are slightly different. Figure 5.2 shows the plot of this data at different temperatures with the actual experimental data also indicated on the graph. The experimental data agreed well with the thermodynamic predictions. Based on the location of the experimental data, it is also reasonable to conclude weld pool equilibrium was roughly 1600^0C.

5.2 Phase II: Oxidizing Potential With Paint Primers

The purpose of this experimental phase was to determine the oxidizing potential of the chosen fluxes with the combined effects of a primer coating. The fluxes used were the $CaCO_3$, SiO_2, Fe_2O_3, and FeO. The experiments also had as an objective the determination of the effect of increasing primer thickness on weld metal oxygen content. It was postulated that because of the chemical composition of the primers (see Section 2.4) that by increasing the primer thickness, the oxygen levels should increase along with the level of diffusible hydrogen. For the experiments to be successful, it would be necessary to maintain tight control on the primer thickness of the weld samples. However, the control of the coating thickness is relatively difficult in small coupons and when mechanically coated.

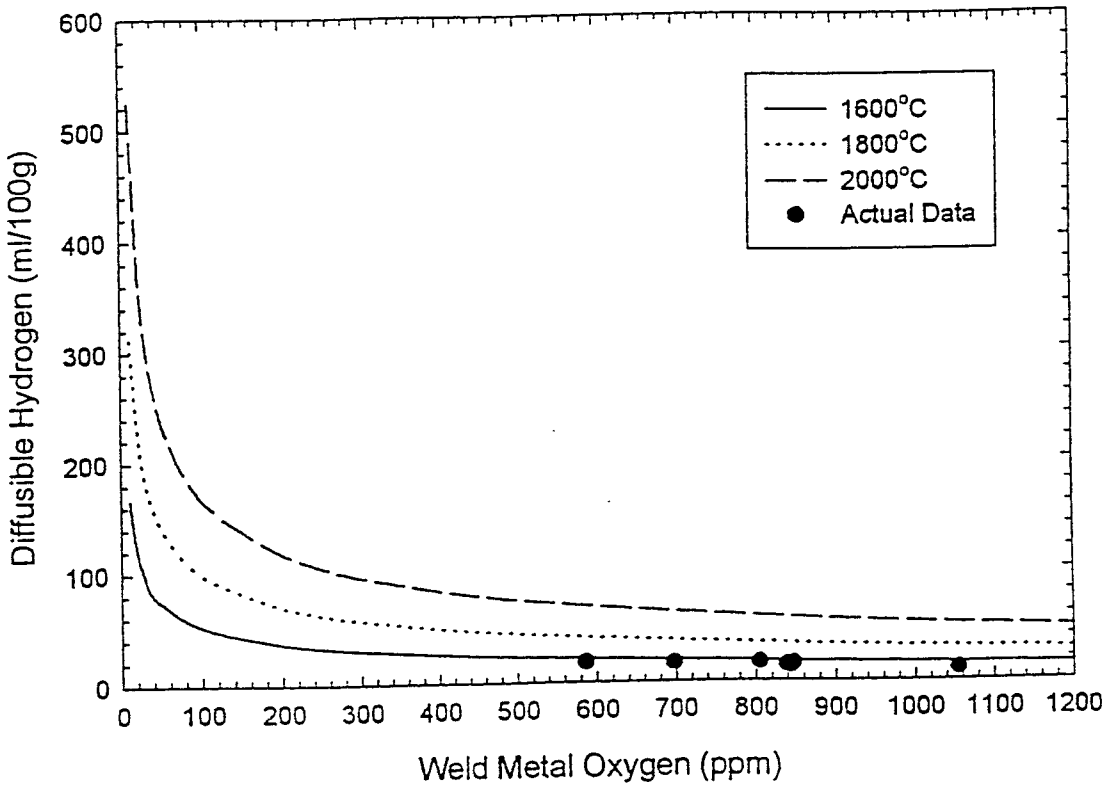

Figure 5.2 Plot of weld metal hydrogen versus weld metal oxygen content from thermodynamic data.

5.2.1 Primer Thickness Testing Guidelines

Samples were received from Ingalls Shipbuilding for the determination of the actual coating thickness. It was originally proposed the following primer thicknesses would tested: 0, 0.5, 1.0, 2.0, and 4.0 mils. When checked with a manual Mikrotest Thickness Gage, the samples showed large variations in the prescribed thicknesses. Most samples were sent back to be recoated. This procedure had to be done several times to achieve the necessary amount of samples with the prescribed primer thickness. The primer used at this point was the Interplate NQA238 which was an inorganic, zinc ethyl-silicate primer. It was determined that the accuracy of the manual thickness gage at the primer thicknesses tested was quite low. It was decided that a more accurate gage, Positector 6000 Model F2, should be obtained. This particular gage is capable of averaging several measurements and giving a variance of the measurements which would be beneficial.

To ensure the consistency of the primer coating and that only correct sample thicknesses would be tested, some guidelines to determine which samples would be satisfactory for testing were established. The guidelines set forth were as follows: 1) Each sample shall be measured at least 5 times with an average and a variance being determined; 2) If the average fell within ± 10 pct. of the specified value, the sample was acceptable; and 3) The variance must be within the range of ± 20 pct. of the average. The 0.5 mil primer thickness was changed to 1.5 mils because trying to achieve that low thickness was too difficult. With these guidelines in place, the necessary primer thicknesses and amount of samples for our experiments was achieved.

5.2.2 Oxidizing Potential of Fluxes

The weld experiments for Phase II began with testing only the 0, 1.0 and 4.0 mil samples because of the limited number of samples at the time. As was stated, it was necessary to determine what effect that the primer would have on the weld metal oxygen content, but also what affect the thickness of the added layer of flux would have on the weld metal oxygen content. The different thickness of the flux additions would include 0, 1/16 in., 1/8 in., and ¼ in. This series of flux additions should give an idea of what each of the fluxes contributes in the way of oxygen to the weld metal and allow for the determination of the amounts to be incorporated in the FCA welding consumables. The flux layer thickness was controlled by cutting copper strips to specified widths to accommodate the proper flux thickness. These strips were placed on the sides of the samples as shown in Figure 4.1 to protect the copper mold block and achieve the proper flux thickness. Once the fluxes were placed upon the samples, the welding took place.

The first welding experiments involved the SiO_2, Fe_2O_3, and $CaCO_3$ fluxes at the specified thicknesses with the 0, 1.0, and 4.0 mils primer thicknesses (Interplate NQA238). A combination of about thirty welds were made at 27 V and 290 ipm WFS. Photographs were taken of the welds so comparisons could be made. The $CaCO_3$ proved the most weldable, followed by the SiO_2, and Fe_2O_3. As single additions, the bead appearance resulted from Fe_2O_3 was quite rough, and not smooth like the $CaCO_3$. SiO_2

gave a very smooth weld bead, but the wetability of the toe was poor indicating very little penetration of the weld bead into the base metal.

The welds were sectioned for interstitial analysis of oxygen. These results showed that the primer had little or no effect on the oxygen level of the weld metal with increasing primer thickness. It is possible that the effects of the flux additions were too overpowering for the primer. This finding also points out the flux modification of the FCAW consumables would be able to affect and moderate the effect of the primer. Increasing the flux thickness also had little effect on weld metal oxygen content, e.g. SiO_2 ($\approx$1000ppm) and $CaCO_3$ ($\approx$550ppm). Only the Fe_2O_3 appeared to have an oxygen content that increased with increasing primer and flux thickness (1000 ppm to 1500 ppm) which can be seen in Figure 5.3.

At this point, the FeO flux addition was also tested in the same manner which involved another ten welds. While providing the highest weld metal oxygen content, the amount of oxygen in the weld metal as a result of the FeO flux addition ($\approx$ 1800 ppm) was not affected by the primer and flux thickness. The appearance of these welds were the poorest due to the high viscosity of the slag and weld metal. The slag was extremely thick and difficult to remove from the weld bead. It had the poorest detachability on the ¼ in. flux thickness. Analysis of the FeO flux addition by XRD showed it was actually a 50/50 weight percent mixture of FeO and Fe_2O_3. Overall, the FeO flux proved to be the least

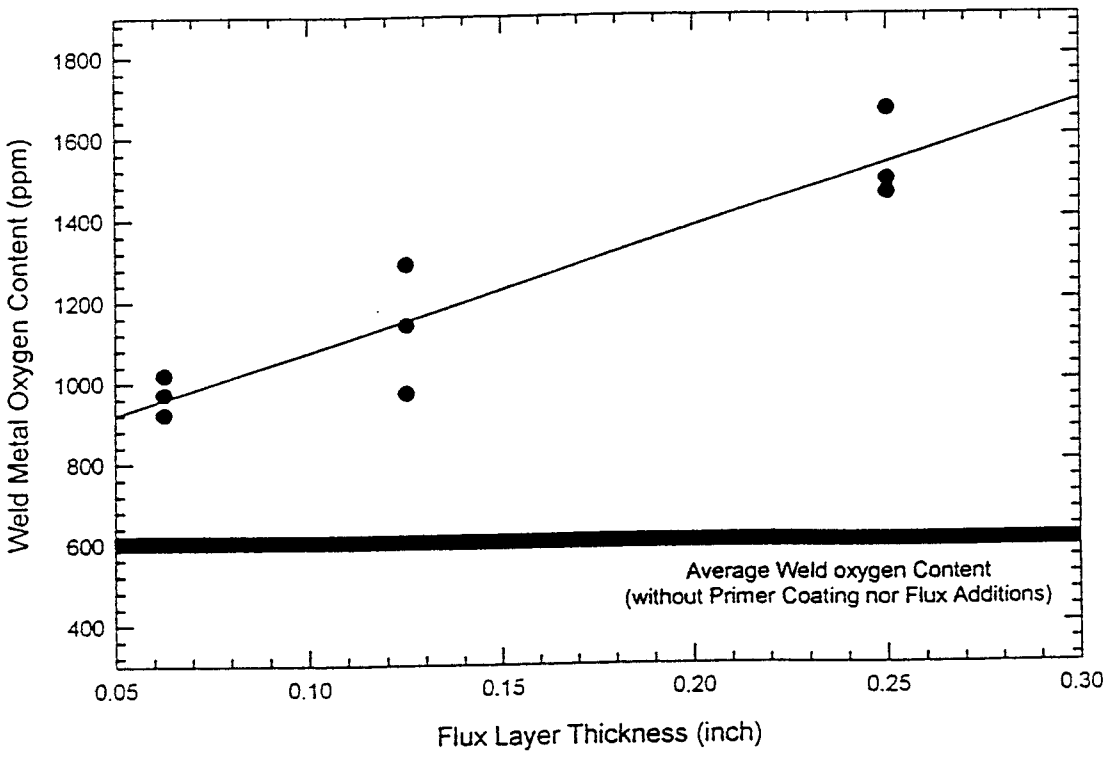

Figure 5.3 Effect of Fe_2O_3 flux thickness on weld metal oxygen content.

weldable, but had the highest oxidizing potential, followed by the Fe_2O_3, SiO_2, and $CaCO_3$. One difficulty in testing the welds with such high oxygen was that Leco does not make any calibration standards that are higher than about 400 ppm [O]. No other commercial establishments were found to offer higher steel oxygen standards. The lack of these higher oxygen standards might cause the results not to be 100 pct. accurate, but the consistency of the results did not appear to cause any concerns.

The next step in the analysis was to determine if the effects of the individual flux additions were additive. For example, if the oxygen content of flux A is 600 ppm and flux B is 700 ppm, is the overall oxygen content of the two fluxes together 1300 ppm? Fluxes were mixed in the following molar combinations: 1) FeO-SiO_2; 2) Fe_2O_3-SiO_2; 3) $CaCO_3$-SiO_2; 4) $CaCO_3$-FeO-SiO_2; and 5) $CaCO_3$-Fe_2O_3-SiO_2. The fluxes were spread on the samples in a 1/8 in. thickness and welded. All the combinations exhibited good weldability. Slag detachability was good, except that it was difficult to remove from the toe area on combination #4. The poor slag detachability was attributed to the presence of FeO which promoted poor viscosity. Information supplied by ESAB indicated that Fe_2O_3 and FeO both decrease viscosity when added to a Si-based flux such as used here.

The results of the oxygen analysis were as follows: 1) 1106 ppm; 2) 1143 ppm; 3) 593 ppm; 4) 719 ppm; and 5) 935 ppm. The effects are not additive. As $CaCO_3$ is added to the mix, it decreases the oxygen level slightly in the weld and promotes weldability. This finding agrees with established trends for effects of $CaCO_3$ additions. The CO_2

provided by the decomposition of $CaCO_3$ provides shielding gas and displaces oxygen and nitrogen. The CaO produced provides arc stabilization and slag viscosity control.

5.2.3 Weld Pool Functions of Fluxes

Most flux ingredients perform several functions. As stated, $CaCO_3$ provides shielding gas, slag formers, arc stabilizers, and a weld pool refiners. The main function of SiO_2 is that of a slag former. The slag is a mixture of glass and crystalline structure. It must melt below the melt temperature of steel ($\approx 1450^0$C), have density less than steel to reduce slag entrapment, proper viscosity in the temperature range of 1450 to 1550^0C, and detachability. Slag detachability can be a big problem. Slags that contain spinels of complex oxides in the form $(M_1M_2)O_4$ are not easily removed (42,43,44). It has been reported that if $(CaO)_2$-SiO_2, Cr_2TiO_5, and $FeTiO_5$ are present, including the CaO-CaF_2-SiO_2 and CaO-TiO_2-SiO_2 systems, the slag readily detaches from the weld deposit (41).

Fe_2O_3 is much like SiO_2 in that it provides many of the same functions such as being a slag former and controller of physical properties. It can be an arc stabilizer and controller of slag viscosity. It has also been shown from these welding experiments that the Fe_2O_3 produces a thick, viscous slag which is not easily removed, and the bead appearance is quite poor. The results from the binary and ternary flux mixtures, oxidizing potential, and appearance can be seen in Figure 5.4. It can be seen that the ternary mixture of Fe_2O_3-$CaCO_3$-SiO_2 provided the best overall properties.

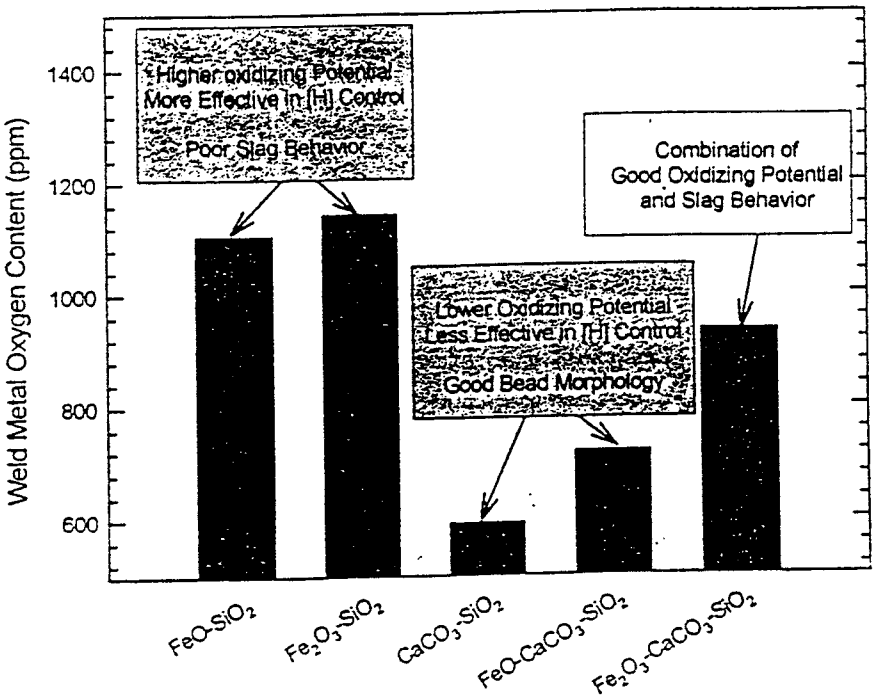

Figure 5.4 Effect of binary and ternary flux additions on weld metal oxygen content.

5.2.4 Inorganic Primer / Diffusible Hydrogen Interaction

Before any further testing of the ternary flux combinations was done, it was decided that the effect of primer thickness on diffusible hydrogen production should be evaluated. Samples with the following primer thicknesses were chosen for testing: 0, 1.25, 2.48, 5.0 and 5.08 mils. The last sample was degassed in a furnace at 300^0C to determine what effect baking would have on primer stability and diffusible hydrogen production. The interstitial analysis results for oxygen revealed nothing other than the fact that the average oxygen level was about 600 ppm.

The results of the diffusible hydrogen tests for these specimens can be seen in Figure 5.5. It clearly shows that as the primer thickness increases up to 5 mils, the level of diffusible hydrogen produced increases seven fold from a sample with no primer coating or flux layer (7.97 ml/100g to 74.3 ml/100g). The baking of the sample had very little effect on the level of diffusible hydrogen produced. It only decreased to about 72 ml/100g. This result indicates that baking a primer-coated samples will have very little effect on the level of diffusible hydrogen produced.

It should be noted that the shipbuilding industry almost never uses a high primer thickness like 4.0 mils. They generally use a primer thickness of 0.75 to 1.0 mils on the average. However, as was indicated when testing primer thickness on the samples, the primer thickness can vary as much as ±1.5 mils. Thus, the experimental program included the samples with the higher primer thickness coating. The descriptions of the effects of

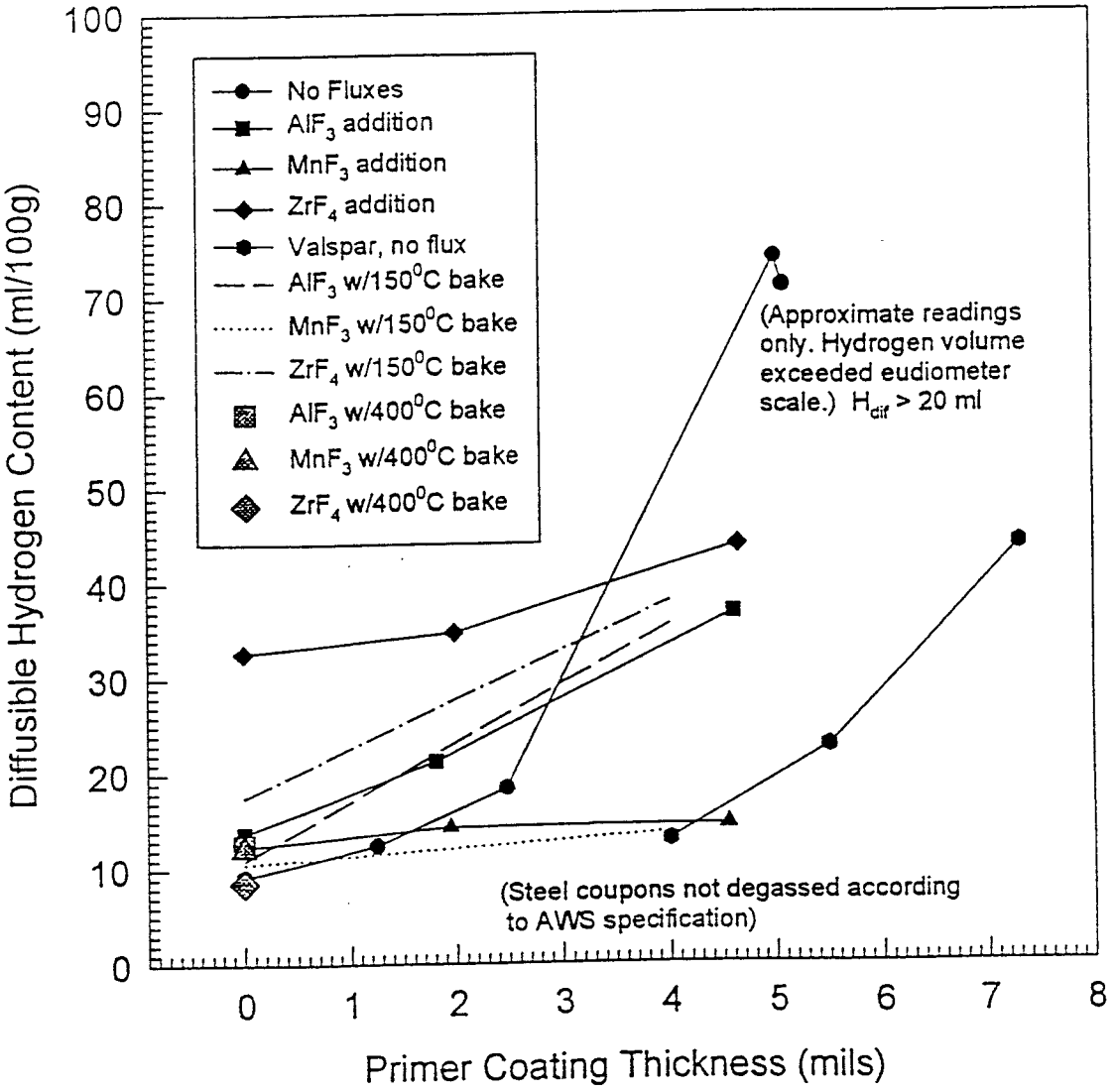

Figure 5.5 Effect of primer thickness, primer type, and fluoride additions on weld metal diffusible hydrogen content.

the fluoride flux additions and Valspar primer will be presented later.

5.2.5 Final Flux Combination Development

With information from the chemical analysis and the previous weld experiments, a test matrix was developed to examine the effects of the flux additions in various levels. The $CaCO_3$ was only tested in two molar levels, 0.25 and 0.5, because it appeared to lower the weld metal oxygen content, but did contribute to good weldability and slag detachability. Because the SiO_2 and Fe_2O_3 affected the oxygen levels more, they would be tested at three molar levels: SiO_2 = 1.0, 2.0, and 3.0; Fe_2O_3 = 1.0, 1.5, and 2.0. The fluxes were weighed out according to their molecular weights to constitute the necessary moles. A total of eighteen different flux combinations with five different primer (Interplate NQA238) thicknesses of 0, 1.0, 1.5, 2.0, and 4.0 mils were tested. Because it was determined that flux depth had little or no effect on oxygen levels, the flux depth of 1/16 in. was chosen for testing. The electrode was baked at 150^0C overnight, and the flux combinations were baked at 400^0C to remove any absorbed moisture. The welding parameters used were 27 V and 290 ipm WFS.

The welding experiments involved ninety samples being welded. All of the combinations performed quite well with only minor differences in arc stability and weldability. As the level of Fe_2O_3 was increased, the cooling rate appeared to decrease because the samples remained hotter for a longer period. Bead width appeared to increase slightly with increasing primer thickness and flux addition levels. This observation could

be the result of increased fluidity of the weld pool from the increased level of Fe_2O_3 in the flux.

Surface defects appeared to increase as the primer level approached 4.0 mils which contributed to the violent, explosive starts when starting a weld on the primer and increased spatter at higher primer thicknesses. Unfortunately, there were no clear-cut trends as far as flux composition and bead appearance.

Select samples were analyzed for chemical composition and ranked according to the level of weld metal oxygen. The fluxes chosen had high (#14 and #7), medium (#18 and #17), and low (#12 and #6) oxygen levels. The oxygen level for the "high" samples was about 830 ppm, 750 ppm for the "medium" samples, and 660 ppm for the "low" samples. The oxygen levels were based on an average of all five of the primer-coated samples. The chemical analysis of samples with 0, 1.0, and 4.0 mils primer can be seen in Table 5.2. The carbon levels varied from 0.06 to 0.086 wt. pct. depending on the primer thickness, despite the results in Table 5.1 indicating that the carbon levels did not vary at all. The reason for the variation observed in Table 5.2 is likely due to the primer, contamination of the flux and samples, or increased carbon levels in the flux or electrode. Examination of Table 5.2 shows that as the level of $CaCO_3$ is increased in the added flux, the carbon levels increase in samples with 0 or 1.0 mils primer. Several other elements, such as sulfur, chromium, nickel, and molybdenum did not vary greatly indicating that

Sample	Flux	$CaCO_3$	SiO_2	Fe_2O_3	Primer	[O]ppm	C	Si	Mn	Ti	Al	V
31	7	0.5	1	1.5	0	832	0.072	0.15	0.68	0.009	0.01	0.021
66	14	0.25	1	2	0	796	0.07	0.15	0.66	0.008	0.007	0.021
86	18	0.25	3	2	0	764	0.06	0.18	0.67	0.01	0.01	0.02
56	12	0.25	3	1.5	0	728	0.067	0.21	0.8	0.011	0.012	0.026
81	17	0.5	3	2	0	702	0.071	0.15	0.62	0.007	0.01	0.019
26	6	0.25	3	1	0	643	0.066	0.2	0.85	0.017	0.01	0.026
87	18	0.25	3	2	1 mil	813	0.07	0.17	0.7	0.01	0.012	0.02
67	14	0.25	1	2	1 mil	797	0.071	0.15	0.67	0.01	0.008	0.02
27	6	0.25	3	1	1 mil	761	0.067	0.22	0.79	0.015	0.01	0.026
32	7	0.5	1	1.5	1 mil	747	0.071	0.16	0.69	0.01	0.01	0.022
82	17	0.5	3	2	1 mil	653	0.086	0.22	0.81	0.018	0.01	0.025
57	12	0.25	3	1.5	1 mil	640	0.072	0.23	0.78	0.022	0.008	0.028
35	7	0.5	1	1.5	4 mils	837	0.082	0.18	0.78	0.011	0.01	0.024
70	14	0.25	1	2	4 mils	834	0.067	0.14	0.64	0.01	0.006	0.018
85	17	0.5	3	2	4 mils	817	0.066	0.23	0.9	0.022	0.01	0.027
90	18	0.25	3	2	4 mils	761	0.07	0.25	0.92	0.025	0.01	0.03
30	6	0.25	3	1	4 mils	703	0.075	0.23	0.89	0.02	0.01	0.027
60	12	0.25	3	1.5	4 mils	702	0.076	0.22	0.85	0.015	0.007	0.026

Table 5.2 Chemical analysis of selected Phase II welds.

the flux and primer additions had little or no effect on their composition. In the flux combinations with the highest levels of SiO_2 added, the level of silicon in the weld metal is the highest, as is manganese in most cases. Other ingredients such as titanium, aluminum, and vanadium show no clear trends in this regards. It also appears that as oxygen levels are increased in the weld, the levels of silicon, manganese and titanium tend to decrease.

Observations of the welds indicated that Fluxes #14 and #7 had the roughest looking appearance, which suggests that they probably had the highest oxygen contents. Fluxes #4 and #6 had the best overall appearance, which suggests that their oxygen levels are much lower. These assumptions were proven through interstitial analysis for oxygen. The results of the tests can be seen in Table 5.3. These results indicate that the assumptions were supported by the oxygen results. Fluxes #14 and #7 had average oxygen levels of 834 ppm and 830 ppm. Fluxes #4 and #6 had average oxygen levels of 676 ppm and 666 ppm. The results of the chemical and oxygen analysis along with the overall appearance, do give us an idea about how to determine the best combination.

5.2.6 Organic Primer: [H]-[O] Interactions

Welds were also made with the Valspar V13F40 primer to perform diffusible hydrogen tests. Since the Interplate primer was the focus of this research, the Valspar primer was only tested at a thickness of 4.0 mils. When subjected to the thickness testing criteria, samples were produced from 4.0 to 7.3 mils for testing. The levels of diffusible

Flux Combo	Moles of $CaCO_3$	Moles of SiO_2	Moles of Fe_2O_3
1	0.5	1	1
2	0.25	1	1
3	0.5	2	1
4	0.25	2	1
5	0.5	3	1
6	0.25	3	1
7	0.5	1	1.5
8	0.25	1	1.5
9	0.5	2	1.5
10	0.25	2	1.5
11	0.5	3	1.5
12	0.25	3	1.5
13	0.5	1	2
14	0.25	1	2
15	0.5	2	2
16	0.25	2	2
17	0.5	3	2
18	0.25	3	2

Table 5.3 Flux combinations and compositions used for oxygen analysis in Phase II.

hydrogen observed were lower than those produced using the inorganic primer.

As it is seen in Figure 5.5, at about 5 mils primer thickness, the inorganic Interplate primer produces about 3.5 times the amount of hydrogen that the organic Valspar primer does. It was expected that the organic primer would produce more diffusible hydrogen than the inorganic primer. However, this was not the case. The Valspar samples with only the 4.0 mils thickness were also welded with the 18 combinations of the oxide fluxes at a thickness of 1/16 in (1.6 mm). The weld tests indicated that some arc instability, thick fumes, spatter, and a slightly higher current level existed.

When subjected to interstitial analysis for oxygen, the Valspar samples produced results that were quite similar to the results on the Interplate samples. As the primer thickness increased for the Valspar samples, the oxygen levels increased slightly. The results for the Valspar samples agree closely in some cases with the Interplate samples when tested on the flux combinations. Flux combinations #14 (high), #17 (medium), and #5 (low) were used for testing with the fluorides. The comparison of the oxygen results (ppm) for the Interplate and Valspar primers at 4.0 mils for the flux combinations are as follows:

Flux Combination	Interplate	Valspar
14	834	773
17	817	741
5	597	616

These results agree well, while some of the other flux combinations do not agree as well. Those results include:

Flux Combination	Interplate	Valspar
9	845	647
6	703	550
11	696	581

5.2.7 Hydrogen-Fluorine Interaction

As indicated earlier, if the oxygen level is increased too high, the mechanical properties of the weld are affected negatively due to the formation of inclusions and large grain-boundary ferrite grains in the microstructure. This deterioration of mechanical properties limits the maximum level of oxygen in the weld metal, despite the effectiveness of hydrogen mitigation by oxygen increase. Another mechanism must be developed to lower hydrogen. This mechanism was the one discussed in Section 2.2 (Hydrogen-Fluorine Relationship). The premise was the same as the case for oxygen. An increase in the fluorine content in the weld metal should results in a decrease in diffusible hydrogen production. The fluoride compounds selected for testing included AlF_3, MnF_3, and ZrF_4. They were selected on the basis of availability and thermal stability.

MnF_3 is available in a red, monoclinic crystalline form with a bulk density of 3.54 g/cm^3. It is also mildly hygroscopic and will react with water. It will begin to decompose at temperature exceeding 600^0C. AlF_3 is available in a white, hexagonal crystalline form

with a bulk density of 3.10 g/cm^3. It is mildly soluble in water. AlF_3 has a sublimation point at 1276^{0}C. ZrF_4 comes in a white, monoclinic crystalline form with a bulk density of 4.43 g/cm^3. It is slightly soluble in water and has a sublimation point of 912^{0}C. None of the manufacturers of these fluorides had determined a particle size, so that information was unavailable. When handling these fluorides, care was taken not to touch or inhale them in by wearing rubber gloves and a filter mask.

To examine the effects of the fluorides and the Interplate primer on diffusible hydrogen levels, test welds were made on samples with 0, ≈1.9, and ≈4.6 mils primer. Samples with the odd primer thickness were used because these tests were not originally accounted for in the test matrix. Therefore, substitute samples that did not fit the requirements for earlier tests were used. The welds were made with 100 pct. CO_2 shielding gas and not the 96/4 CO_2-H_2 mixture, so as to compare with the previous results. The welds done with no primer exhibited good stability and very little spatter. As the primer thickness increased, spatter and fume generation increased significantly. The results of the diffusible hydrogen tests can be seen in Figure 5.5. The levels of hydrogen are noticeably higher compared to the welds done with "no fluxes".

As mentioned, some of the fluorides are relatively hygroscopic to a certain degree. For this reason, the fluorides were baked at 400^{0}C overnight as were the oxide fluxes, and welded over samples with no primer. The welding arc indicated some slight instability and increased spatter for the baked fluorides as primer thickness increased. The test results

showed that the hydrogen level decreased by a factor of eight for ZrF_4. Samples covered by MnF_3 and AlF_3 showed hydrogen levels that didn't decrease much, if any, as seen in Figure 5.5. It was decided to run a few more samples with about 4.0 mils primer, and to once again use the baking temperature of 400^0C overnight. The results of these tests had hydrogen levels approaching those samples done with no baking. This fact indicates that the fluorides begin to breakdown when the baking temperature is too high and long.

It was decided to try a lower baking temperature of 150^0C for one hour. The arc stability and lack of spatter was quite good for the samples with no primer. Of course, as the primer thickness increased, spatter and fume generation increased. Arc stability remained quite good. The results of the tests are once again seen in Figure 5.5. These tests showed that the reduction of hydrogen is the greatest in ZrF_4, followed by MnF_3 and AlF_3. The MnF_3 and AlF_3 appeared to be insensitive to primer thickness and baking temperature to a certain degree, unlike the ZrF_4. However, at higher primer thickness, the MnF_3 produces the lowest diffusible hydrogen levels as compared to the samples welded with no flux.

At this point, it was decided to see what effects that a flux combination with high (#14), medium (#17), and low (#5) level of oxygen would have on weldability when combined with the three types of fluorides. The fluorides were added to the combinations in mole levels of 0.5 and 1.0. Prior to welding, the combinations were baked at 150^0C for one hour. The Interplate primer was tested in thicknesses of 0, 1.0 and 5.0 mils. A

thickness of 1.5 mils was used when the 1.0 mil samples ran out. Arc instability increased with increasing primer thickness as did the amount of spatter. Arc instability was the greatest in the samples with the ZrF_4. They also had current levels that were slightly lower than the other samples. The samples with the best arc stability were those with the AlF_3. They also had current levels that were slightly higher than the samples with the ZrF_4. The samples with the MnF_3 appeared to suffer from slight case of "arc wander". This arc wandering could possibly be due to either magnetic or thermal arc blow. Overall, all the samples welded quite satisfactorily.

The next step was to section the weld samples made with the fluorides (AlF_3, MnF_3, and ZrF_4), Valspar primer, and the oxide/fluoride combinations for oxygen analysis. The oxygen content of our base weld was about 586 ppm. When comparing this value to those values of the fluoride samples, the fluorides lowered the level of oxygen in the weld metal. This effect is most pronounced with the MnF_3 as the levels dropped from 586 ppm to about 460 ppm. All of the other fluorides had drops in oxygen levels. The level of oxygen does increase as the primer thickness increases in all cases for the fluorides.

The fluorides that were combined with the high (#14), medium (#17), and low (#5) oxygen level flux combinations showed that as primer level increased, so did the oxygen level for all the different fluorides. The fluorides were mixed in levels of 0.5 and 1.0 mils. The oxygen levels were generally higher in the samples with only 0.5 mils of the fluorides. As the fluoride level increased, the weld metal oxygen decreased. The oxygen levels were

lowest in samples with the ZrF_4, followed by the MnF_3 and AlF_3. These results agree closely with the results from oxygen analysis on the individual fluorides where the AlF_3 produced the highest overall oxygen levels followed by the MnF_3 and ZrF_4.

5.2.8 Microstructural Characterization of Phase II Welds

Microstructural characterization was done on some of the previous welds to determine how each of the flux components and primers affected the microstructure. The samples looked at included the DH-36 steel plate, reference weld (with 0, 1.0 and 4.0 mils Interplate), welds that resulted from each oxide flux (0 and 4.0 mils Interplate), each fluoride flux (0 and ≈4.0 mils Interplate), and selected flux combinations (#14, #17, #5, #11, and #1; 0 and 4.0 mils Interplate and Valspar). The analysis began with examination of each of the microstructures at 200X and 500X at specific locations within the weld metal. This location was about 4 mm into the weld metal along the toe and 1 mm downward. As expected, increasing the amount of weld metal oxygen resulted in a decrease of the amount of acicular ferrite, and an increase in grain-boundary ferrite.

$CaCO_3$ produced about 600ppm [O], followed by SiO_2 (1000ppm), Fe_2O_3 (1200ppm), and FeO (1800ppm). The average amount of AF decreased in each as follows: $54 \rightarrow 29 \rightarrow 17 \rightarrow 2$ volume percent. These data show that a three-fold increase in oxygen can produce a twenty-five-fold decrease in the amount of AF or a four-fold increase in grain-boundary ferrite. Similar variations were found in the welds made. The

amount of AF produced with Flux #5 (≈ 630 ppm) gave a microstructure with about 37 pct. AF, whereas Flux #14 (≈ 830 ppm) produced only 14 pct. AF. As the amount of GBF increased, so did the FS phase in some cases. Most of the welds made with the fluorides produced oxygen levels about 500 ppm. Because the oxygen levels were well below the reference weld level, the amount of AF produced was also higher, roughly 80 vol. pct., with only minor variations between fluorides. The fluorine appears to refine the grain size of the microstructure while decreasing the oxygen content of the weld. Even though the primers did not affect the oxygen levels to any great degree, but they do affect the overall microstructure. More AF is produced with the Valspar than the Interplate primer. Because the oxygen levels produced by each primer were similar, there must be something in the chemical composition of the Valspar primer that accounts for this. This result would account for the increased levels of AF and decreased levels of FS-phase.

The next step was to take hardness measurements of the weld beads to determine the overall hardenability of the weld metal produced with the different primers and fluxes. The hardness measurements were made on top of the weld beads after the tops of the weld beads were ground off to provide a flat surface for the test. It should be pointed out that these particular samples were air cooled, and not quenched as occurs with the diffusible hydrogen testing. The results of the hardness tests can be seen in Table 5.4 along with the oxygen contents of the weld metal. It is clear to see that as the oxygen content of the weld metal increases, the weld metal hardness decreases. This is further supported by the

Sample Description	Weld metal Oxygen (ppm)	Weld Metal Hardness (Vickers)
No Primer (NP)	586	186.0
1.0 mil Interplate	577	192.5
4.0 mils Interplate	619	192.0
SiO_2, NP	1050	177.6
SiO_2, 4 mils Interplate	892	178.8
Fe_2O_3, NP	971	147.9
Fe_2O_3, 4 mils Interplate	921	149.7
$CaCO_3$, NP	555	189.0
$CaCO_3$, 4 mils Interplate	586	204.0
FeO, NP	1738	106.0
FeO, 4 mils Interplate	1730	154.5
Flux 14, NP	796	138.0
Flux 14, 4 mils Interplate	834	147.0
Flux 14, 4 mils Valspar	773	155.1
Flux 17, NP	702	142.5
Flux 17, 4 mils Interplate	817	159.9
Flux 17, 4 mils Valspar	741	151.5
Flux 5, NP	647	158.1
Flux 5, 4 mils Interplate	597	181.0
Flux 5, 4 mils Valspar	616	158.1
Flux 11, NP	540	153.0
Flux 11, 4 mils Interplate	696	163.8
Flux 11, 4 mils Valspar	581	162.6
Flux 1, NP	715	157.5
Flux 1, 4 mils Interplate	794	166.6
Flux 1, 4 mils Valspar	761	153.3
MnF_3, NP	466	182.5
AlF_3, NP	538	198.0
ZrF_4, NP	498	182.0

Table 5.4 Weld metal hardness for selected Phase II welds (not quenched).

graph in Figure 5.6. This decrease in hardness is due to increases in the amount of the blocky grain boundary ferrite (GBF) that is produced from the high oxygen contents.

Figure 5.7 shows the microstructures of welds made with FeO (1738 ppm) and $CaCO_3$ (555 ppm) fluxes. It is clear to see that the weld produced with the FeO is almost entirely GBF with a Vicker's hardness of 106, while the weld made with $CaCO_3$ is a typical weld microstructure consisting of acicular ferrite, grain boundary ferrite and FS phase with a Vicker's hardness of 189. Welds made with the Interplate primer produced a hardness (192.5 H_V) greater than the base weld (186 H_V), which indicates that the primers also assisted in refining the weld metal microstructure, as seen in Figure 5.8.

Grain refinement is also observed in using the fluoride fluxes. They also produced microstructures that were highly refined compared to the reference weld (Figure 5.8). The hardness, in general, did not change much, except for the welds made with and AlF_3 layer. It could be due to the fact that there are stable carbides produced within lower bainite structures in steels containing aluminum (45) which increase the hardness of the steel or weld metal, or it could be due to the precipitation of fine AlN particles that pin the austenite grains (46).

The mechanism of grain size control results from the aluminum that does not combine with oxygen, but combines with nitrogen to from the fine nitride particles that pin grain boundaries. Whatever the reason, all fluoride welds show some degree of grain refinement which would be beneficial in controlling grain size in welds containing high

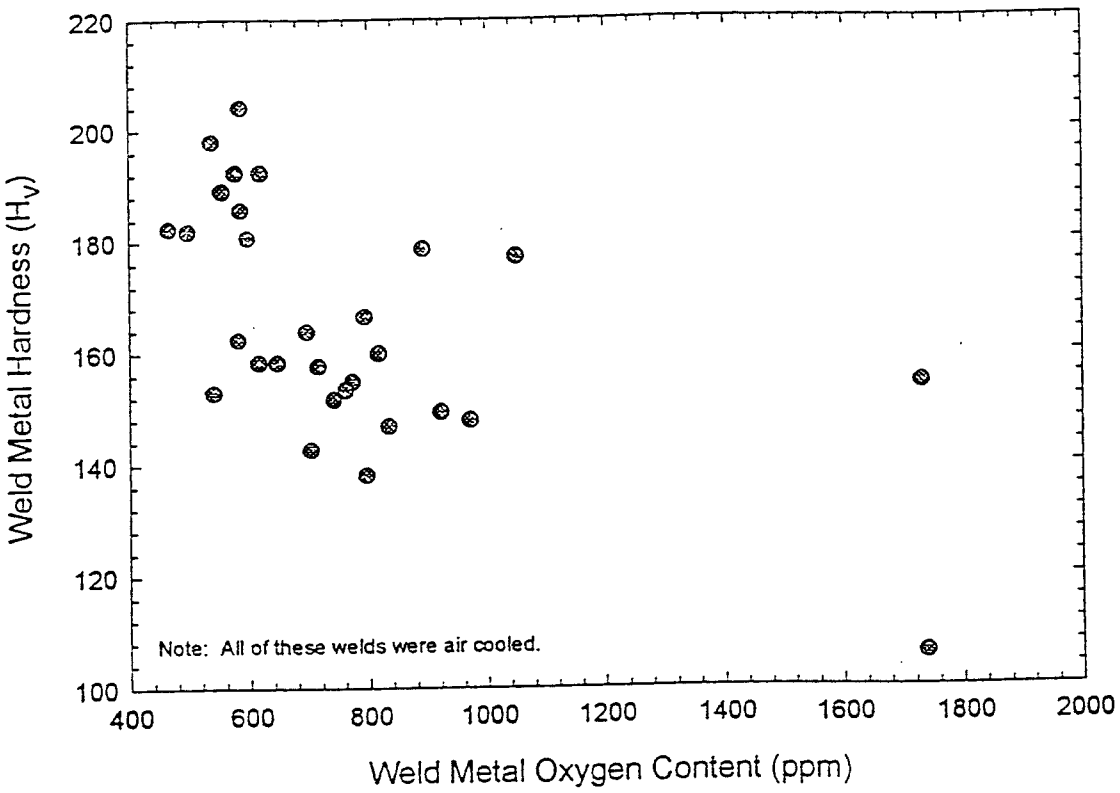

Figure 5.6 Effect of weld metal oxygen content on weld metal hardness (Phase II).

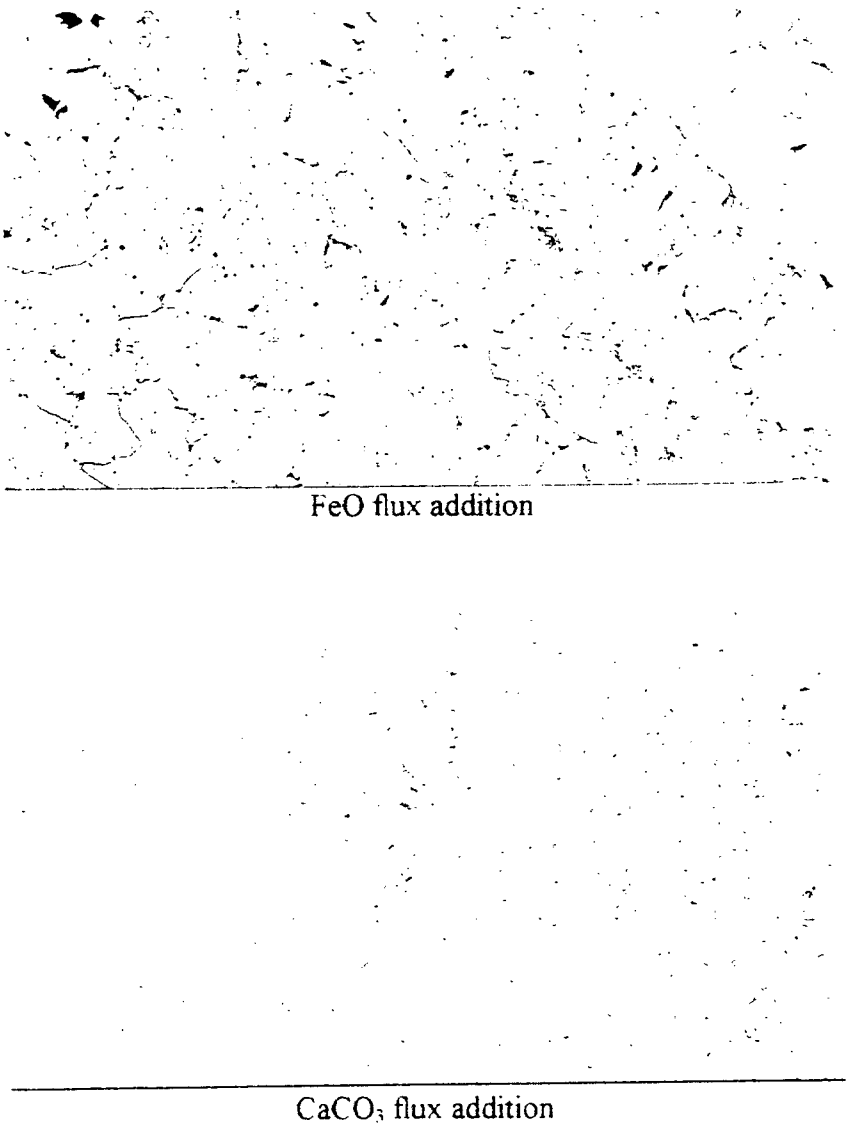

Figure 5.7 Microstructures of welds made with commercial FCAW electrode, and FeO and $CaCO_3$ flux additions (200X).

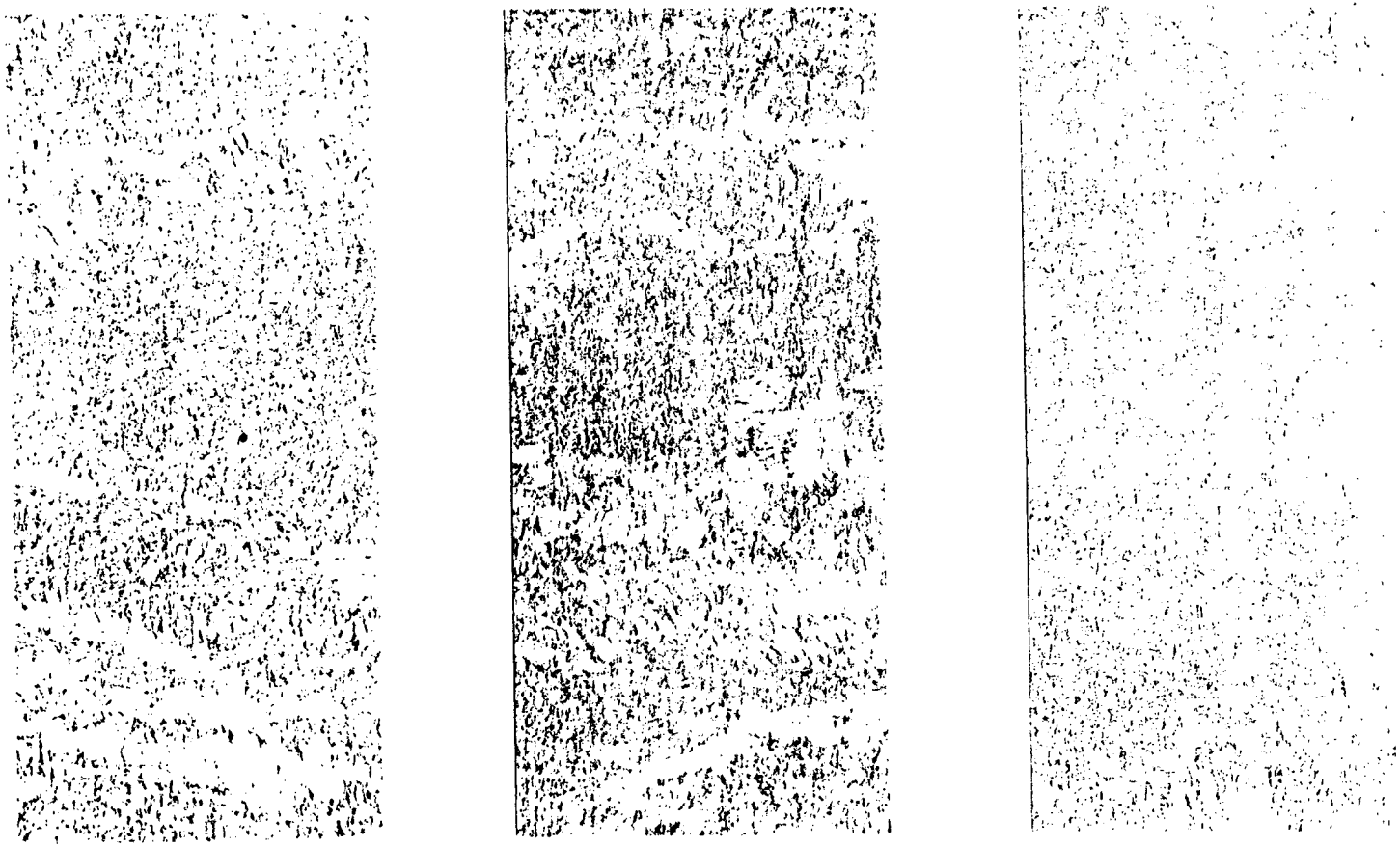

No Primer

4.0 mils Interplate

MnF_3 Additions

Figure 5.8 Microstructures of welds made with commercial FCAW electrodes on samples with no primer, 4.0 mils Interplate, and MnF_3 flux addition (200X).

oxygen levels. Higher oxygen levels not only produce a low hardness, but also large grain sizes. Therefore, control of the grain size would be extremely important. This concluded the work done in Phase II of the project, and gave the guidelines necessary to develop several experimental FCA welding consumables for Phase III.

5.3 Phase III: Formulation of Experimental FCAW Electrodes

The results of Phase II provided the basis for developing some experimental FCA welding electrodes for testing on the basis of diffusible hydrogen, interstitial oxygen, chemical analysis, and mechanical properties. Ingalls Shipbuilding would perform all the multi-pass welds in a flat and vertical position from which two all-weld-metal tensile specimens, two transverse tensile specimens, and ten Charpy V-notch specimens would be machined for testing according to AWS B4.0. Ingalls would also be responsible for performing fillet weld break tests according to AWS B4.0. CSM would be responsible for the mechanical testing and performing bead-on-plate welds for diffusible hydrogen testing, oxygen analysis, and chemical analysis of the weld metal.

5.3.1 Electrode Formulation and Manufacture

The first step was to set some guidelines for the development of the experimental electrode formulations. It was decided early on that four different experimental electrodes

would be manufactured by ESAB Welding and Cutting Products for testing. It was also desired to have a final product that would produce a high level of weld metal oxygen. However, it has been clearly shown that too high of an oxygen content destroys mechanical properties as well as the optimal microstructure. It was decided to limit the oxygen levels produced by the electrodes to about 650 and 750 ppm. The oxygen level produced by the base electrode on the base material was around 600 ppm [O]. The desired levels should be produced by basing the electrodes on the flux combinations #11 (0.5 $CaCO_3$/3.0 SiO_2/1.5 Fe_2O_3) and #1 (0.5 $CaCO_3$/1.0 SiO_2/1.0 Fe_2O_3). It was also desired to add 0.5 moles of MnF_3 to these two electrodes because it is less hygroscopic and less sensitive to increased primer thickness than the other fluorides, which would accommodate the variations in primer thickness present in the industrial setting. MnF_3 also produced the lowest hydrogen levels at the lower baking temperature.

These desired goals were sent to ESAB where they expressed some concern about modifying the Dual Shield II 71 Ultra wire because it already contains strong deoxidizers, which should reduce the weld metal oxygen content to about 450 to 600 ppm. Adding oxide compounds to increase the weld metal oxygen level would have negative effects on the welding performance of the wire. It may also be difficult to get the desired oxides into the wire. It was suggested that the strong deoxidizers could be removed or that another product (Dual Shield 7000) could be used to achieve the desired oxygen levels. There was some concern whether the higher oxygen in the weld metal gave the improved

performance when welding over primer, or whether the actual reactions with the oxide compounds were producing the improved performance. It appeared as if the improvements were a result of the latter which made the removal of the deoxidizers unnecessary. Since all of the previous work was based upon the Dual Shield II 71 Ultra wire, it made sense to continue with it.

Trying to modify an existing product proved to be a difficult task. Changing a consumable can affect the chemistry of the slag and weld pool, which can also make any prediction of chemical reactions difficult in subsequent work. It is difficult to incorporate these oxides into the consumable because of the difficulty that exists in determining the exact amount of flux that was used in the experiments since they were placed on top of the samples prior to welding. It was suggested that two approaches might be followed to incorporate the additions. The first would be to just add in the additions as desired. The second would be to develop a wire that would generate the desired oxygen content with alloying requirements based on chemical analysis results. It was determined that just adding in the desired oxides would be the best approach with modifications made to accommodate weldability.

To determine the amounts of the fluxes to be added to our electrode, several calculations were made based on our flux combinations and the chemical analysis of the Dual Shield II 71 Ultra flux as analyzed. The first step was to determine the weight of the electrode per inch which turned out to be about 0.245 g/in (0.01 g/mm). Next, the flux

weight in the wire used to make one inch of weld was determined. This was based on a fill ratio of 20 pct. (flux/metal), even though this is not the exact figure. The flux weight used in one inch of weld is about 1.013 g. The percentage of each of the flux components was calculated based on the chemical analysis results that were determined. The volume of added flux was based on a flux layer thickness of 1/64 in. (0.4 mm) over a distance of 17/32 in. (13.5 mm) which represents the distance over an average weld bead or the perimeter of a half-cylinder. The volume of added flux turned out to be 0.0083 in^3 or 0.136 cm^3. The next step was to calculate the percentage of the flux components in the added flux, and then the weight of each. The densities used are "apparent" densities based on the grain size of the fluxes determined by ESAB.

These formulations were again sent to ESAB for further review and suggestions to improve or eliminate any possible problems. It was noticed that the assumption of the 20 pct. fill percentage was too high. The Dual Shield products have a fill percentage of 12.5 pct. which changed the weight of flux per inch to 0.633 g. ESAB did not foresee any problems as far as weldability. The only problem was the availability of Fe_2O_3 in the necessary size. Because they were not able to locate a supply of the hematite (Fe_2O_3) in the required size, it was decided to substitute magnetite (Fe_3O_4), which would change the oxidizing potential, but it was determined through some thermodynamic calculations not to a large degree. With this change in mind, the final compositions as proposed by ESAB can be seen in Table 5.5 using the Fe_3O_4 instead of the Fe_2O_3. To accommodate our flux

Electrode	% ESAB Slag	% ESAB FeAlloys	% Fe	%$CaCO_3$	% SiO_2	% Fe_2O_3	% MnF_3
UA-632	***	***	***	***	***	***	***
UA-633	63.25	23.00	1.90	1.25	4.35	6.25	0.00
UA-634	63.25	23.00	1.35	1.10	4.10	6.00	1.20
UA-635	63.25	23.00	3.00	1.90	2.30	6.55	0.00
UA-636	63.25	23.00	2.20	1.65	2.00	6.00	1.90

Table 5.5 Composition of experimental electrodes used in Phase III.

additions, a higher fill percentage and thinner strip had to be used. The ESAB slag and Fe alloys were balanced to get the same weight percentages in the original wire.

5.3.2 Welding of Experimental FCAW Electrodes

Aside from the 4 experimental compositions of the electrodes shown in Table 5.5, ESAB made another electrode with an increased fill percentage based on the Dual Shield II 71 Ultra for comparison with the experimental FCA welding electrodes. The electrodes were tested on samples for diffusible hydrogen testing over mercury. Because these samples were coated with both the Valspar and Interplate primers, they were not cleaned nor degassed according to the specification so the hydrogen levels were expected to be somewhat higher. The samples tested were coated with no primer, 1.5 and 4.0 mils Interplate, and 1.5 and 4.0 mils Valspar. According to ESAB, they were a bit concerned about how the flux additions would affect the weldability. However, they noted that the electrodes performed quite well which was also substantiated by the CSM welding experiments. It was difficult to determine any variations in transfer modes, arc stability, and overall performance since they all performed well. They all had increased spatter and fume generation as the primer thickness increased which is expected. The Valspar primer appeared to create the most spatter and fumes when welded over as compared to the Interplate.

5.3.3 [H]-[O] Analysis

The welding of the experimental electrodes were followed by the diffusible hydrogen tests and interstitial analysis for oxygen. The results of these tests can be seen in Table 5.6. The diffusible hydrogen results show that as the primer thickness increased, the amount of hydrogen also increased. Again, the Valspar (zinc, epoxy based) primer produced less hydrogen than did the Interplate (zinc, ethyl-silicate based) primer. The results show that UA-636 (containing Flux #1 and MnF_3) produced the lowest average diffusible hydrogen overall at about 13.33 ml/100g, followed by UA-632 (commercial product) at 14.95 ml/100g.

In the case of UA-632 (commercial product), which is based upon the Dual Shield II71 Ultra with an increased fill percentage, the results are much lower for the diffusible hydrogen at higher primer thickness than those obtained in Figure 5.5. This result could be due to the increased fill percentage of the electrode since nothing else was changed. Nevertheless, the experimental electrodes all produced lower hydrogen values with increasing primer thickness.

When these results are plotted against the weld metal oxygen results, as seen in Figure 5.9, a downward trend in diffusible hydrogen for increasing oxygen levels is established for each of the electrodes and primer combinations. This trend was established during verification of the *hydrogen-oxygen* equilibrium. As was stated in Section 5.3, the reference weld made with the base electrode resulted in an oxygen content of 600 ppm,

Diffusible Hydrogen (ml/100g)					
Electrode	No Primer	1.5 mils I	4.0 mils I	1.5 mils V	4.0 mils V
UA-632	10.11	12.4	20.97	11.72	19.57
UA-633	13.53	14.94	19.39	14.27	15.68
UA-634	9.23	15.92	19.82	16.41	19.55
UA-635	11.61	14.91	28.08	34.85	16.03
UA-636	9.64	10.87	15.77	10.97	19.42
Interstitial Oxygen (ppm)					
Electrode	No Primer	1.5 mils I	4.0 mils I	1.5 mils V	4.0 mils V
UA-632	540	604	562	564	575
UA-633	662	655	674	639	590
UA-634	681	700	725	712	677
UA-635	596	599	591	617	627
UA-636	653	673	665	655	662

Table 5.6 Results of the weld metal diffusible hydrogen and oxygen analysis for each electrode, primer type and primer thickness used.

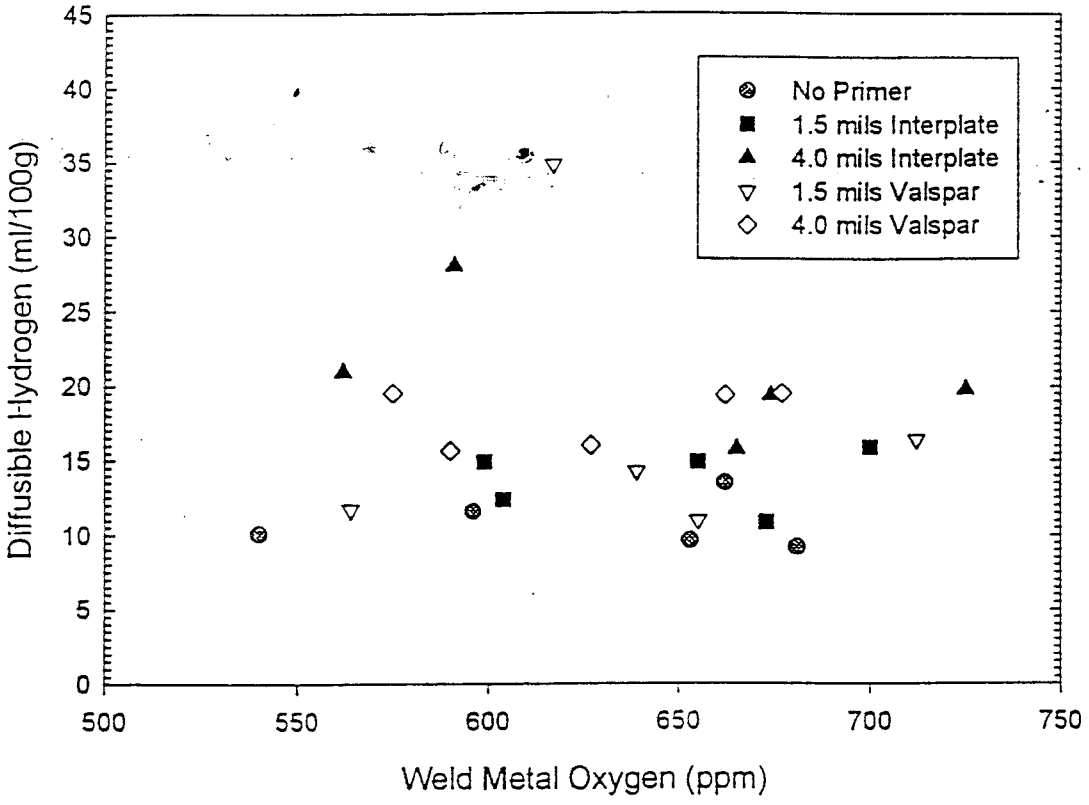

Figure 5.9 Plot of weld metal diffusible hydrogen as a function of weld metal oxygen content for the Phase III welds.

and oxygen levels of 650 and 750 ppm were desired with the flux additions.

One thing that was quite unexpected was the fact that as the MnF_3 was added to the two other experimental electrodes, the oxygen levels increased about 70 ppm. This result should not happen since the percentage of the added oxidizing components dropped in each electrode dropped. Examining the free energy of formation (ΔG_f^0) data for the formation of $H_2O_{(g)}$ and $HF_{(g)}$ helps to explain the reason for this occurrence. The data shows that the free energy of formation for $HF_{(g)}$ is more negative than the free energy of formation for $H_2O_{(g)}$ which indicates that $HF_{(g)}$ is likely to form before the $H_2O_{(g)}$. As a result, more oxygen becomes available to form oxide inclusions which would increase the weld metal oxygen content.

Because there are so many competing reactions taking place, this analysis may be somewhat oversimplified, but it does give a plausible explanation for this increased oxygen occurrence. Oxygen in the weld environment can affect the weld metal properties by the precipitation of non-metallic inclusions, by oxidizing alloy additions, and by causing CO porosity. Oxides precipitate in the liquid metal as it cools, and appear in the solidified weld as spherical inclusions. They are composed mainly of the oxides of silicon, manganese and any other deoxidants that may be present.

5.3.4 Hardenability of Welds

The next step was to examine the hardenability of the individual welds made with each primer and primer thickness. Because these welds were also used for the diffusible hydrogen testing, they had been quenched in ice water immediately after welding making them suitable for hardenability testing. The hardness for each weld made on the different primers and primer thicknesses can be seen in Table 5.7. The Vickers hardness (H_V) of each weld made on "no primer" were quite similar to one another. Differences in the readings can be attributed to the chemistry of the weld metal which affects hardenability. The hardness of the welds made with the electrodes containing MnF_3 additions (UA-634 and UA-636) appear to help refine the microstructure as seen by the hardness increases. This result could be attributed to the change in the level of oxidizing and fluoride flux additions, and the fact that there are several competing reactions taking place which affect the microstructure.

The hardness of the weld metals produced by quenching compared to air cooling indicates that the weld metal produced by the experimental FCAW consumables is quite hardenable. Hardenability is defined as the "susceptibility to hardening by rapid cooling" or "the capacity of a steel to transform partially or completely from austenite to some percentage of martensite" (47,48). The Vicker's hardness of the air-cooled welds made with no primer were 189.0 (UA-632), 182.0 (UA-633), 182.5 (UA-634), 180.5 (UA-635), and 185.5 (UA-636). Upon quenching, the hardness increased by an average of 86 points.

Electrode	Primer	Thickness	Weld metal Oxygen (ppm)	Weld Metal Hardness (Vickers)
UA-632	NP	0	540	275.5
	Interplate	1.5 mils	604	272.0
	Interplate	4.0 mils	562	323.4
	Valspar	1.5 mils	564	316.4
	Valspar	4.0 mils	575	306.8
UA-633	NP	0	662	277.6
	Interplate	1.5 mils	655	274.1
	Interplate	4.0 mils	674	286.0
	Valspar	1.5 mils	639	263.6
	Valspar	4.0 mils	590	283.2
UA-634	NP	0	681	274.8
	Interplate	1.5 mils	700	302.0
	Interplate	4.0 mils	725	318.0
	Valspar	1.5 mils	712	309.2
	Valspar	4.0 mils	677	314.8
UA-635	NP	0	596	259.4
	Interplate	1.5 mils	599	272.0
	Interplate	4.0 mils	591	346.8
	Valspar	1.5 mils	617	354.0
	Valspar	4.0 mils	627	365.7
UA-636	NP	0	653	261.8
	Interplate	1.5 mils	673	264.8
	Interplate	4.0 mils	665	307.6
	Valspar	1.5 mils	655	276.9
	Valspar	4.0 mils	662	292.4

Table 5.7 Weld metal hardness results from experimental electrodes for Phase III welds (quenched).

Generally, steels containing less than 0.3 wt. pct. carbon (e.g. DH-36 plate contains 0.06%) tend to be difficult to harden, and are usually used comprised of a ferrite-pearlite microstructure (46). This type of microstructure is typical of welds made with an E71T-1 electrode. Because these types of welds do not contain high levels of carbon or alloying additions, a martensitic microstructure cannot be obtained to promote high strength, fatigue and wear resistance. Therefore, these properties must be enhanced through alloying with elements such as manganese and silicon, and with microalloying additions of vanadium, niobium (or columbium) and titanium.

The results also showed that increasing the primer thickness assists with increasing the hardenability of the weld metal. Using the results for UA-636 as an example, the weld metal hardness for the sample with no primer was 261.8 H_V. As the Interplate primer thickness increased from 1.5 to 4.0 mils, the hardness increased from 264.8 to 307.6 H_V. As the Valspar primer increased from 1.5 to 4.0 mils, the hardness increased from 276.9 to 292.4 H_V. The other electrodes exhibited similar results. As has been mentioned before, some of the hardness differences could be explained by microstructural differences brought on by differences in chemical composition of the weld metal.

5.3.5 Mechanical Testing

The mechanical testing performed on each of the experimental electrodes provided some very encouraging results. The actual acceptance criteria for the mechanical tests

included AWS A5.20 (Specification for Carbon Steel Electrodes for FCAW) and Mil-E--24403/1D (Electrodes - Welding, Flux-Cored, Ordinary Strength and Low Alloy). These specifications governed the properties of the original electrode used (Dual Shield II71 Ultra) in the early experiments. Because samples were welded in both the flat and vertical position, separate tests were conducted for each position as far as tensile and Charpy tests.

The results that were obtained for the all-weld-metal tensile samples in the flat and vertical positions can be seen in Figure 5.10. The strain rate for each of these tests 0.5 in/in of gage length, per minute. The stress-strain diagrams for each of the electrodes exhibited discontinuous yielding in the weld metal with upper and lower yield points (49). In low-carbon steels, the upper yield point can be associated with small amounts of interstitial or substitutional impurities. Carbon or nitrogen atoms readily diffuse to the position of minimum energy just below the extra plane of atoms in a positive edge dislocation. The elastic interaction is so strong that the impurity atmosphere becomes completely saturated and condenses into a row of atoms along the core of the dislocation. When the dislocation line is pulled free from the influence of the solute atoms, yielding can occur at lower stress. This explains the origin of the upper and lower yield point.

In the flat position, only UA-633 failed to pass both the YS and UTS requirements. For the all-weld-metal samples, only UA-635 and UA-636 samples passed both standards. The best performing electrode was UA-636 with 66.3 ksi (457 MPa) σ_{ys}, 71.7 ksi (494 MPa) σ_{uts}, and 29.4 pct. elongation. In the vertical position, only UA-633

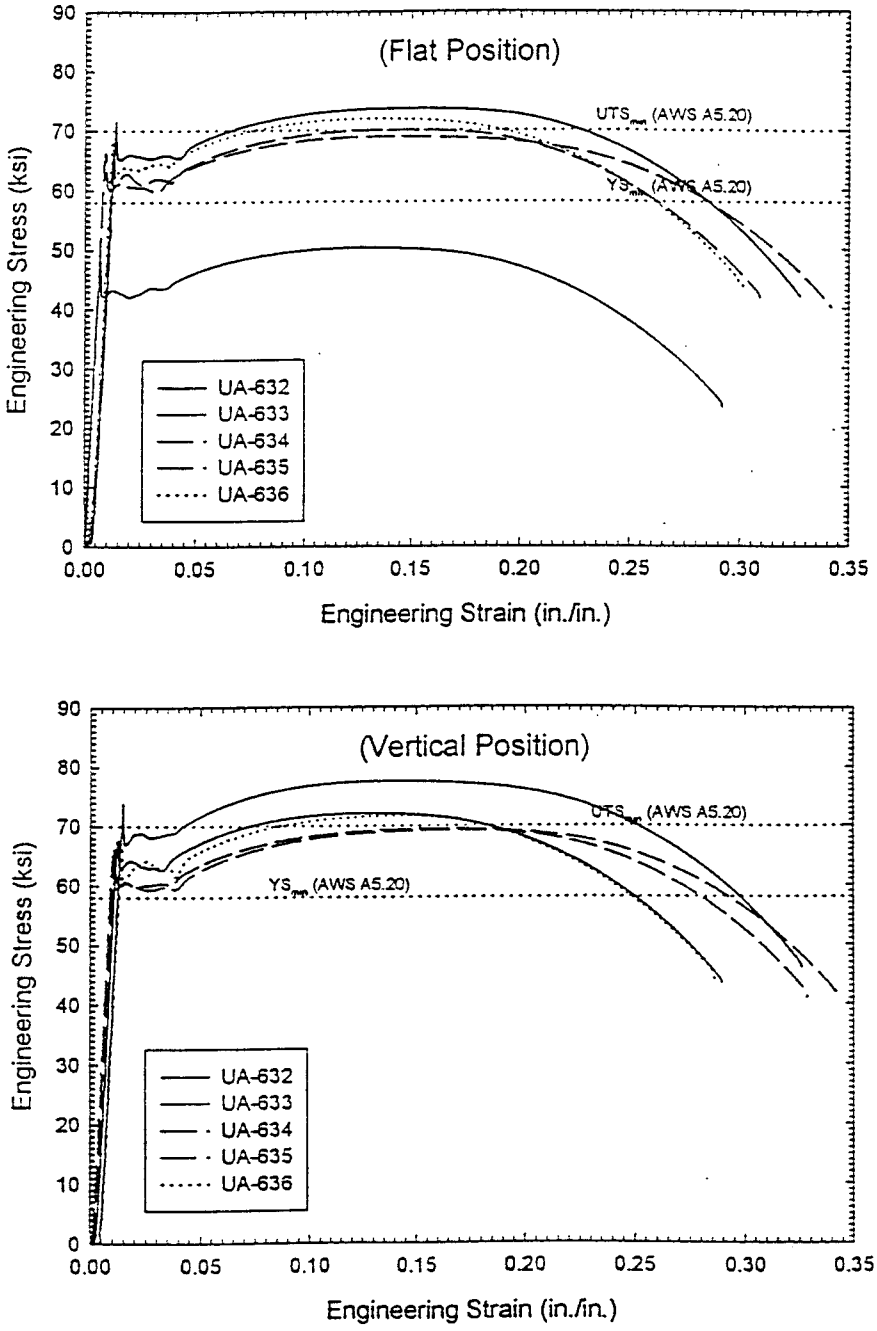

Figure 5.10 Stress-strain diagrams for tensile samples welded in the flat and vertical positions for Phase III.

and UA-636 passed according to the specifications. UA-633 performed the best at 65.2 ksi (450 MPa) σ_{ys}, 72.2 ksi (498 MPa) σ_{uts}, and 28.9 pct. elongation, followed closely by UA-636 at 61.6 ksi (425 MPa) σ_{ys}, 70.3 ksi (485 MPa) σ_{uts}, and 29.5 pct. elongation. The electrode that was based on the ESAB commercial product, the UA-632 electrode, performed better than most of the experimental electrodes in certain situations. The results of these tests can be seen in Table 5.8.

In the tensile fracture of moderately ductile metals, the plastic deformation produces a necked region (49). Necking begins at the point of plastic instability where the increase in strength due to strain hardening fails to compensate for the decrease in cross-sectional area. Fracture begins at the center of the specimen due to microvoids, and then extends by a shear separation producing what is known as a "cup-and-cone" fracture surface. These microvoids can be formed at sites containing inclusions, second-phase particles, or fine oxide particles. Each one of the all-weld-metal samples exhibited this type of surface. The necking, or fracture, did not necessarily occur in the center of the 2.00 in. (50.8 mm) gage length. Fracture mostly occurred slightly off-center of the 2.00 in. (50.8 mm) gage length for all of the flat and several of the vertical samples. Fracture occurred nearly 5/8 in. off-center for samples produced with UA-633 and UA-636. This just indicates that there was a higher fraction of inclusions or oxide particles located there to initiate the fracture. The strength of the weld metal was not affected by the location of fracture within the gage length.

	UA-632	UA-632	UA-633	UA-633	UA-634	UA-634	UA-635	UA-635	UA-636	UA-636	Acceptance Standards	
Properties	CSM	Ingalls	CSM	Ingalls	CSM	Ingalls	CSM	Ingalls	CSM	Ingalls	AWS A5.20	Mil-E-24403/1D
Yield Strength (ksi; flat)	68.3	61.6	42.7	57.1	62.6	57.2	64.7	59.4	66.3	59.8	58.0	60 AW / 55 SR
Yield Strength (ksi; vertical)	70.4	57.1	65.2	52.4	58.8	51.8	60.4	58.3	61.6	59.1	58.0	60 AW / 55 SR
Ultimate Tensile Strength (ksi; flat)	73.8	77	49.0	70.7	67.6	74.5	70.0	76.2	71.7	76.2	70.0	70.0
Ultimate Tensile Strength (ksi; vertical)	77.6	80.6	72.2	76.5	66.2	73.5	67.1	74.4	70.3	76.0	70.0	70.0
Elongation (%; flat)	32.7	31	31.3	27.5	32.8	28.0	31.9	27.5	29.4	28.0	22.0	22.0
Elongation (%; vertical)	32.7	32	28.9	26.5	34.2	30.0	33.0	29.0	29.5	29.5	22.0	22.0
Reduction of Area (%; flat)	74.7	62.2	73.5	58.4	72.6	58.9	73.2	56.9	71.8	57.9	***	***
Reduction of Area (%; vertical)	70.9	61.5	71.7	55.0	71.9	61.1	71.4	57.5	70.2	59.0	***	***
Charpy V-Notch (ft-lbs; flat)												
*@ 20°C	135.5	***	94.0	***	108.0	***	128.0	***	137.0	***	***	***
*@ 0°C	108	***	71.0	***	83.5	***	97.0	***	64.5	***	***	30.0
*@ -20°C	68	***	52.5	***	37.0	***	32.0	***	36.0	***	20.0	20.0
*@ -40°C	15	***	30.0	***	8.0	***	7.0	***	17.0	***	***	***
Charpy V-Notch (ft-lbs; vertical)												
*@ 20°C	137.5	***	60.5	***	133.5	***	144.0	***	152.5	***	***	***
*@ 0°C	101	***	60.5	***	110.5	***	125.0	***	132.5	***	***	30.0
*@ -20°C	14.5	***	27.5	***	73.5	***	107.6	***	52.0	***	20.0	20.0
*@ -40°C	6.5	***	8.0	***	22.0	***	17.6	***	10.0	***	***	***

Table 5.8 Mechanical test results on experimental FCAW electrodes for Phase III.

The transverse tensile specimens were performed by Ingalls Shipbuilding because they possessed the necessary equipment to test the specimens. The transverse samples welded in the flat position all passed requirements, except for UA-633. UA-632 performed the best at 61.6 ksi (425 MPa) σ_{ys}, 77.0 ksi (531 MPa) σ_{uts}, and 31.0 pct. elongation, followed by UA-636 at 59.8 ksi (412 MPa) σ_{ys}, 76.2 ksi (525 MPa) σ_{uts}, and 28.0 pct. elongation. For the samples welded in the vertical position, only UA-635 and UA-636 passed the requirements. UA-636 performed the best with results of 59.1 ksi (408 ksi) σ_{ys}, 76.0 ksi (524 ksi) σ_{uts}, and 29.5 pct. elongation. These results are comparable to those obtained with the all-weld-metal samples. The differences occur mainly because of the different strain rates used in each set of tests. The all-weld-metal tests used a strain rate of 0.5 in/in, while the transverse tests used rates from 0.007 to 0.05 in/in because the equipment used wasn't computer controlled for the same reason the transverse tensile test data generated could not be plotted as stress-strain curves.

The impact energy absorbed for each of the electrodes was determined using the Charpy V-notch test apparatus and samples as described in Section 4.7. The test specimens were machined out of the same weld metal as the tensile specimens. Multi-pass welds were made in both the flat and vertical positions. All of the electrodes provided samples that passed the criteria set forth in the specifications of 20 ft-lbs at a test temperature of -20^0C (-4^0F). The results of the tests at these temperatures are shown in Table 5.8. Figure 5.11 shows the impact energy absorbed for each of the electrodes in the

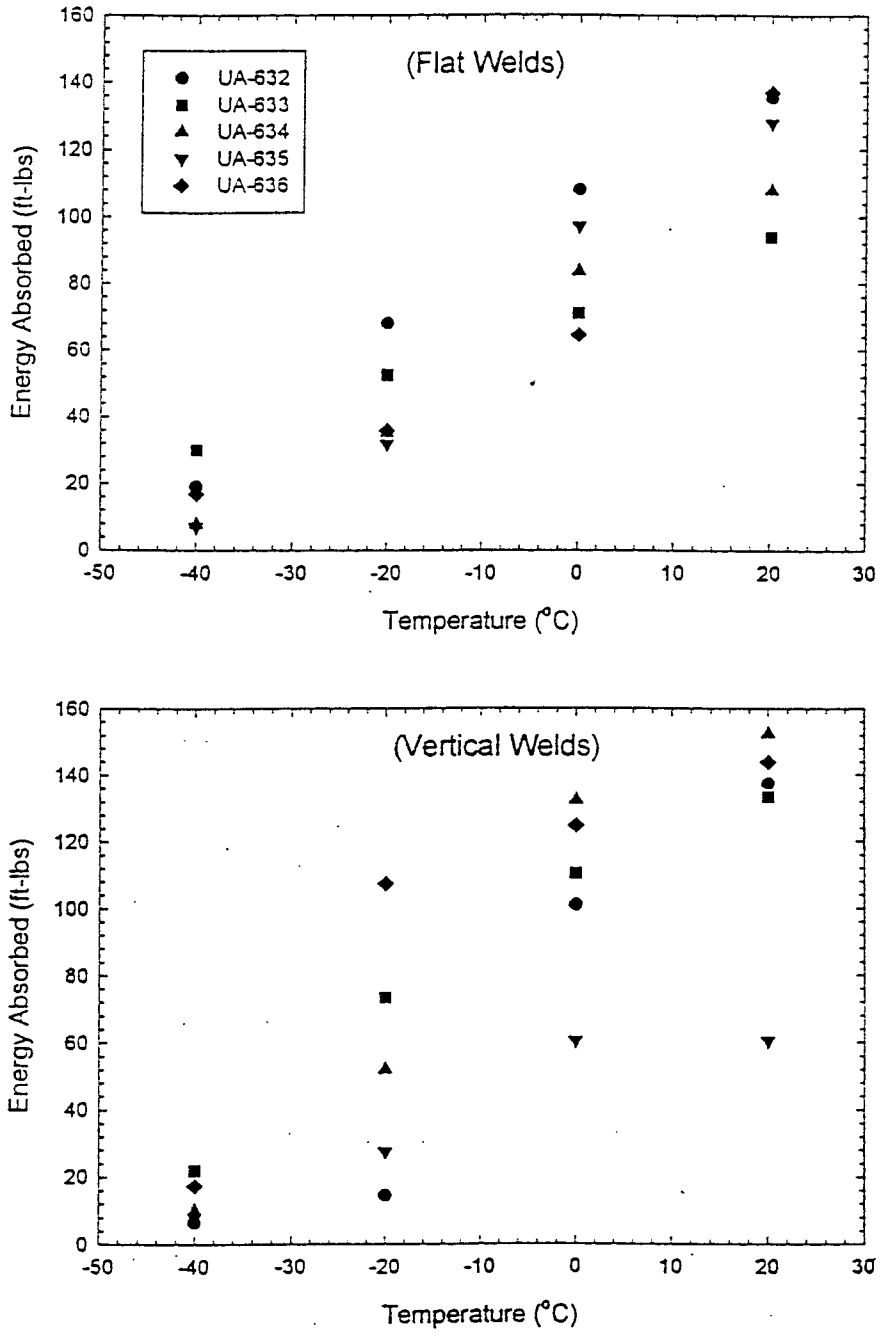

Figure 5.11 Charpy V-notch impact energy for samples welded in the flat and vertical positions for Phase III.

flat and vertical positions. The temperature range, as stated, was set at 20^0C to -40^0C due to the limited number of samples.

Most of the samples tested did provide adequate data to construct a typical ductile-to-brittle transition temperature (DBTT) curve for each of the electrodes (50). The DBTT is the temperature at which the fracture surface exhibits roughly a 50/50 mix of ductile (rough or fibrous) and brittle (irregular, small bright facets) fracture modes (49,50). The Charpy samples showed a nice transition in the fracture surfaces from being nearly 100 percent ductile at 20^0C to nearly 100 percent brittle at -40^0C.

The easiest definition of this transition temperature is stated as the average between the upper and lower shelf energy values (49). The DBTT appears to be around -10^0C (14^0F) for each of the electrodes. The transition temperature can also be defined as the temperature at which a Charpy specimen breaks with a fixed amount of energy (50). This result is the type of criteria used in the AWS and Military specifications (see Table 5.8). For the flat welds, UA-633 appeared to perform the best overall. For the vertical welds, UA-635 appeared to perform the best overall. It is important to remember that each of the electrodes passed the requirements set forth in the specifications, so any one would be acceptable to use. Each of the electrodes performed better in the vertical position as compared to the flat position as far as energy absorbed. There are several variables that affect the transition temperature of steel weld metals, including microstructure and chemical composition. It has been shown in the literature that a weld

microstructure with about 70 percent acicular ferrite is the best at arresting crack propagation (51). The microstructure is affected by the amount of oxygen in the weld metal, along with other elements such as carbon, phosphorus and manganese. Carbon and phosphorus tend to increase the transition temperature, while manganese lowers it (50). This result is one reason that low carbon steels contain a liberal amount of manganese in both the FCAW consumable and the base material. Besides lowering the transition temperature, the manganese also helps to increase hardenability of the weld metal.

Welding in the vertical-up position appears to allow time for inclusions within the weld metal to float upward as the weld pool progresses, which also keeps the inclusions from being trapped in the solidifying weld pool. In the upper-shelf temperature region, ductile fracture occurs by microvoid coalescence. Microvoids are initiated at inclusion/matrix interfaces which leads to a decrease in upper-shelf energy with increasing inclusion content. This means that the cleaner the weld metal, the higher the energy absorbed.

One other possibility could be the fact that different welding parameters were used during each pass in the making of the multi-pass welds. Each electrode did not take the same number of passes to complete each set of welds in both the flat and vertical positions. For example, in the flat position, UA-633 took nineteen passes to complete the weld, and UA-635 took sixteen passes with the others falling in between. For the vertical position, all of the electrodes took ten passes to complete, but UA-636 took only eight

passes. The number of passes would affect the properties possessed by the weld metals.

Another factor for the differences in properties could be the heat input. The heat input is calculated using the current (I), voltage (V), travel speed (s), and process efficiency (η) (14). The heat input equation is as follows:

$$H.I.=\frac{I\times V}{s}(\eta) \quad \text{.....(5.3.1)}$$

The process efficiency is determined by the welding process used. For FCA welding, it is roughly 0.75 (52). The average current, voltage, travel speed, and heat input for the flat welds can be seen in the following:

Electrode	Current (A)	Voltage (V)	Speed (ipm)	H.I. (kJ/mm)
UA-632	213.3	26.6	12.0	1.23
UA-633	213.6	26.2	12.5	1.11
UA-634	215.6	27.1	11.6	1.26
UA-635	209.7	26.3	12.0	1.17
UA-636	221.8	25.5	12.0	1.20

These values are quite similar to one another with only minor differences. Because the heat input is based upon basically three different variables, there are several combinations that can give the same amount of heat input. These all affect the type of weld metal one would obtain as far as mechanical properties. The average current, voltage, travel speed, and heat input for the vertical welds can be seen in the following:

Electrode	Current (A)	Voltage (V)	Speed (ipm)	H.I. (kJ/mm)
UA-632	209.8	25.6	6.4	2.04
UA-633	197.5	25.5	5.8	2.10
UA-634	193.5	26.5	5.6	2.21
UA-635	189.5	26.1	5.7	2.06
UA-636	195	25.9	4.9	2.44

It is easy to see that the vertical welds were subjected to almost twice the amount of heat input to which the flat welds were subjected. The current, voltage and travel speed were higher for the flat welds than for the vertical welds. However, the travel speed for the vertical welds was fifty percent less. This is the key for the high heat input of the vertical welds.

Multi-pass welds can lead to refinement of the microstructure which in turn improves toughness (52). Each resulting pass, or weld thermal cycle, can effectively refine or "normalize" the previous weld metal. The net effect of reheating the heat-affected zone (HAZ) produces the refinement rather than causing larger prior austenite grain sizes. The larger the number of passes, or beads, results in a greater volume of reheated weld metal, or recrystallized weld metal. The increased amount of grain refined weld metal results in the removal of segregation products, and will also result in higher notch toughness (52). This can also be the case when fewer (larger) runs are used. This would produce an increase in the amount of recrystallized weld metal. This reheating can also cause microalloying additions (e.g. Nb, V, Ti, etc.) to create grain hardening and reduce toughness. The weld centerline at which the Charpy V-notch is generally located can

experience severe segregation during higher speeds in welding. It is clear to see that there are several factors which affect the amount of energy absorbed. The higher energy absorbed by the vertical Charpy samples is very likely a combination of having cleaner weld metal and the fact that they were produced with fewer passes at slower speeds and higher heat input.

The fillet weld break tests were performed by Ingalls Shipbuilding on samples with no primer, 1.5 and 4.0 mils Interplate, and 1.5 and 4.0 mils Valspar. The welding parameters used for each of the electrodes were similar and averaged 230 A, 27 V, and 8.4 ipm travel speed. These parameters produced an average heat input of 1.75 kJ/mm. The tests showed exactly how the experimental electrodes performed when welding over primers in an identical environment. The purpose of this test is to determine the soundness of fillet welded joints. This test is qualitative in nature with acceptance determined by the extent and nature of flaws present. The fillet weld specimen, as shown in Figure 4.4, has one leg bent upon the other so as to place the root of the weld in tension. The load is maintained until the legs of the joint come in contact with each other or the specimen fractures. The fracture surface is then examined visually for evidence of cracks, inclusions or lack of penetration.

The observations of the first side welds made in the fillet weld break tests are shown in Table 5.9. Tests were done with each of the four experimental electrodes, along with UA-632 (commercial product). Each of the electrodes produced significant amounts

UA-632 (Commercial)	UA-633	UA-634	UA-635	UA-636
*fumes and spatter increased with increasing primer thickness	*less fumes that UA-632; Valspar produced less spatter than the Interplate	*Same as the UA-633	*Same as the UA-633	*Same as the UA-633
*exposed porosity & worm tracks on the 2nd side welds were less than on the 1st side	*exposed porosity & worm tracks on 2nd side weld, except on the 1.5 mil Interplate. It had worm tracks or pin holes on either side.	*pin holes & worm tracks on the surface of 2nd side welds of each samples were less than that generated on the first side welds	*pin holes & worm tracks on the surface of 2nd side welds of each samples were less than that generated on the first side welds	*pin holes & worm tracks on the surface of 2nd side welds of each samples were less than that generated on the first side welds
*unstable arc, spray to globular	*fairly stable spray arc transfer	*Valspar - stable spray arc transfer; Interplate - spray to globular	*fairly stable spray arc transfer	*produced a slightly unstable arc then alternated between spray and globular
*voltage variations due to primer thickness differences	*voltage variations due to primer thickness differences	*voltage variations due to primer thickness differences	*voltage variations due to primer thickness differences	*voltage variations due to primer thickness differences
*smoke generated made it difficult to breath and perform weld inspection	*smoke generated made it difficult to breath and perform weld inspection	*smoke generated made it difficult to breath and perform weld inspection	*smoke generated made it difficult to breath and perform weld inspection	*smoke generated made it difficult to breath and perform weld inspection
Visual Inspection of First Side Welds (1VPA & 1IPA - 1.5 mil Primer)	*Visual Inspection of First Side Welds (2VPA & 2IPA - 1.5 mil Primer)*	*Visual Inspection of First Side Welds (3VPA & 3IPA - 1.5 mil Primer)*	*Visual Inspection of First Side Welds (4VPA & 4IPA - 1.5 mil Primer)*	*Visual Inspection of First Side Welds (5VPA & 5IPA - 1.5 mil Primer)*
1VPA: minor worm tracks and 4 pinholes visible in initial 25% of fillet weld length	2VPA: random pin holes & worm tracks were formed in the initial 50% of weld length	3VPA: total of three randomly dispersed worm tracks were formed in the fillet weld	4VPA: randomly dispersed worm tracks were visible in the initial 12" of the fillet weld	5VPA: no worm tracks or pin holes were visible on the weld surface
1VPB: extensive porosity and worm tracks observed in full length of fillet weld, defects were randomly dispersed over length	2VPB: random pin holes & worm tracks were viable throughout the entire weld length	3VPB: random dispersed pin holes and worm tracks were visible throughout the entire weld length	4VPB: random dispersed worm tracks were visible throughout the entire weld length	5VPB: randomly dispersed pin hole tracks were visible throughout the entire weld length
1IPA: total of 4 pin holes about 1/8" diameter were observed in initial 25% of length of fillet weld	2IPA: no exposed pin holes or worm tracks visible	3IPA: visual inspection of the weld surface showed 5 pin holes about 3/32" to 1/8" diameter	4IPA: no worm tracks or pin holes were visible on the weld surface	5IPA: one pinhole formed in fillet weld
1IPB: minor worm tracks were viable in the initial 10% of fillet weld length	2IPB: pin holes were visible throughout the entire length of the weld, nine of the pinholes about 1/8" diameter	3IPB: ten pin holes were formed in the fillet weld and were primarily concentrated between 18" and 27" along the weld length	4IPB: visual inspection of the weld surface showed two pin holes and worm tracks in the first 12" of the weld	5IPB: pin holes and worm tracks were formed in the first 27"
X-Ray Inspection	*X-Ray Inspection*	*X-Ray Inspection*	*X-Ray Inspection*	*X-Ray Inspection*
Accepted	Accepted	Accepted	Accepted	Accepted

Table 5.9 Observations of first-side fillet welds made for the fillet weld break tests for Phase III.

of fumes and spatter as the primer thickness increased. The Valspar primer (zinc, epoxy based) produced less spatter than did the Interplate primer (zinc, ethyl-silicate based). It appeared that the commercial electrode (UA-632) produced slightly more fumes than the other electrodes. This decrease in fume levels could be due to lesser amounts of volatile flux constituents in the experimental electrodes or possibly due to shifts in the partial pressures of gasses within the welding arc. The transfer mode of each electrode varied from one to the other. UA-632 had an unstable arc in which the transfer mode switched between spray and globular transfer modes, while UA-633 had fairly stable, spray arc transfer. There were also differences in transfer modes depending on which primer was used. UA-634 produced a stable, spray arc transfer with the Valspar, and a spray to globular transfer with the Interplate.

With these minor variations in arc stability and transfer modes, there were significant differences in the level of weld discontinuities produced. The commercial product (UA-632) produced significant amounts of pinholes and visible worm tracks in the samples with only 1.5 mils of each primer. Samples coated with 4.0 mils of each primer produced extensive amounts of porosity and worm tracks throughout the entire weld lengths. Electrodes UA-633 and UA-634 produced no exposed pin holes or worm tracks on samples with 1.5 mils Interplate. However, there were random pin holes and worm tracks on the other samples, as well as the samples welded with UA-635.

Examination of the results from the UA-636 indicated that it performed quite well,

even at higher primer thickness. On the samples with 1.5 mils of the primers, only the Interplate had one visible pin hole on the weld surface, while the Valspar had none. The samples with 4.0 mils of the primers both had small amounts of randomly dispersed pinholes. The other electrodes produced much higher levels of discontinuities than the UA-636. It appears that UA-636 performs the best with regards to the level of discontinuities produced for the first side welds.

Conclusions about the second-side welds are not as forthcoming. Each of the electrodes welded on samples with no primer produced very minor amounts of porosity as evidenced by the example in Figure 5.12. Examples of the other electrodes welded on the different primers at the different thicknesses can also be seen in Figures 5.13 through 5.16. They each produced varying levels of porosity and worm tracks. Figure 5.13, which was done with UA-634 over 1.5 mils of Interplate primer, shows an extremely high level of worm tracks. Figure 5.15, which was done with UA-636 over 4.0 mils of Interplate primer, has a high level of large pores. It does appear that UA-636 produced the lowest content of discontinuities overall. Based on these results and the first-side weld observations, UA-636 appears to perform the best.

5.3.6 Weld Metal Chemical Analysis

The results of the chemical analysis of the bead-on-plate welds made with the experimental electrodes can be seen in Table 5.10, along with the weld metal carbon

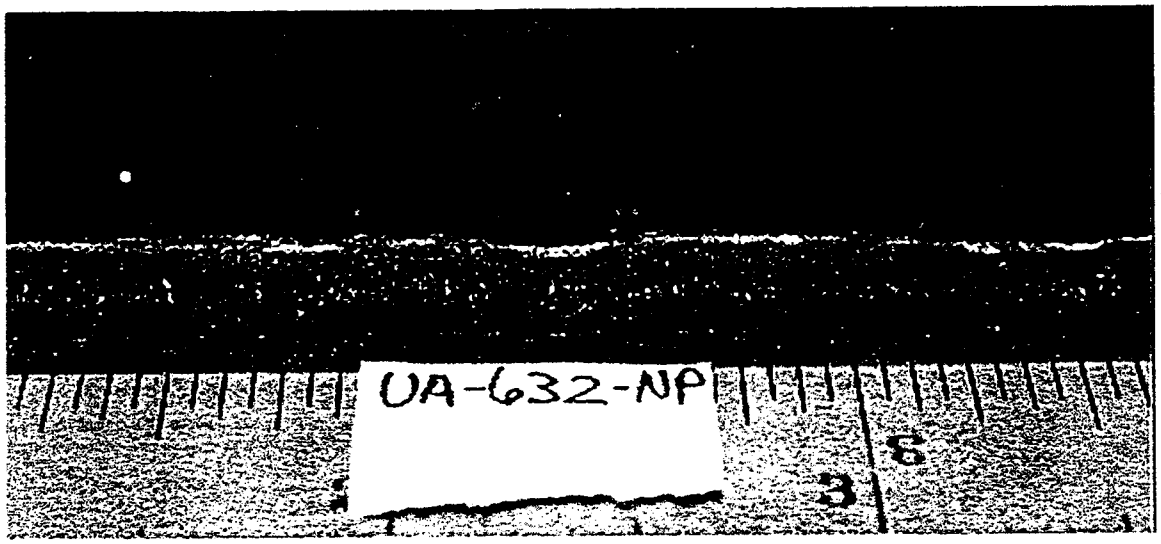

Figure 5.12 Photograph of weld made with UA-632 on "no primer".

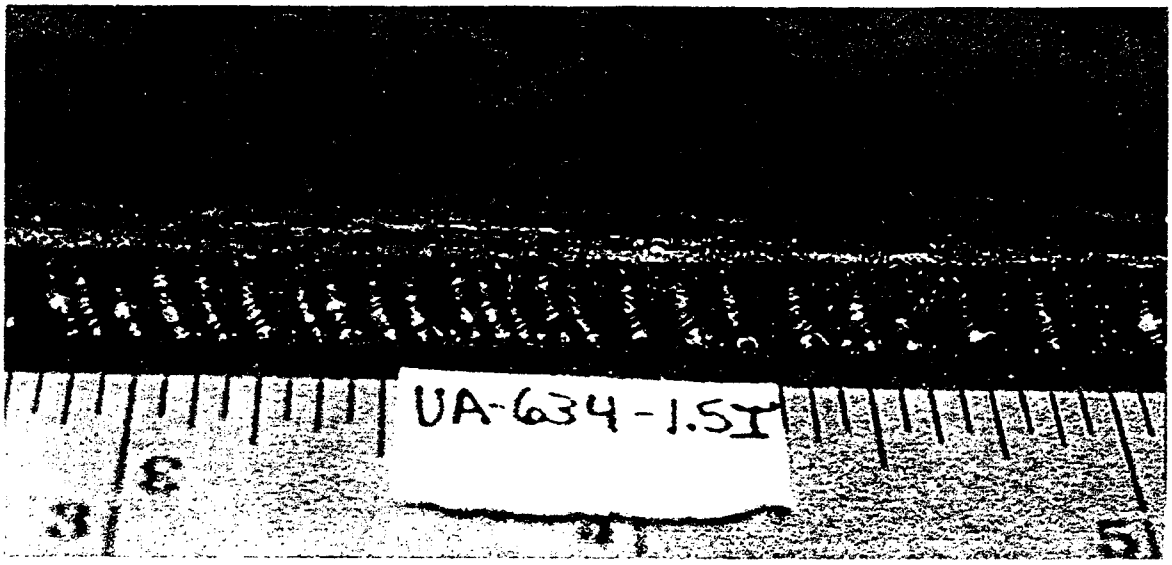

Figure 5.13 Photograph of weld made with UA-634 on 1.5 mils of Interplate NQA238.

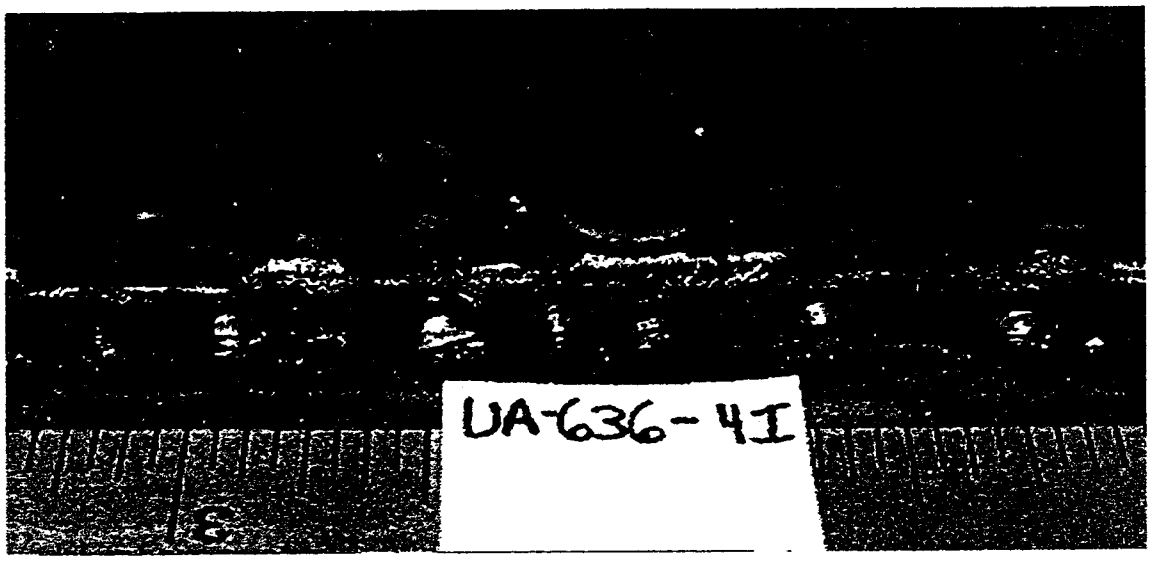

Figure 5.14 Photograph of weld made with UA-636 on 4.0 mils of Interplate NQA238.

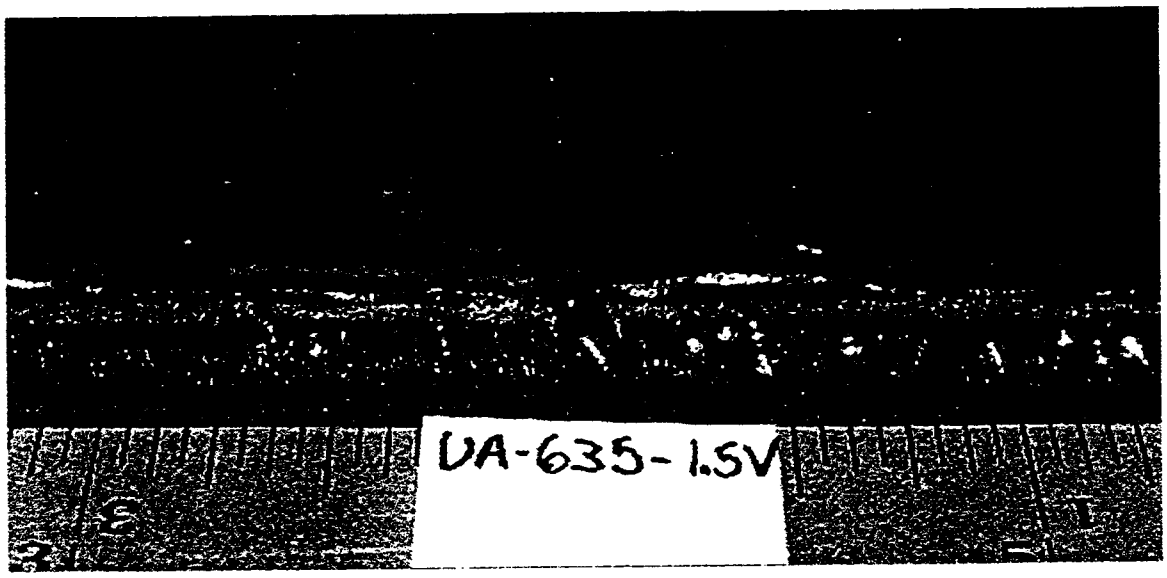

Figure 5.15 Photograph of weld made with UA-635 on 1.5 mils of Valspar V13F40.

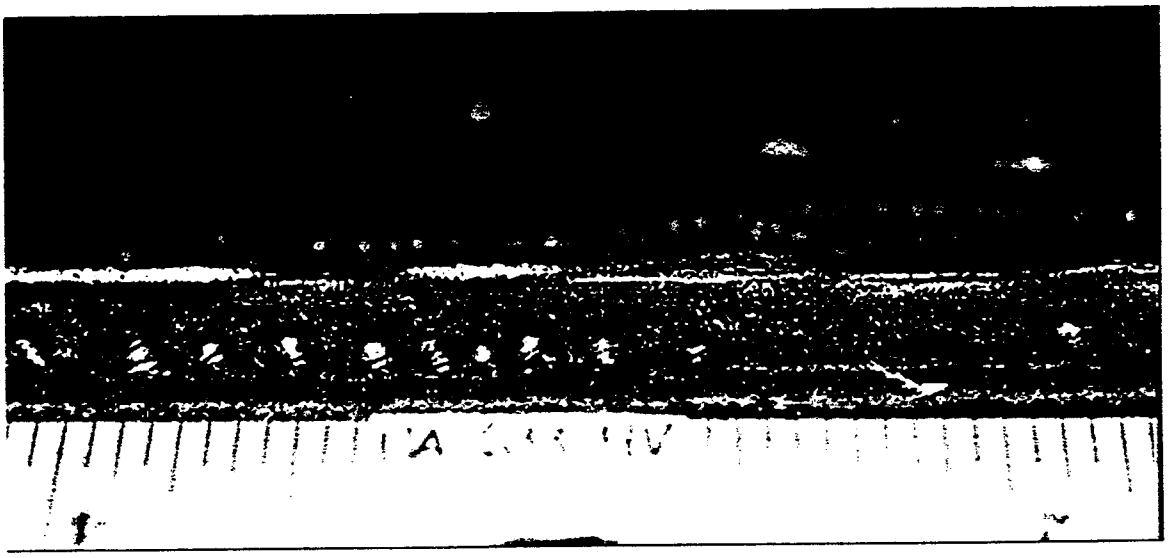

Figure 5.16 Photograph of weld made with UA-633 on 4.0 mils of Valspar V13F40.

Electrode	Primer	Thickness	C	Si	Mn	Cu	Cr	Ni	Mo	Cb	Ti	Al	V	B	P_{cm}
UA-632	none	none	0.0419	0.32	1.27	0.020	0.04	0.03	0.01	0.021	0.048	<.01	0.031	0.0025	0.1329
	1.5 mils	Interplate	0.042	0.34	1.28	0.020	0.03	0.03	0.01	0.018	0.040	0.01	0.030	0.0027	0.1375
	4.0 mils	Interplate	0.043	0.34	1.29	0.020	0.04	0.03	0.01	0.021	0.051	0.01	0.032	0.0027	0.1397
	1.5 mils	Valspar	0.044	0.32	1.27	0.020	0.03	0.03	0.01	0.025	0.042	0.01	0.032	0.0025	0.1375
	4.0 mils	Valspar	0.043	0.34	1.29	0.020	0.04	0.04	0.01	0.021	0.041	<.01	0.030	0.0025	0.1387
UA-633	none	none	0.0449	0.23	1.08	0.020	0.03	0.03	0.01	0.010	0.025	<.01	0.032	0.0015	0.127
	1.5 mils	Interplate	0.047	0.24	1.10	0.020	0.03	0.04	0.01	0.010	0.030	<.01	0.030	0.0018	0.1258
	4.0 mils	Interplate	0.048	0.24	1.06	0.020	0.03	0.03	0.01	0.010	0.030	0.017	0.030	0.0029	0.1302
	1.5 mils	Valspar	0.048	0.25	1.11	0.020	0.04	0.03	0.01	0.010	0.031	0.01	0.031	0.0018	0.1281
	4.0 mils	Valspar	0.046	0.25	1.13	0.020	0.03	0.03	0.01	0.010	0.028	0.01	0.028	0.0019	0.1268
UA-634	none	none	0.0458	0.30	1.12	0.020	0.03	0.03	0.01	0.015	0.030	0.025	0.030	0.0019	0.1282
	1.5 mils	Interplate	0.052	0.28	1.09	0.020	0.03	0.03	0.01	0.013	0.028	0.01	0.031	0.0016	0.1306
	4.0 mils	Interplate	0.056	0.30	1.10	0.020	0.03	0.04	0.01	0.016	0.035	0.047	0.032	0.0020	0.138
	1.5 mils	Valspar	0.052	0.31	1.16	0.020	0.03	0.04	0.01	0.013	0.033	<.01	0.031	0.0019	0.1368
	4.0 mils	Valspar	0.047	0.31	1.09	0.020	0.03	0.04	0.01	0.012	0.034	<.01	0.028	0.0020	0.1285
UA-635	none	none	0.0459	0.28	1.14	0.020	0.03	0.04	0.01	0.010	0.032	<.01	0.030	0.0019	0.1287
	1.5 mils	Interplate	0.045	0.29	1.15	0.020	0.04	0.03	0.01	0.013	0.036	<.01	0.031	0.0021	0.1299
	4.0 mils	Interplate	0.046	0.30	1.12	0.020	0.04	0.04	0.01	0.013	0.035	0.01	0.030	0.0021	0.1298
	1.5 mils	Valspar	0.045	0.31	1.17	0.020	0.04	0.04	0.01	0.012	0.036	<.01	0.029	0.0020	0.1311
	4.0 mils	Valspar	0.042	0.30	1.12	0.020	0.03	0.04	0.01	0.014	0.027	<.01	0.030	0.0019	0.1243
UA-636	none	none	0.0406	0.25	1.05	0.020	0.03	0.04	0.01	0.010	0.027	<.01	0.027	0.0018	0.1164
	1.5 mils	Interplate	0.042	0.27	1.12	0.019	0.03	0.05	0.01	0.010	0.029	<.01	0.032	0.0019	0.1237
	4.0 mils	Interplate	0.041	0.29	1.17	0.019	0.03	0.04	0.01	0.010	0.032	<.01	0.029	0.0020	0.1259
	1.5 mils	Valspar	0.046	0.31	1.21	0.020	0.04	0.04	0.01	0.015	0.037	0.014	0.031	0.0022	0.1353
	4.0 mils	Valspar	0.045	0.28	1.14	0.020	0.03	0.04	0.01	0.010	0.037	0.032	0.026	0.0020	0.1278

Table 5.10 Chemical analysis of welds made with the experimental FCAW electrodes, and different primers and primer thickness.

equivalent parameter, P_{cm}. P_{cm} is determined using the Ito-Bessyo equation (40). This equation can be used as an indicator of weld metal alloying content as it relates to weld cracking susceptibility . The P_{cm} parameter correlates well with steels that have low carbon (< 0.1 wt. pct.). Steels with a P_{cm} less than 0.2 wt. pct. have shown good resistance to weld cracking. It is clear to see that each one of the weld metals possesses good resistance to weld cracking based on these criteria. This result is not unexpected since the DH-36 base plate and the experimental electrodes are considered to be of low carbon and low alloy content. Production of phases, such as martensite and bainite, that are highly susceptible to weld cracking is kept to a minimum.

It is questionable whether or not carbon equivalent equations have the ability to predict the properties and transformation behavior of weld metals. Precipitates of microalloy additions may form during the weld thermal cycle more predominately then plate martensite of high carbon content (53). Solidification and second phase particles (e.g. inclusions) will also affect the weld metal solid state transformation reactions since oxide inclusions are known to promote ferrite nucleation and should reduce hardenability. Existing carbon equivalent equations do not adequately include the role of the oxide weld metal inclusions into the formulas, which is necessary for reliable prediction of weld metal microstructure and properties.

Liu and Olson (54,55) suggested that for low carbon microalloyed steel weld metals, the desirable size distribution of inclusions would be when the maximum size

distribution is greater than the Zener particle diameter. This condition would promote larger prior austenite grains because inclusions of a size larger than the Zener diameter would not hinder austenite grain growth. Instead of being located on the prior austenite grain boundaries, the inclusions would be located within the grains. Because of this fact, acicular ferrite would nucleate intragranularly on the inclusions, and therefore, would increase the toughness of the weld metal. However, if a large fraction of the inclusions are below the Zener diameter, most of the inclusions will pin the austenite grain boundaries resulting in large fractions of grain boundary ferrite which limit weld metal toughness. Inclusions rich in titanium and aluminum were also found to nucleate acicular ferrite.

To obtain reliable predictability from these carbon equivalent equations, a combination of carbon equivalent, basicity and equations concerning nitrogen and sulfur should be used to understand weld metal transformation and properties (53). As was mentioned earlier, the basicity index can be used as a measure of expected weld cleanliness and mechanical properties. The higher the basicity, the cleaner a weld metal is with respect to non-metallic inclusions, and the lower the weld metal oxygen content. Figure 5.17 plots the weld metal oxygen content against what is called the "added oxygen potential" basicity index (B.I.+). Because the exact composition of the experimental electrodes is not available, only the added oxide fluxes can be used in the calculations. It is clear to see that an increase in "B.I.+" results in lower weld metal oxygen or lower oxidizing potential. This result means that the oxidizing potential of the electrode will

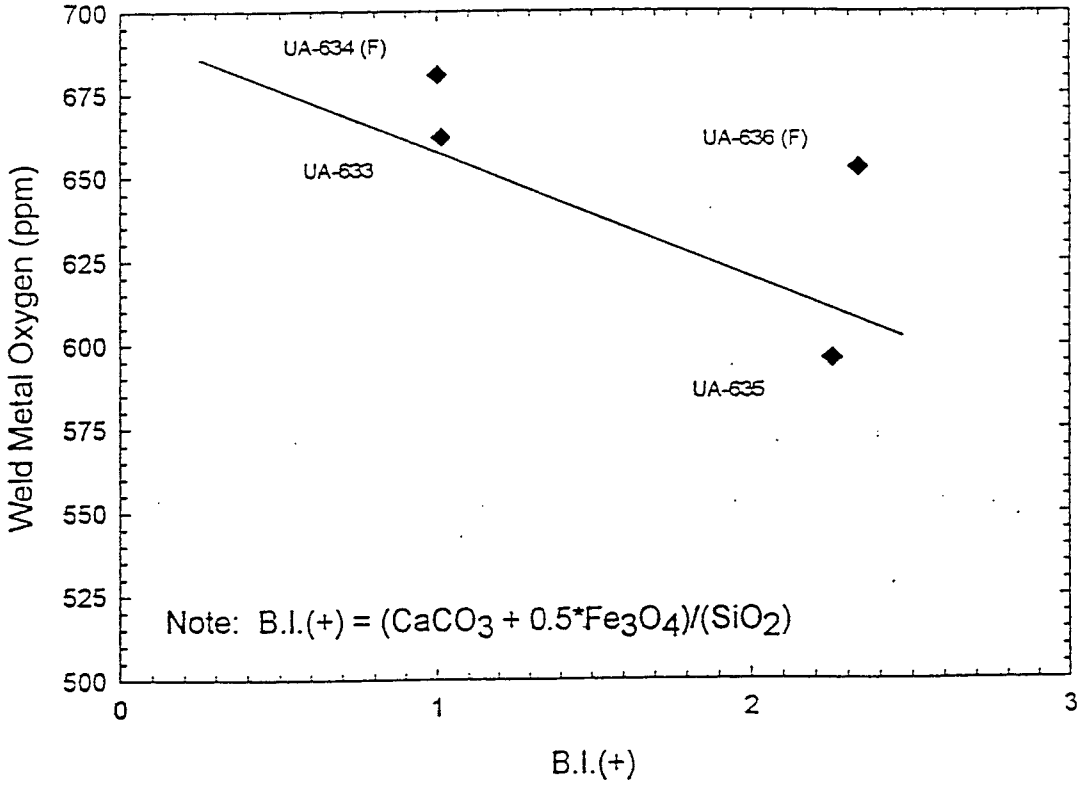

Figure 5.17 Effect of "added oxygen potential" basicity index, B.I. (+) on weld metal oxygen content.

determine the weld metal composition and microstructural make-up.

The type of electrodes used in these experiments were rutile-based, meaning that they contain around fifty percent TiO_2. Since the weld metal that was produced by the experimental electrodes contains substantial levels of titanium, it is expected that they must also contain high levels of inclusions. As mentioned previously, inclusions are used to nucleate acicular ferrite intragranularly in austenite grains. High weld metal toughness is produced from high levels of acicular ferrite within the weld metal.

Examination of the Charpy impact data compared with the chemical analysis data indicates that as the level of titanium is increased within the weld metal, the energy absorbed also increases as shown in Figure 5.18. The CVN values approach a maximum higher levels, although not substantially. This result of course occurs around titanium contents of 0.027 wt. pct. (e.g. UA-636 levels) and decrease slightly at only at the higher test temperatures. As the test temperature approaches -40^0C (-40^0F), the energy absorbed is about 12 ft-lbs. This same situation also exists for silicon as shown in Figure 5.19. The maximum CVN values exist around 0.25 wt. pct silicon (e.g. UA-636 levels) and decrease slightly as the percentage of silicon increases.

This situation should exist for manganese. However, it exhibits minimum CVN energy around 1.08 wt. pct. and increases from there (Figure 5.20). This is also the case with carbon. It approaches a minimum around 0.045 wt. pct. (Figure 5.21). It is not known why manganese and carbon behave this way. Increases in carbon should produce

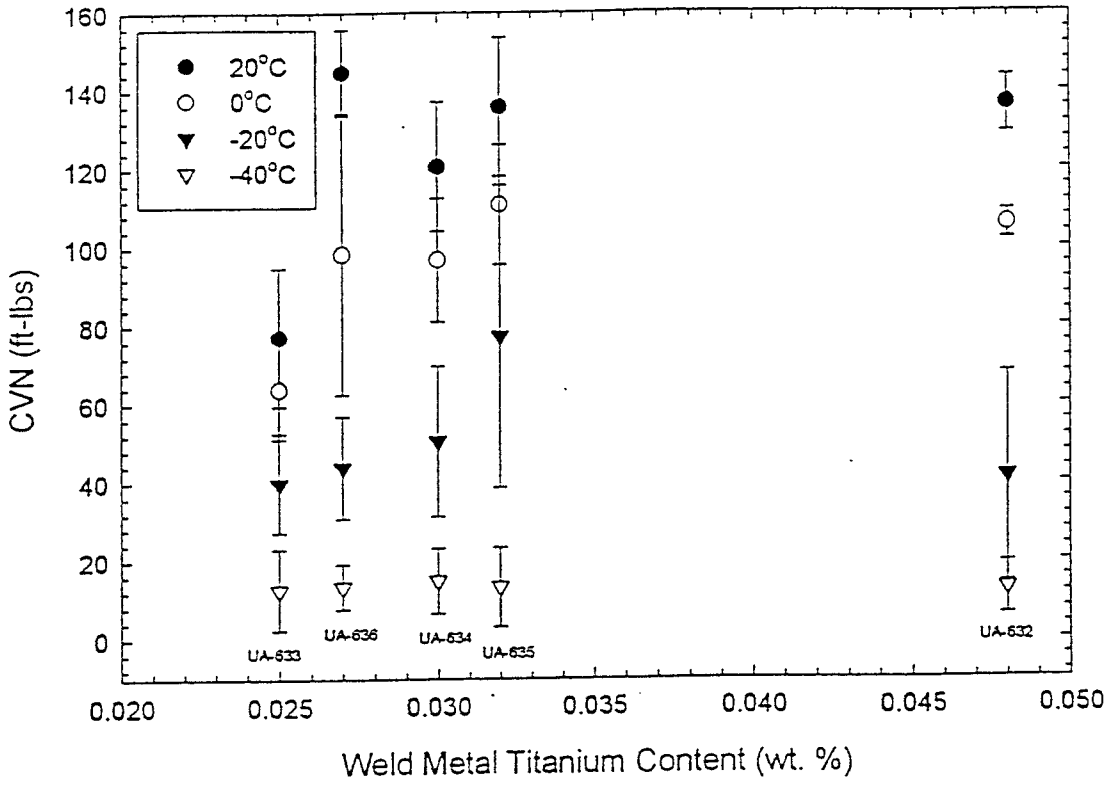

Figure 5.18 Effect of weld metal titanium content on Charpy impact energy absorption.

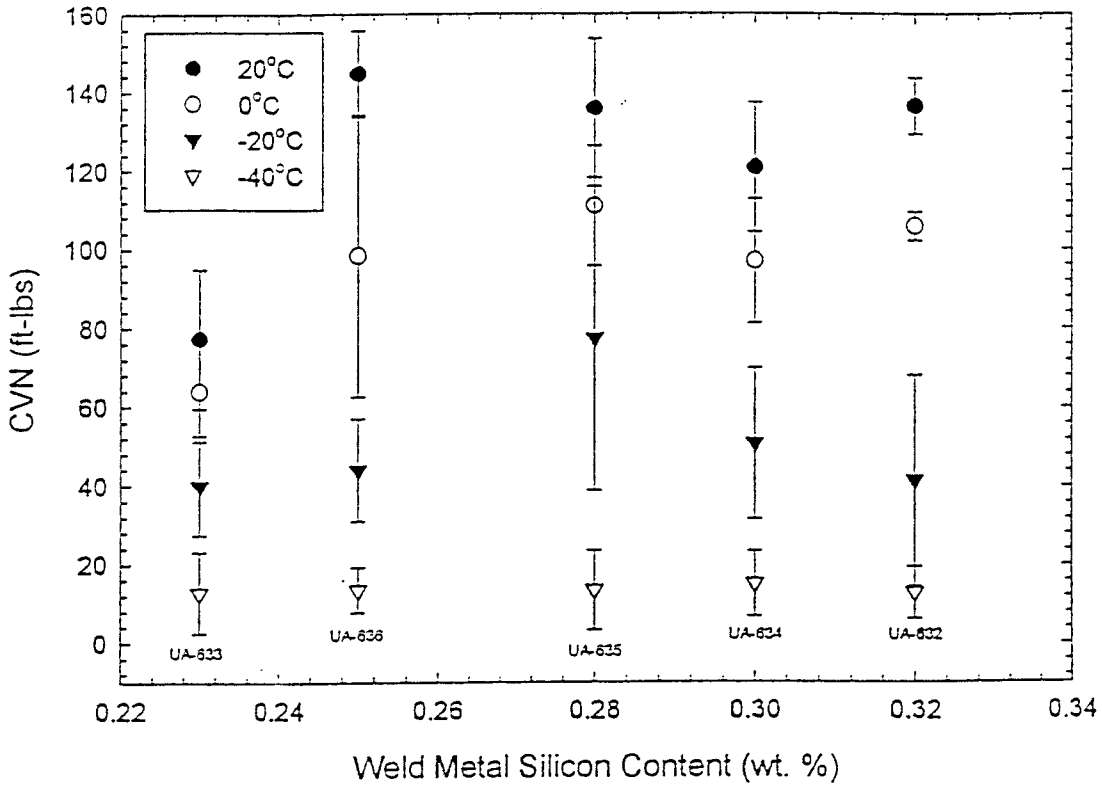

Figure 5.19 Effect of weld metal silicon content on Charpy impact energy absorption.

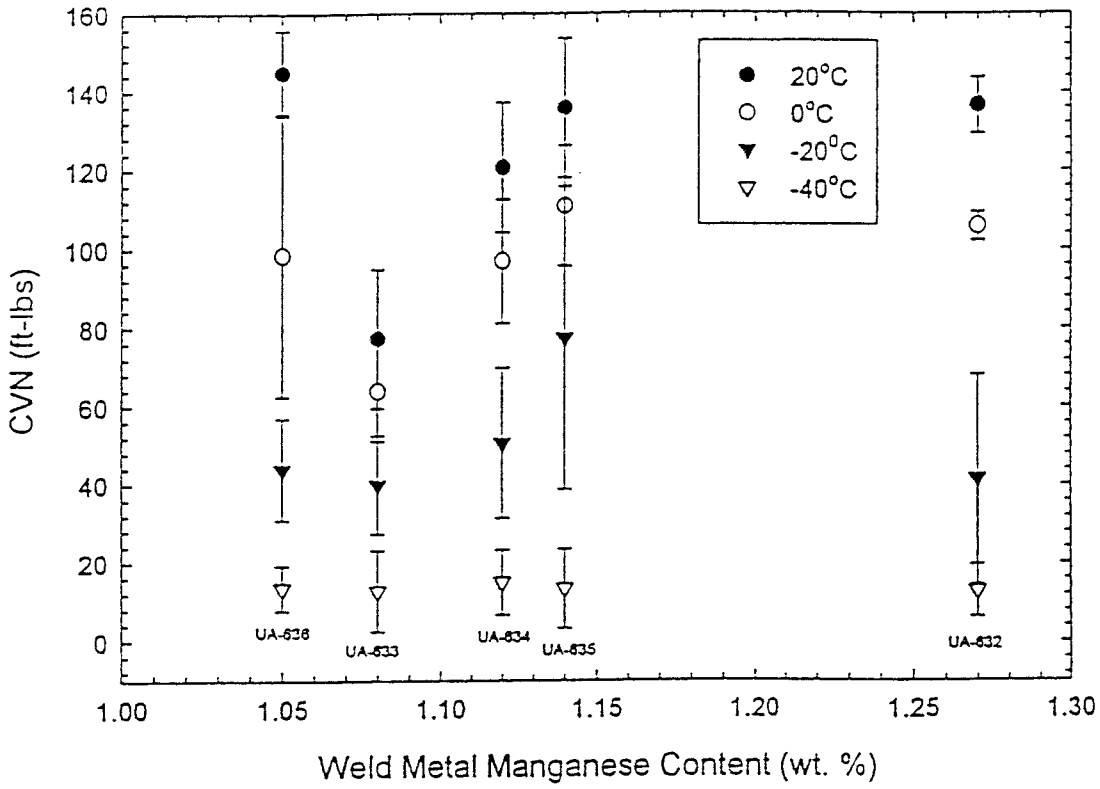

Figure 5.20 Effect of weld metal manganese content on Charpy impact energy absorption.

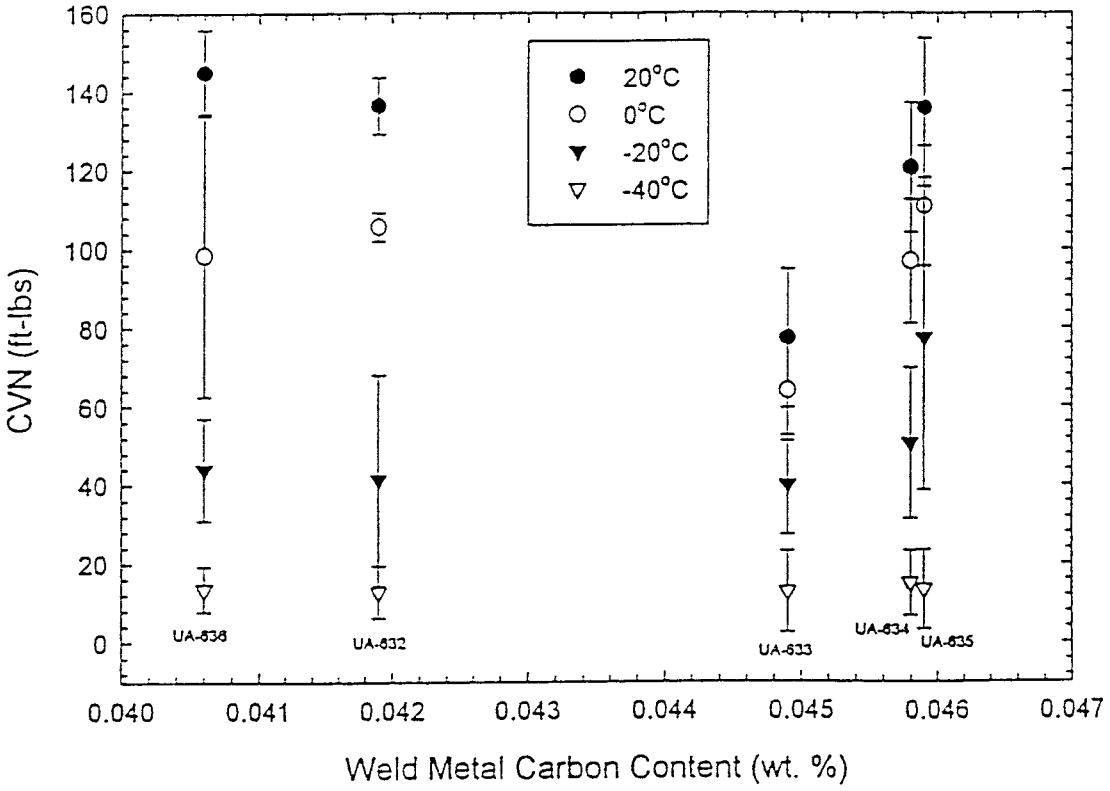

Figure 5.21 Effect of weld metal carbon content on Charpy impact energy absorption.

decreases in CVN energy, while increases in manganese should produce increases in CVN energy up to a point. This indicates the complexity of reactions taking place between the slag and weld metal. When the concentrations reach a certain point, other reactions become dominate and can affect the impact energy absorbed by changing the microstructure.

This same sort of situation exists when examining the tensile strengths of the weld metal. Each curve follows the same pattern as with the CVN data. The lowest yield strengths and ultimate tensile strengths occur around the same values as for the CVN data. There appears to be some correlation between alloying additions and the maximum levels attainable for tensile strength and impact energy absorption. Generally, it is expected that as the strength of the weld metal increases, the toughness should decrease. However, when examining Figure 5.18 which shows the toughness data plotted against increases in titanium levels, it is easy to see that this assumption is not necessarily true. This result could be due to defects in the weld metal or the type of microstructure generated.

The lowest strength and toughness values occur when using electrode UA-633, and the highest levels occur when using UA-636 and UA-632. This result is also supported by the carbon equivalent parameter (or weld cracking susceptibility), P_{cm}. All of the weld metals produced exhibited low P_{cm} values, and therefore, are not likely to be highly susceptible to weld metal cracking. The lowest P_{cm} value of 0.1164 was produced by UA-636 which means it is the least likely to experience cracking problems, even

compared to the commercial product. Both of these weld metals, coincidentally, have very low aluminum concentrations in the weld metal.

At low weld metal aluminum contents, titanium plays an active role in inclusion formation by entering deoxidation reactions which is what occurs here (56). Weld metal oxygen content will control the size and size distribution of oxides in the weld metal. For a given heat input, base metal composition, electrode composition, and oxide inclusions will control the prior austenite grain size and the number of adequate sites available for the nucleation of acicular ferrite. This situation is the main reason why it is necessary to determine the effect of flux composition on weld metal oxygen concentration.

Other inclusions may form besides oxide inclusions. These inclusions include sulfides, nitrides, carbides, and other compounds. Strengthening mechanisms such as fine carbo-nitride precipitation or solid solution strengthening by silicon, manganese, copper, or molybdenum additions are often not effective in weld metal because the fine precipitates are replaced by the oxide inclusions. The weld metal produced by the experimental electrodes does contain substantial amounts of manganese as seen in the chemical analysis (Table 5.10). Manganese may promote the formation of acicular ferrite by the production of MnS inclusions which may act as nucleation sites. Silicon, on the other hand, is considered to be detrimental to weld metal toughness because it promotes the formation of martensite and bainite phases which strengthen the weld metal. However, since the weld metals contain relatively small amounts silicon, this is not very

likely to occur. Some precipitation strengthening may occur because of the columbium, vanadium and titanium precipitates that may form. As with other alloying elements, a correct balance of microalloying elements is required to promote the formation of acicular ferrite without substantially increasing hardenability.

Elements such as sulfur and phosphorus are never deliberately added to steels because of their tendency to reduce toughness by embrittling grain boundaries. Sulfur and phosphorus are tramp elements found in the metal sheath of the FCA welding electrode and in the base metal. The DH-36 base plate contained about 90 ppm sulfur and 60 ppm phosphorus, while the metal sheath contained about 120 ppm each of sulfur and phosphorus. This resulted in the experimental electrodes producing about 70 to 90 ppm of sulfur and 120 to 170 ppm phosphorus in the weld metal. There have been no optimal sulfur levels reported in the literature regarding the formation of MnS. However, sulfur levels should be maintained at less than 200 ppm, as with the experimental welds, to avoid the potent grain boundary embrittling effects.

Phosphorus concentrations in weld metals are generally kept below 100 ppm, but solidification-induced segregation can raise local concentration to over 500 ppm. Recent work by Kluken et. al. suggests that segregation of phosphorus can increase with the amounts of acicular ferrite (57,58). The growth of delta-ferrite boundaries coincide with the phosphorus-rich regions, and that for some reason stimulates the formation of acicular ferrite. When austenite grain boundaries do not coincide with the phosphorus-rich

regions, ferrite plates grow from the grain boundaries and consume most of the austenite before acicular ferrite is nucleated. This result may explain the higher than anticipated phosphorus levels.

Chapter 6

CONCLUSIONS

The major achievements of this investigation can be summarized in the following conclusions:

1. The *hydrogen-oxygen* equilibrium holds true in weldments despite the faster heating and cooling rates than expected in the equilibrium conditions. Adding high oxidizing potential fluxes, such as $CaCO_3$, SiO_2, FeO, Fe_2O_3, and Fe_3O_4, to a flux-cored arc welding consumable will help to lower the amount of diffusible hydrogen produced in the weld metal.

2. The *hydrogen-fluorine* equilibrium holds true in weldments much like the *hydrogen-oxygen* equilibrium relationship. Fluoride additions to a FCAW consumable will further lower the diffusible hydrogen, especially at a higher primer thickness. The fluoride additions have also been shown to refine the microstructure.

3. Flux thickness, primer type (organic or inorganic) and primer thickness have little or no effect on weld metal oxygen content.

4. Primer type and thickness can greatly affect the amount of diffusible hydrogen produced in weld metal.

5. Surface discontinuities increase as the primer thickness approaches 4.0 mils.

6. Experimental electrode UA-636 performed the best compared to the other consumables on the basis of mechanical properties and levels of diffusible hydrogen produced. Further experiments based upon its composition would be advised.

Chapter 7

AREAS FOR FURTHER RESEARCH

Based on the encouraging results from the previous research, there are several areas that could be examined as far as controlling the amount of diffusible hydrogen produced by welding over primer-coated steels. These areas could include:

1. systematic examination of fluoride-containing fluxes
2. processing parameters (e.g. pulsed arc welding)
3. primer formulations

With the information already established regarding the *hydrogen-oxygen* and *hydrogen-fluorine* equilibrium, it only makes sense that several more fluorides should be examined regarding their ability to control diffusible hydrogen and refine the weld microstructure.

Examination of the processing parameters, or pulsed-arc control in welding would be another good area to examine. It has been shown that the welding parameters, such as voltage and current, can greatly affect arc stability and therefore, the amount of hydrogen pick-up in the weld pool. Optimizing the welding parameters and using pulsed-arc control would be another way to minimize the hydrogen pick-up and control fume production via pulsing.

The same type of examination that was done on the fluxes could also be applied to the primers. The chemical composition could be altered to help minimize several of the problems such as those encountered in welding. It has clearly been shown that altering the composition of an electrode results in different properties being obtained. Because many primers have unknown compositions, such as the electrodes, it would be necessary to have support from a major manufacturer of these primer coatings.

REFERENCES CITED

1. Suga, T., Nagakoa, S., Nakano, T. and Suenaga, K., "An Investigation into Resistance to Porosity Generation in High-Speed Horizontal CO_2 Fillet Welding", *IIW Doc.XII-1456-96*, American Council, AWS, Miami, FL, pg. 275-293.

2. American Welding Society, 1996, *Materials and Applications - Welding Handbook*, Vol. 3, Miami, FL, pg. 446-449.

3. Medieiros, R.C., 1997, "Effect of Oxidizing Electrodes and Polarity on Hydrogen Mitigation in Underwater Wet Welding", Colorado School of Mines, Golden, CO Ph.D. Thesis Number T-5013.

4. Pope, A.M., 1995, "Oxygen and Hydrogen Control in Shielded Metal Underwater Wet Welding", Colorado School of Mines, Golden, CO, Ph.D. Thesis Number T-4720.

5. Liu, S., Olson, D.L. and Ibarra, S., "Underwater Welding", *Welding, Brazing, and Soldering - ASM Handbook*, Vol. 6, 9th Edition, Materials Park, OH, 1993, pg. 1010-1015.

6. Sanchez-Osio, A., Liu, S. and Olson, D.L., "The Effect of Solidification on the Formation and Growth of Inclusions in Low Carbon Steel Welds", *Materials Science and Engineering*, 1996, pg. 122-133.

7. Reeve, L., "The Relation Between the Hydrogen Content of Weld Metal and its Oxygen Content", *The Journal of the Iron and Steel Institute*, ccII (II), 1945, pg. 385-396.

8. Gooch, T.G., "Properties of Underwater Welds, Part 1 - Procedural Trails", *Metal Construction*, March 1983, pg. 164-167.

9. Gooch, T.G., "Properties of Underwater Welds, Part 2 - Mechanical Properties", *Metal Construction*, April 1983, pg. 206-216.

10. Richardson, F.D. and Jeffes, J.H.E., "The Thermodynamics of Substances of Interest in Iron and Steel Making from 0^0C to 2400^0C", *The Journal of the Iron and Steel Institute*, 160 (III), November 1948, pg. 261-270.

11. Sorokin, L.I. and Sidlin, Z.A., "The Effect of Alloying Elements and of Marble in an Electrode Coating on the Susceptibility of a Deposited Nickel Chrome Metal to Pore Formation", *Svar. Proizvod.*, No. 11, 1974, pg. 7-9.

12. Liu, S. and Olson, D.L., "The Effect of Altitude on Welding", *Trends in Welding Research*, ASM International, Materials Park, OH, 1995.

13. American Welding Society, 1985, Guide for Steel Hull Welding, *ANSI/AWS D3.5-85*, Miami, Florida.

14. Lancaster, J.F., *Metallurgy of Welding*, Allen and Unwin, London, 4th Edition, 1987.

15. American Welding Society, 1973, *Welding Handbook - Applications of Welding*, Section 5, 6th Edition, Miami, FL.

16. Marrion, A.R., *The Chemistry and Physics of Coatings*, The Royal Society of Chemistry, 1994.

17. ASM International, 1987, *Metals Handbook - Corrosion*, Volume 13, 9th Edition, Materials Park, OH.

18. Schweitzer, P.A., *Corrosion and Corrosion Protection Handbook*, Marcel Dekker, Inc., New York and Basel, 2nd Edition, 1989.

19. Lee and Neville, *Epoxy Resins*, New York: McGraw-Hill, 1957.

20. Leonard, R.W., "Precoated Steel Sheet", *ASM Handbook: Properties and Selection: Irons, Steels, and High Performance Alloys*, ASM International, Vol. 1, 10th Edition, Materials Park, OH, 1990, pg. 212-225.

21. *Systems and Specifications*, Steel Structures Painting Manual, Volume 2, 7th Edition, 1982.

22. Ross, B, "Welding of primer-coated plate", *Philips Welding Reporter*, 1971/4, pg. 9-13.

23. Huisman, M.D., "Problems related to electric welding of shop-primer-treated material", *Philips Welding Reporter*, 1969/2, pg. 3-6.

24. Hilton, D., Norrish, J. and Stares, I., "Metal Inert Gas welding of primed plate", *Welding Review*, November 1990, pg. 196-200.

25. Asnis, A., Gutman, L.M., Mosenkis, Yu.G. and Baidulov, V.S., "Automatic Welding Through Anti-Corrosion Coatings in a Mixture of CO_2 and Oxygen", *Avt. Svarka*, No. 10, 1975, pg. 39-40.

26. Lucas, W. and Sheldon, J.D., "An assessment of weldable primers", *Welding & Metal Fabrication*, July 1993, pg. 274-277.

27. Matsui, H., Suzuki, H., Yamada, M., Hattori, T. and Shionoya, S., "Application of Arc Welding to Galvanized Steel Sheets", *Toyota Technical Review*, Vol. 45, No. 1, Sept. 1995, pg. 114-123.

28. Scandanavian Review, "MIG weldable shop primers pioneered in Finnish yards", *Shipping World & Shipbuilder*, January/February 1991, pg. 35-37.

29. Malik, L., Pates, M.J. and Morrison, K.G., "Study of the Effect of Welding Processes and Parameters on Weldability of Selected Primers And, By Literature Review, The Effect of Primer Induced Porosity on Joint Performance", *Canadian Coast Guard R&D Project Report*, Transport Canada Report No. TP9710, May 1989.

30. Lucas, W. "An Initial Assessment of the Methods for Determining the Susceptibility of a Primer to Form Porosity", *IIW Doc. XII-1337-93*, American Council, AWS, Miami, FL.

31. National Shipbuilding Research Program, "Improved Fabrication Primer for Protection of Steel", *NSRP-SPC-SP023/1*, 1973.

32. Dallam, C.B. and Damkroger, B.K., "Characterization of Welds", *Welding, Brazing, and Soldering - ASM Handbook*, Vol. 6, 9th Edition, Materials Park, OH, 1993, pg. 97-106.

33. American Welding Society, 1980, "Specification for Low Alloy Steel electrodes for Flux Cored Arc Welding", *AWS A5.29-80*, AWS, Miami, Florida.

34. American Welding Society, 1985, "Standard Methods for Mechanical Testing of Welds", *ANSI/AWS B4.0-85*, AWS, Miami, Florida.

35. American Welding Society, 1988, "Guide for the Visual Inspection of Welds", *ANSI/AWS B1.11-85*, AWS, Miami, Florida.

36. Military Specification, July 1989, "Electrodes - Welding, Flux Cored, Low-Alloy Steel", *MIL-E-24403/2C (SH)*.

37. American Welding Society, 1986, "Standard Methods for Determination of the Diffusible Hydrogen Content of Martensitic, Bainitic, and Ferritic Weld Metal Produced by Arc Welding", *AWS A4.3-86*, AWS, Miami, Florida.

38. Yurioka, N. and Suzuki, H., "Hydrogen assisted cracking in C-Mn and low alloy steel weldments", *International Materials Review*, The Institute of Metals and ASM International, Vol. 35, No. 4, 1990, pg. 217-249.

39. Johnson, M.Q., Frederickson, G.L., Liu, S. and Edwards, G.R., "Consumable Development for Advanced High Strength Steels", *International Trends in Welding Science and Technology*, ASM International, Materials Park, OH, 1992, Pg. 353-358.

40. Ito, Y. and Bessyo, K., 1968, *IIW Doc. IX-567*, American Council, AWS, Miami, Florida.

41. Johnson, M.Q., 1993, "Engineering and Design of Shielded Metal Arc Welding Consumables for High Strength Steel", Colorado School of Mines, Golden, CO, M.S. Thesis T-4286.

42. Gotal'Skii, YuN. and Stretovich, A.D., "On the Mechanism of Bonding of the Slag Crust with the Weld Metal", *Svar. Proizvod.*, No. 10, 1977, pg. 48-50.

43. Gotal'Skii, YuN. and Stretovich, A.D., "The Mechanism of Formation of the Bond Bewtween Slag Crust and Weld Metal", *Svar. Proizvod.*, No. 11, pg. 54-56.

44. Olson, D.L., Edwards, G.R. and Marya, S.K., "The Physical Behavior Associated with Slag Detachability During Welding", *Ferrous Alloy Weldments, Key Eng. Mats.*, Trans. Tech. Publ. Zurich, Switzerland, Vol. 67-70, pg. 253-268.

45. Hehemann, R.H., "Ferrous and Nonferrous Bainitic Structures", *Metals Handbook*, ASM, Vol. 8, 8th Edition, Materials Park, OH, 1973, pg. 194-196.

46. Krauss, G., *Steels: Heat Treatment and Processing Principles*, ASM International, 2nd. Edition, Materials Park, OH, 1990.

47. Grossmann, M.A. and Bain, E.C., *Principles of Heat Treatment*, ASM, 5th Edition, Materials Park, OH, 1964.

48. Siebert, C.A., Doane, D.V. and Breen, D.H., *The Hardneability of Steels - Concepts, Metallurgical Influences, and Industrial Applications*, ASM, Materials Park, OH, 1977.

49. Dieter, G.E., *Mechanical Metallurgy*, New York: McGraw-Hill, 3rd Edition, 1986.

50. Reed-Hill, R.E., *Physical Metallurgy Principles*, PWS Engineering, 2nd Edition, 1973.

51. Vishnu, P.R., "Solid-State Transformations in Weldments", *Welding, Brazing, and Soldering - ASM Handbook*, Vol. 6, 9th Edition, Materials Park, OH, 1993, pg. 70-87.

52. Easterling, K., *Introduction to Physical Metallurgy of Welding*, Butterworth-Heinemann Ltd., Oxford, UK, 2nd Edition, 1992.

53. Liu, S. and Olson, D.L., "The Role of Inclusions in Controlling HSLA Steel Weld Metal Microstructure", *Welding Journal*, Vol. 65, No. 6, 1986, pg. 139s-149s.

54. Ramsay, C.W., Olson, D.L. and Matlock, D.K., "The Influence of Inclusions on the Microstructure and Properties of a High Strength Steel Weld Metal", *Trends in Welding Research*, ASM, Materials Park, OH, 1989.

55. Tulani, S.S., Boinzewski, T. and Eaton, N.F., "Notch Toughness of Commercial and Submerged Arc Weld Metal", *Welding and Metal Fabrication*, Vol. 37, No. 8, 1969, pg. 327-339.

56. Oh, D.W., 1987, "The Influence of Boron and Titanium on Low Carbon Microalloyed Steel Weld Metal", Colorado School of Mines, Golden, CO, M.S. Thesis T-3415.

57. Kluken, A.O. and Grong, O., "Structure Property Relationships in Reheated SA Steel Weld Metal", *Recent Trends in Welding Science and Technology*, ASM International, Materials Park, OH, 1989, pg. 781-786.

58. Kluken, A.O., Grong, O. and Rorvik, R., "Solidification Microstructure and Phase Transformations in Al-Ti-Si-Mn Deoxidized Steel Weld Metals", *Met. Trans. A*, 21A, 1990, pg. 2047-2058.

OTHER REFERENCES

ASM International, "Joint Evaluation and Quality Control", *Welding, Brazing, and Soldering - ASM Handbook*, Vol. 6, 9th Edition, Materials Park, OH, 1993, pg. 1073-1128.

ASM International, "Selection of Carbon and Low-Alloy Steels", *Welding, Brazing, and Soldering - ASM Handbook*, Vol. 6, 9th Edition, Materials Park, OH, 1993, pg. 405-428.

Ahlblom, B., "Oxygen and its Role in Determining Weld Metal Microstructure and Toughness - A State-of-the-Art Review", *IIW Doc. IX-1322-84*, American Council, AWS, Miami, FL, 1984.

American Welding Society, *Welding Journal*, Welding Workbook Datasheet No. 213b, February 1998, pg. 56.

American Welding Society, 1991, *Welding Processes - Welding Handbook*, Vol. 2, 8th Edition, Miami, FL, pg. 157-190.

AWS Research Committee on Health and Safety, *Fumes and Gases in the Welding Environment*, American Welding Society, 1979, Miami, Florida.

Bailey, N. and Davis, M.L.E., "Fluxes for submerged-arc welding ferritic steels, Pt. 1: Manufacture, quality control, physical properties, and weldability", *The Welding Institute*, Report M84/75.

Bailey, N. and Pargeter, R.J., "The Influence of Flux Type on the Strength and Toughness of Mild Steel Weld Metal, Part 4", *The Welding Institute*, Report 124/1980, Cambridge, UK, 1980.

Bailey, N. and Regelous, G.R., "Recent developments in Transvarestraint testing", *The Welding Institute Research Bulletin*, August 1976, pg.201-204.

Bhadeshia, H.K.D.H., "Models for Acicular Ferrite", *International Trends in Welding Science and Technology*, ASM International, Materials Park, OH, 1992, pg. 213-222.

Bilyk, G.B and Kuplevatskii, L.M., "Increasing the stability of melting of self shielding flux cored wires", *Svar. Proizvod.*, No. 4, 1986, pg. 25-26.

Blodgett, O.W., *Design of Weldments*, The James F. Lincoln Arc Welding Foundation, 8th Edition, Cleveland, OH, 1976.

Bracarense, A.Q. and Liu, S., "Control of covered electrode heating by flux ingredients substitution", *Welding Metal and Fabrication*, May 1994.

Brahma, D and Boom, R., *Fundamentals of Steelmaking Metallurgy*, Prentice Hall International (UK) Limited, 1993.

Campbell, R.D. and Walsh, D.W., "Weldability Testing", *Welding, Brazing, and Soldering - ASM Handbook*, Vol. 6, 9th Edition, Materials Park, OH, 1993, pg. 603-613.

Cary, H. and Barhorst, S., "Welding Equipment for Complex Arc Welding Processes", *Trends in Welding Research*, ASM International, Materials Park, OH, 1986, pg. 783-793.

Chew, B., "Moisture Loss and Regain by Some Basic Flux Covered Electrodes", *Welding Journal*, May 1976, pg. 128s-134s.

Christensen, N. and Chipman, J., *Welding Research Council Bulletin*, No. 15, 1953.

Coe, F.R., "Fluxes and Slags in Arc Welding", *The Welding Institute*, Report 39/1977/M, Cambridge, UK.

Davis, M.L.E., "An Introduction to Welding Fluxes for Mild and Low Alloy Steels", *The Welding Institute*, Cambridge, UK, 1981.

Drzeniek, I.H., "Flux-cored wire electrodes - cross-sectional shape, production, characteristics", *Welding and Cutting*, No. 10, 1987.

Fasiska, E.J., Wagenblast, H.W. and Nasta, M., *Characterization of Arc Welding Fume*, American Welding Society, 1983, Miami, Florida.

Ferree, S.E., "New Generation of Cored Wires Creates Less Fume and Spatter", *Welding Journal*, Vol. 74, No. 12, 1995, pg. 45-49.

Francis, R.E., Jones, J.E. and Olson, D.L., "Effect of Shielding Gas Oxygen Activity on Weld Metal microstructure of GMA Welded Microalloyed HSLA Steel", *Welding Journal*, Vol. 69, No. 11, 1990, pg. 408-415.

French, I.E. and Bosworth, M.R., "A Comparison of Pulsed and Conventional Welding with Basic Flux Cored and Metal Cored Welding Wires", *Welding Journal*, June 1995, pg. 197s-205s.

Frost, R.H., Olson, D.L. and Liu, S., "Influence of Solidification on Inclusion Formation in Welds", *International Trends in Welding Science and Technology*, ASM International, Materials Park, OH, 1992, pg. 205-209.

Fox, A.G., Eakes, M.W. and Franke, G.L., "The Effect of Small Changes in Flux Basicity on the Acicular Ferrite Content and Mechanical Properties of Submerged Arc Weld Metal of Navy HY-100 Steel", *Welding Journal*, Vol. 75, No. 10, 1995, pg. 330s-342s.

Gaskell, D.R., *Introduction to Metallurgical Thermodynamics*, New York: McGraw-Hill, 2nd Edition, 1981, pg. 287.

Gooch, T.G. and Hart, P.H.M., "Solid State Phase Transformations in Steel During Welding", *Trends in Welding Research*, ASM International, Materials Park, OH, 1986, pg. 161-176.

Goodwin, G.M., "Development of a New Hot-Cracking Test - The Sigmajig", *Welding Journal*, Vol. 66, No. 2, 1987, pg. 33s-38s.

Graville, B., "A survey review of weld metal hydrogen cracking", *Welding in the World*, Vol. 24, No. 9/10, 1986, pg. 2-8.

Grong, O. and Matlock, D.K., "Microstructural development in mild and low-alloy steel weld metals", *International Metals Reviews*, Vol. 31, No. 1, 1986, pg. 27-48.

Gustafsson, J. and Heinäkari, M., "Experiences with CIM in Shipbuilding", *Welding Journal*, Vol. 70, No. 3, March 1991, pg. 27-32.

Heile, R.F. and Hill, D.C., "Particle Fume Generation in Arc Welding Processes", *Welding Journal*, July 1975, pg. 201s-210s.

Henderson, I.D., Senff, U.E. and Wilson, A.J., "Fume Generation and Chemical Analysis of Fume for a Selected Range of Flux-Cored Structural Steel Wires - AWRA Document P9-44-85", *Australian Welding Research*, December 1986, pg. 11-18.

Hrivnak, I., "The Mutual Relationship and Interdependence of Developments in Steel Metallurgy and Welding Technology", *Welding in the World*, Vol. 16, No. 1.

Huisman, M.D., "Flux- and metal-cored wires, a productive alternative to stick electrodes and solid wires", *Svetsaren*, Vol. 51, No. 1-2, 1996, pg. 6-14.

Ibarra, S., Grubbs, C.E. and Liu, S., "State-of-the-Art and Practice of Underwater Wet Welding of Steel", *International Workshop on Underwater Welding of Marine Structures*, American Bureau of Shipping, 1995, pg. 49-112.

Ibarra, S., Liu, S. and Olson, D.L., "Effect of Water Depth on Underwater Wet Weld Metal Porosity Formation", *International Conference on Underwater Wet Welding*, American Welding Society, Miami, FL, 1992, pg. 54-69.

Ibarra, S., Grubbs, C.E. and Olson, D.L., "The Nature of Metallurgical Reactions in Underwater Welding", *Offshore Technology Conference*, OTC 5388, 1987, pg. 277-281.

Jackson, C.E., "Fluxes and Slags in Arc Welding", *WRC Bulletin*, Welding Research Council, No. 190, New York, NY, 1973.

Kamada, M., Kanbe, Y., Suzuki, T. and Maki, S., "Flux Cored Electrode Development for Zinc-Primer Painted Steel Plate", *Welding Journal*, March 1993, pg. 49-54.

Katoh, M. and Kerr, H.R., "Investigation of Heat-Affected Zone Cracking of GTA Welds of Al-Mg-Si Alloys Using the Varestraint Test", *Welding Journal*, Vol. 66, No. 12, pg. 360s-368s.

Kline, M.D. and Doyle, T.E., "Programmable Automated Welding System", *Welding and Weld Automation in Shipbuilding*, The TMS Society, 1996, pg. 187-193.

Lin, W., Lippold, J.C. and Baeslack III, W.A., "An Evaluation of Heat-Affected Zone Liquation Cracking Susceptibility", *Welding Journal*, Vol. 72, No. 4, 1993, pg. 135s-153s.

Lin, W., Baeslack III, W.A. and Lippold, J.C., "A Method for Predicting HAZ Liquation Cracking using the Gleeble Hot Ductility and Spot-Varestraint Tests", *Edison Welding Institute Research Report*, MR9111, October 1991.

The Lincoln Electric Company, *The Procedure Handbook of Arc Welding*, 12th Edition, Cleveland, OH, 1973.

Lippold, J.C., Shademan, S.S. and Baeslack III, W.A., "The Effect of Specimen Strength and Thickness on Cracking Susceptibility during the Sigmajig Weldability Test", *Welding Journal*, Vol. 75, No. 3, 1996, pg. 81s-92s.

Liu, S. and Indacochea, J.E., "Weldability of Steels", *ASM Handbook: Properties and Selection: Irons, Steels, and High Performance Alloys*, ASM International, Vol. 1, 10th Edition, Materials Park, OH, 1990, pg.603-613.

Lundin, C.D., Menon, R., Lee, C.H. and Osorio, V., "New Concepts in Varestraint Testing for Hot Cracking", *Welding Research: The State of the Art*, October 1985, pg. 33-42.

Lundin, C.D., Lingenfelter, A.C., Grotke, G.E., Lessmann, G.G. and Matthews, S.J., "The Varestraint Test", *Welding Research Council Bulletin*, No. 280, August 1982.

McKeown, D., "Hydrogen and its control in weld metal", *Metal Construction*, Vol. 17, No. 10, October 1985, pg. 655-661.

Mejías, H.D., Pérez, T.E. and De Vedia, L., "Microstructure and Mechanical Properties of Self-Shielded Flux-Cored Arc Weld Metal", *Trends in Welding Research*, ASM International, Materials Park, OH, 1986, pg. 503-507.

Meyer, D.W., "Flux-Cored Arc Welding", *Welding, Brazing, and Soldering - ASM Handbook*, Vol. 6, 9th Edition, Materials Park, OH, 1993, pg. 186-189.

Middle, J.E., "Welding Preprimed BS 4360 Constructional Steel", *W&J Leigh - Metagard G 240 A*, pg. 245-250.

Moreton, J. and Jenkins, N, "Pollutants from paints when welding primed steel - new test method proposed", *Metal Construction*, Vol. 16, No. 10, 1984, pg. 605-607.

Muan, A. and Osborn, E.F., *Phase Equilibria Among Oxides in Steelmaking*, Addison-Wesley Publishing Company, Inc., 1965.

Nelson, T., Lippold, J.C., Lin, W. and Baeslack III, W.A., "Evaluation of the Circular Patch Test for Assessing Weld Solidification Cracking", *Edison Welding Institute Research Report*, MR9407, November 1994.

Nykänen, E., "Shipbuilding at Kvaerner Masa Yards Helsinki New Shipyard", *Svetsaren*, Vol. 51, No. 1-2, 1996, pg. 66-68.

Olson, D.L. and Liu, S., "The Physical and Chemical Behavior of Steel Welding Consumables", *Trends in Welding Research*, ASM International, Materials Park, OH, 1995, pg. 299-307.

Olson, D.L., Liu, S., Frost, R.H., Edwards, G.R. and Fleming, D.A., "Nature and Behavior of Fluxes Used for Welding", *Welding, Brazing, and Soldering - ASM Handbook*, Vol. 6, 9th Edition, Materials Park, OH, 1993, pg. 55-63.

Olson, D.L. and Ibarra, S. "Underwater Welding Metallurgy", *First OMAE Specialty Symposium on Offshore and Arctic Frontiers*, American Society of Mechanical Engineers, 1986, pg. 439-447.

Pehlke, R.D., Porter, W.F. and Urban, R.F., *BOF Steelmaking, Vol. I: Introduction, Theory and Design, Part I*, Iron and Steel Society (AIME), 1982.

Pfluger, A.R. and Lewis, R.E., *Weld Imperfections - Proceedings of a Symposium at Lockheed Palo Alto Research Lab*, Addison-Wesley Publishing Company, 1968.

Pope, A.M., Liu, S. and Olson, D.L., "Effects of the Electrode Oxidizing Potential on Underwater Wet Welds", *Proceedings of the 13th International Conference on Offshore Mechanics and Arctic Engineering*, American Society of Mechanical Engineers, 1994, pg. 361-368.

Rawlings, G.N. and Wilken, K., "Comparing the effectiveness of new hot cracking test methods", *Welding and Cutting*, 4/1992.

"Safe Welding on Coated Steel", *Canadian Welder and Fabricator*, March-April 1991, pg. 13-14.

Savage, W.F. and Lundin, C.D., "Application of the Varestraint Technique to the Study of Weldability", *Welding Journal*, November 1966, pg. 497s-503s.

Savage, W.F. and Lundin, C.D., "The Varestraint Test", *Welding Journal*, October 1965, pg. 433s-442s.

Schumann, G.O. and French, I.E., "The Influence of Welding Variables on Weld Metal Mechanical and Microstructural Properties from Conventional and Microalloyed Rutile Flux-Cored Wires", *Trends in Welding Research*, ASM International, Materials Park, OH, 1995, pg. 525-534.

Solomon, H.D., "Fundamentals of Weld Solidification", *Welding, Brazing, and Soldering - ASM Handbook*, Vol. 6, 9th Edition, Materials Park, OH, 1993, pg. 45-54.

Strangwood, M. and Bhadeshia, H.K.D.H., "The Mechanism of Acicular Ferrite Formation in Steel Weld Deposits", *Trends in Welding Research*, ASM International, Materials Park, OH, 1986, pg. 209-213.

Terashima, H. and Tsuboi, J., *Metal Construction*, Vol. 14, 1982, pg. 648-654.

Turkdogan, E.T., *Physiochemical Properties of Molten Slags and Glasses*, The Metals Society, 1983.

Vaidya, V.V., "Flux Cored Arc Welding Wires - Factors Affecting Selection", *Canadian Welder and Fabricator*, November 1989.

Vuik, J., "An update of the state-of-the-art of weld metal hydrogen cracking", *Welding in the World*, Vol. 31, No. 5, 1993, pg. 23-32.

Webber, J., "AWS Shipbuilding Conference Stresses Need for New Methods", *Welding Journal*, Vol. 68, No.1, January 1989, pg.63-65.

Welding Rod Division, The Japan Welding Engineering Society, "Researches on Fumes and Gases Emitted by Welding Primed Steels", *IIW/IIS Doc. VIII-1257-84*, American Council, AWS, Miami, FL.

Wilken, K. and Kleistner, H., "The classification and evaluation of hot cracking tests for weldments", *Welding in the World*, Vol. 28, No. 7/8, 1990, pg. 126-143.

Yang, J.R. and Bhadeshia, H.K.D.H., "Thermodynamics of the Acicular Ferrite Transformation in Alloy-Steel Weld Deposits", *Trends in Welding Research*, ASM International, Materials Park, OH, 1986, pg. 187-191.

For more information about the
National Shipbuilding Research Program
please visit:

http://www.nsrp.org/

or

http://www.USAShipbuilding.com/